

Technical Support of the U.S. DOE Biomass Power Program in the Development of Biomass to Electricity Technologies.

Richard L. Bain and Ralph P. Overend
National Renewable Energy Laboratory
Industrial Technologies Division
1617 Cole Boulevard
Golden, CO 80401-3393

Keywords: Biomass, Electric Power, R&D

INTRODUCTION

In the USA the period since 1973 to the present, has resulted in a dramatic upswing in bioenergy use and applications uses especially in the thermal and electrical applications of mainly wood residues. The wood processing and pulp and paper sectors became about 70% self sufficient in energy in that period and the amount of grid connected electrical capacity increased from less than 200 MW in 1978 to over 7,500 MW_e today. This dramatic growth stimulated in part by federal tax policy and state utility regulatory actions, occurred after the Public Utilities Regulatory Policies Act (PURPA) of 1978 guaranteed small electricity producers that utilities would purchase electricity at a price equal to the utilities' avoided cost.

More than 70 percent of biomass power is cogenerated with process heat. Wood-fired systems account for 88 percent, agricultural waste (3%), landfill gas (8%), and anaerobic digesters (1%). There are nearly 1000 wood-fired plants in the U.S., typically ranging from 10 to 25 MW_e. Only a third of these plants offer electricity for sale. The rest are owned and operated by the paper and wood products industries for their own use. Most of today's biomass grid connected power installations are the smaller scale independent power and cogeneration systems. To date, utilities have been involved in only a handful of dedicated wood-fired plants in the 40 to 50 MW_e size range, and in some co-firing of wood and municipal solid waste in conventional coal-fired plants.

Net plant heat rates for 25 MW_e plants in the California PG&E service territory average approximately 18 percent efficiency (17,000 Btu/kWh). By comparison the 43 MW_e utility-operated plant at Kettle Falls, Washington has a reported heat rate of 26% efficiency (14,382 Btu/kWh). However, the advantageous power purchase agreements that were negotiated under PURPA in the 1980s are no longer available at high rates of avoided costs. As a result a number of plants are closing as their power contracts come up for renewal. They could be competitive in today's environment using low cost waste and residue fuels if their efficiency was much higher as has been demonstrated in the sugar industry of Hawaii where the power plants operate for a major part of the year as CHP installations. Investments in efficient steam cycles has resulted in a competitive rate of power generation under PURPA. Low pressure boilers were systematically replaced by higher pressure boiler systems of larger capacity in the period 1960 through 1980 with the average steam pressure and temperature increasing from 1.3 MPa and 210 °C to 4.4 MPa and 380 °C. Meanwhile the net steam consumption in the mills decreased significantly from 600 kg /tc to about 300-400 kg/tc, resulting in a power output of about 60 kWh/tc on average with the best mills reaching over 100 kWh/tc.

Biomass Power Efficiency Advances are Needed in order to be competitive with low cost fossil fuels, especially in stand alone power generation, will require a considerable increase in the power to heat ratio and will require advanced technologies - such as the use of IGCC (Integrated Gasification Combined Cycles) as illustrated in Table 1.

As can be seen, the increase in efficiency has two effects: it reduces the capital cost on a kW basis, and it reduces the sensitivity of the final cost of electricity to the fuel cost component.

The USDOE Biomass Power Program is working to address the issues of making biomass competitive by working with today's industry to increase its reliability and to develop advanced systems for increased efficiency and environmental performance.

The pathways under discussion are included in Figure 1.

Support for today's Industry: In general the biomass power industry has displayed good reliability, however, in the case of the IPP Biomass fueled stations in California, operational difficulties

rapidly emerged when using non-wood biomass fuels¹. The operational difficulties were caused by the deposition of mineral matter on the heat exchange surfaces (boiler tubes, superheaters, and water walls) and by the agglomeration of ash and inert fluid bed materials. This problem is one that is costly as it results in down-time for tube cleaning and repair, and because there is considerable interest in the development of dedicated crops such as short rotation woody crops and herbaceous energy crops for bioenergy applications it could be a problem that would affect the long term large scale deployment of biomass fuels in both electricity generation and the production of liquid fuels. For this reason the USDOE through NREL initiated a collaborative study with industry on the ash deposition problem² with the goal of establishing the root cause of the difficulties in using non-traditional biomass fuels.

While the nature of the direct combustion boiler problem is of current concern, NREL also recognized that these same issues may have to be addressed in the non-combustion processes such as fast pyrolysis, and gasification that convert biomass into intermediate fuels that would be used in very high efficiency generation systems based on gas turbines. Gas turbines are extremely sensitive to both mineral matter and to alkali metals. For the state-of-the-art turbines with turbine inlet temperatures of 1260°C (2300 °F) the manufacturer's specifications call for less than 300 ppb of alkali metal in the hot section. Since high efficiency biomass to electric conversion is a goal of the USDOE Biomass Power Program³ a program of testing non-woody and short rotation biomass feedstocks in gasifiers and fast pyrolysis processes was instituted.

The Ash Deposition Problem was addressed by conducting extensive fuels and deposits analysis and through an extensive collaboration the cause was identified. The project received over 700 different fuels analyses from the participants, however, the majority of these did not have the critical ash analysis data. However, this may not have been such a bad omission since the project has established that there are major problems with the standard ash determination methods that are accepted as standards for coal materials. The ASTM methods for coal prepare an ash at 800 °C which is then used for the pyrometric cone analysis to determine if there will be a slagging or sticky problem. Unfortunately the critical element causing the ash deposition and fouling problem is potassium and it is known that this and other mineral matter from biomass will evaporate from the ash at 800 °C, decreasing its mass and altering its fusion properties⁴. Potassium is a key component of cellular function and in plants it can be present at 1000 times the concentration of sodium. As much as 35% of the ash in annual plants can be alkali which drastically reduces the ash fusion temperature from greater than 1300 °C in the case of wood ash to about 700 °C where the potassium can form a eutectic with the plant's silica or the sand medium of the fluidized bed⁵. Work with the MBMS system at NREL has shown that the form in which potassium is transported can be very diverse including oxides, hydroxide, sulphite/ate, and chlorides as volatiles⁶.

Gasification Developments: Commercial biomass gasifiers are already in use to generate process heat and steam. Current development activities are focused on producing electricity and, to some extent, liquid fuels, and involve integrating gasification with various cleanup systems to ensure a high-quality and reliable gas product. At this time, there is no clear preference for a single gasifier system. The Global Environment Facility⁷, is evaluating two systems offered by Scandinavian commercial developers for the CHESF project in NE Brasil. The evaluation will compare the advantages and disadvantages of using air gasification at high pressure (Bioflo) or at low pressure (the TPS system). High-pressure gasification would have to meet the pressure requirements of the chosen turbine on all system components, including the gas clean-up system; the low-pressure system would carry out the gas cleaning before compressing the fuel gas to the turbine operating pressure. Air blown systems only produce a low-heating value gas (less than 150 Btu/ft³, 5-6 MJ/Nm³), and a significant loss in efficiency is imposed if the gas must be cooled to ambient temperatures prior to being compressed. For this reason, the American and Scandinavian gasification programs are emphasizing using hot gas clean-up systems for the air-blown, low heating value gasifiers that will be operated at pressure.

The U.S. program has a dual-pathway strategy involving both low and medium heating value gas production. One high pressure system is capable of generating either low or medium heating value gases according to whether it is an air- or oxygen-blown variant, and is the Renugas® system developed by IGT. The low-pressure strategy in the U.S. is based around two developers of medium heating value gas systems who do not use oxygen, rather use indirect gasification to produce gases having heating values of 350-450 Btu/ft³ (15 - 20 MJ/Nm³). Cooling and quenching the gas does not incur a significant efficiency penalty and, compared with low-heating value gas, there are essentially no modifications required in the turbine combustors to handle the

medium-heating value gas fuels.

The Pacific International Center for High Technology Research (PICHTR) Project (>6 MW):

The U.S. Department of Energy (DOE) and the state of Hawaii have joined with PICHTR in a cost-shared cooperative project to scale up the Institute of Gas Technology (IGT) Renugas® pressurized air/oxygen gasifier to a 45-90 ton/day engineering development unit (EDU) operating at 1-2 MPa using bagasse and wood as feed. The site is the HC&S sugar mill at Paia, Maui, Hawaii, and NREL is providing project oversight in addition to systems analysis. The first phase, which is now being commissioned consists of the design, construction, and preliminary operation of the gasifier to generate hot, unprocessed gas. The gasifier is designed to operate with either air or oxygen at pressures up to 2.2 MPa, at typical operating temperatures of 850°-900° C. In Phase 1, the gasifier will be operated for about four months at a feed rate of 45 ton/day at a maximum pressure of 1 MPa. Following the end of Phase 1 in late 1995, a hot-gas cleanup unit and gas turbine will be added to the system to generate 3-5 MW of electricity.

The Vermont Gasifier Project with FERCO and the McNeil Generating Station (>15MW)

Future Energy Resources Company (FERCO) of Atlanta, GA, is the licensee of the Battelle indirect gasification system, and the scaleup is at the site of the Burlington Electric Department's McNeil station in Burlington, VT. The project, which is in two phases, will first take feedstock from the 50 MWe station and after gasification will return the gas to the boiler. The scale of operation is about 200 tpd. The second phase will incorporate approximately 15 MW_e of turbine electricity generation. The project is jointly funded by USDOE and FERCO and presently construction forecast to start in Fall 1995.

National Renewable Energy Laboratory (NREL) Activities: The research strategy is guided by systems analysis and technoeconomic assessments of gasifier-based power cycles. In the laboratory, research is ongoing to develop catalysts for hot gas conditioning, and use of advanced instrumentation and chemometrics for feedstock characterization and evaluation. One element of this research is using advanced mass spectrometry to characterize alkali metal speciation under gasification and combustion of biomass conditions. This work has been extended to develop and using a transportable molecular beam mass spectrometer (TMBMS) for real time measurement of hot stream composition to 500 atomic mass units (amu). The TMBMS is being used by both Battelle and IGT to measure gasifier and catalyst performance in the field.

ACKNOWLEDGMENTS

This work was performed under contract N^o DE-AC36-83CH10093 to the US Department of Energy. Special thanks go to our colleagues at NREL: Foster Abglevor, Thomas A. Milne, David Dayton, Jim Diebold, David Gratson, Esteban Chornet, Robert Evans, John Scahill, Steven Czernik, and Kevin Craig for their helpful discussions on this theme.

REFERENCES

1. Jane Hughes Turnbull. 1993 *Use of Biomass in Electric Power Generation the California Experience*, Biomass and Bioenergy Vol. 4. pp 75-84.
2. Alkali Deposits found in biomass power plants: a preliminary investigation of their extent and nature. NREL Subcontract TZ-2-1-11226-1. Principal Investigator Thomas R. Miles of Thomas R. Miles Consulting Design Engineers. Participants: Delano Energy Company Inc.; Electric Power Research Institute; Elkraft Power Company (Denmark); Foster Wheeler Energy Corporation; Hydra Co Operations Inc.; Mendota Biomass Power, Inc.; National Wood Energy Association; Sithe Energies, Inc.; Thermo Electron Energy Systems; Wheelabrator Environmental Systems Inc.; Woodland Biomass Power Ltd.; Western Area Power Authority; Sandia National Laboratories; Hazen Research Inc.; Al Duzy and Associates; University of California Davis; U.S. Dept. of the Interior, Bureau of Mines; Appel Consultants, Inc.
3. Electricity from Biomass National Biomass Power Program Five-Year Plan (FY1994-FY1998) Solar Thermal and Biomass Power Division, Office of Solar Energy Conversion, U.S. Department of Energy, Washington, D.C. Draft April 1994.
4. M.K. Misra, K.W. Ragland, and A.J. Baker. 1993 *Wood Ash Composition as a Function of the Furnace Temperature*, Biomass and Bioenergy Vol. 4. pp 103-116.

5. A. Ergundler, and A.E. Ghaly. 1993 *Agglomeration of Silica Sand in a Fluidized Bed Gasifier Operating on Wheat Straw*, Biomass and Bioenergy Vol. 4. pp 135-147. See also the phase diagram for $\text{SiO}_2 - \text{K}_2\text{O} \cdot \text{SiO}_2$ in E.M. Levin, H.F. McMurdie, and F.P. Hall, 1956. *Phase Diagrams for Ceramists*. The Am. Ceramic Soc. Inc.:Columbus OH.
6. D. Dayton, and T.A. Milne. "Alkali, Chlorine, SO_x , and NO_x Release During Combustion of Pyrolysis Oils and Chars." in Ed. T.A. Milne. Proceedings Biomass Pyrolysis Oil Properties and Combustion Meeting. September 26-28, 1994 Estes park Colorado. NREL-CP-430-7215. pp 296-308.
7. P. Elliott, and R. Booth. 1993. *Brazilian Biomass Power Demonstration Project*. Special Project Brief. Shell International:London, U.K.

Table 1. Comparison of present day steam generation with IGCC

Cost factors (£/kWh)	Steam Generation	IGCC
Operations and Maintenance	0.5	0.5
Fuel only Cost	3.6	1.6
Capital Recovery	4.2	3.0-3.5
Cost of Electricity	8.3	5.1-5.6

Notes to Table 1. Assuming a marginal cost of fuel of \$2/million Btu (or approximately \$40/tonne of dry biomass), a load factor of 85% (base loaded), and a return on capital invested of 8%/year, it is possible to see the effect of the new technology. Both plants are approximately 50 MW_e capacity. The efficiency of the steam plant is about 20%, while the IGCC is estimated to have an efficiency of 45%. The capital cost of the steam plant is \$1.8/W, while that of the IGCC is expected to be in the range of \$1.3 to \$1.5/W.

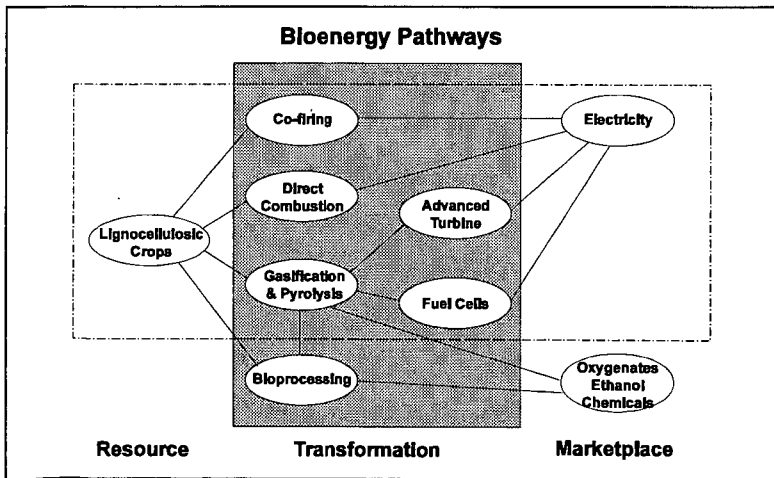


FIGURE 1: Bioenergy pathways.

HOT GAS CLEANUP IN BIOMASS GASIFICATION - REVIEW OF ACTIVITIES WITHIN EC SPONSORED R&D PROGRAMS

Anders L. Hallgren, Dept. of Chem. Eng. II
P.O.B. 124, Chemical Center, University of Lund
S-221 00 Lund, Sweden

Keywords: biomass gasification, hot gas cleanup, filtering, alkali measurements

INTRODUCTION

The use of biomass as an alternative fuel source attracts presently considerable interest in the European Community. A variety of R&D projects are currently active in investigating the prospects for biomass conversion processes in power and heat production.

Renewable energies in general are seen as one of the major options for energy supply, offering substantial advantages regarding environmental protection and CO₂ emissions. Because of their decentralize character they may also offer considerable potential in rural areas.

Within the European Commission (EC) research and technical development programs, several R&D and demonstration projects are being carried out reflecting issues in utilizing biomass or alternative solid fuels for power and heat production. Apart from being a potential environmental-friendly conversion route, the motives for introducing biomass in heat and power production is of course being able to replace the use of fossil fuels and to find alternative applications for existing agricultural areas.

One of the main technical issues is the gas cleanup process for clean gas utilizations and IGCC (Integrated Gasification Combined Cycle) concepts. Potential advantages are expected if the gas cleaning process can be accomplished at enhanced temperatures. Available options for integrated hot gas cleanup are being tested ranging from particulate removal to emission control. An overview of the ongoing projects in the area is presented in the following.

A new generation of gasifiers suitable for gasification of biomass and so called alternative solid fuels are under development. A PFB biomass gasifier test rig (Figure 2) has been installed at the Dept. of Chem. Eng. II (University of Lund). The system includes an integrated hot gas cleanup system that forms the basis for the activities at the department within two EC Joule II programs [1]. Progress from these efforts are presented and discussed.

PROSPECTS FOR BIOMASS UTILIZATION

At present about 80 % of the energy consumption within the European Union is from the use of fossil fuels. Within the power and heat production, some 40 % of the production is produced from coal utilization. These production systems have often modest efficiency and contribute to a large extent to the global emissions of nitrogen oxides, sulfur oxide, carbon oxide, and particulate matter [2]. Until today natural gas and fossil fuels have been regarded as the most economic and appropriate fuel for heat and power production where biofuels (biomass, agro- and forestry residues) may be believed to be the more environmental friendly alternative in the long run.

In many regions of Europe there is a steady and continuous production of biomass residues. The growing of biomass for energy production, combined with the utilization of agricultural and forestry residues, is an alternative energy resource in many areas that today is likely to be not too far from a commercial status. One driving force for this development is the tax structure including the exclusion of biomass from recently imposed CO₂ tax on fossil fuels. In some regions farmers may even be

encouraged to grow energy crops on land that during the last years has been taken out of production to balance the farming industry.

To meet the environmental challenges, improved technologies are needed. The current technologies involve combined cycle concepts where improved performances are needed. Novel solutions and continuous developments of integrated systems offer encouraging prospects for enhanced efficiency and more economical power generation. The improvements also have to involve fuel flexible systems accepting a broad variety of different solid fuels. Since the awareness of potential environmental-friendly alternatives has increased and the restrictions with respect to emissions has been reinforced, the interest for utilizing renewable fuels in heat and power production has correspondingly grown. With IGCC technology and renewable energy sources it is possible to get a both ecological acceptable and a highly efficient concept for heat and power production.

INTEGRATED HOT GAS CLEANING FOR IGCC PROCESSES

For a successful implementation of biomass gasification in commercial fuel gas production, the effluent gas must conform to allowable limits regarding particulate and other impurities. For IGCC applications there are potential advantages with gas cleanup at high temperatures and elevated pressures.

The fuel gas from gasification processes contains various amounts of impurities and particulate originating from the solid fuel and attrition products from the bed material. Advanced filtration technology today partially offers solutions to some of these problems. Especially the integration of these systems in larger scales has to be surveyed more carefully.

Hot gas cleaning also imply chemical manipulations of the product gas to meet environmental as well as technical standards. High molecular weight products, tars, and other components like alkali trace elements may cause in the condensed phase severe operational problems. These have to be removed before the gas product can qualify as fuel for gas engine or gas turbine purposes.

Within the so called JOULE II NON-NUCLEAR ENERGIES research framework several multi-partner projects have been drawn together embracing technical programs from a variety of R&D organizations, including industrial partners, from the current member states of the European Community. An unique opportunity is hereby given to establish expert networks designed to address key technical issues. Some of the networks are dealing with issues connected with particulate removal and emission control. A presentation of three projects working with biomass related hot gas cleanup is given below.

Current research projects in the EC Joule II Non-Nuclear Energy Program

- INTEGRATED HOT FUEL GAS CLEANING FOR ADVANCED COMBINED CYCLE PURPOSES (JOU2/CT93/0431) is a sub-project incorporated in a vast EC program project called CLEAN COAL TECHNOLOGY R&D. As the name implies, the project essentially deals with topics reflecting coal gasification and combustion. Likewise the sub-project is aimed to cover integrated gas cleanup issues in coal related advanced gasification systems. However, the need for fuel flexibility for such systems has been recognized and alternative solid fuels are considered and included in the studies.

The project organization and work, as for most EC project programs, is based on a close scientific and technical co-operation between the project partners organized in groups based on scientific areas. A typical project structure is shown in Figure 1. This project is one of the bigger projects within the Joule II program and the activities comprise a broad range of research tasks within hot gas cleaning. From techno-economic modeling studies via cycle control studies to fundamental and applied emission control investigations, the project has a total budget of close to 8 million ECU, an equivalent of 6 million USD. The grant from the European Commission is here about 3.5 million USD. The project is co-ordinated by CRE (Coal Research Establishment) in England.

- COMPARISONS OF ENTRAINED PHASE AND FLUIDIZED BED GASIFICATION OF BIOMASS WITH RESPECT

TO PROBLEMS RELATED TO FEEDING AND HOT GAS CLEANING (JOU2/CT93/0347) is another Joule II project focusing on integrated gas cleanup for advanced gasification systems. The project work is a co-operation between Coal Research Establishment (CRE) in the UK, Deutsche Montan Technologie (DMT) in Germany, and LIT in Sweden. The objective with the project is to collect end-user-oriented information for process development in advanced thermochemical conversion of biomass. Integrated pressurized hot gas cleansing units at DMT and LIT have been provided with different filters (filter types; materials) to find the most suitable filtering system for biomass gasification purposes. The project is co-ordinated by DMT and has a total budget of 1 million ECU (750.000 USD).

- ADVANCED AND INTEGRATED BIOMASS GASIFICATION WITH HOT AND CATALYTIC FLUE GAS CLEANING FOR ELECTRICITY PRODUCTION AND OTHER END PRODUCTS (JOU2/CT93/0399) is a project coordinated by the University of Madrid (Spain) dealing with catalytic reforming and optimization of the gas product. Specific focus is put upon catalytic methane steam reforming, hydrocracking, and the use of water-gas shift catalysis. Together with Danish Technical Institute (DTI) in Denmark cereal straw is converted in a fluidized bed gasifier with a down stream catalytic reformer. The total budget for a 36 months work period is 300.000 ECU (225.000 USD).

The above mentioned project are being carried out during 1994-96. Periodically, technical meetings as well as progress meetings are held through out the course of the projects to monitor and to assess the project progress. Apart from the Joule II program other EC sponsored research programs as well as various national research programs are undertaken within the individual countries in the European Community.

Project work at Lund Institute of Technology (LIT)

LIT takes part in two of the above mentioned projects with studies investigating the influence of different bed materials, the effect from biomass ash on the bed behavior in PCFB gasification of biomass, and hot gas particulate removal. The distribution of alkali species in the gasification products is additionally studied including an assessment for their reduction or removal [3].

Vapor-phase alkali metals (Na, K) may form condensed compounds in the temperature interval 400-550 °C. These alkali compounds are capable of drastically enhance hot corrosion on metallic surfaces in the process system, cementing deposited particulate, and support agglomeration tendencies of the bed material in a fluidized bed gasifier. Enhanced tendency for agglomerations in the bed, due to sticky layers of alkali condensations on the particle surfaces, has been found in systems utilizing biomass.

Specifically of interest is to what extent the alkali compounds in the fuel are converted into the gas phase and how to reduce the alkali concentration. At equilibrium the alkali content in the gas phase is strongly influenced by the temperature as well as by the pressure. At increasing pressures in the system the alkali content in the gas phase is reduced largely due to condensation mechanisms. The temperature in certain parts of the conversion system must be kept high enough to suppress such condensation mechanisms. Consequently, to reach efficient reduction this suggests that gas phase alkali capture must take place at temperatures above 600 °C that put distinct requirements on adequate on-line monitoring.

At LIT sorbents for hot gas alkali removal are studied and the efficiency of these sorbents are being evaluated. Routine on-line methods for monitoring alkali components directly in the hot gas phase are very scarcely reported in the literature. Current alkali measurements techniques are mainly based on batch sampling and laser spectroscopy, methods that both are being tested and evaluated within the Joule II program.

An instrument for plasma assisted alkali monitoring in the gas phase, developed by the University of Tampere (Finland), will be tested with the test rig at LIT. The method is based on optical spectroscopy of alkali metals heated by a thermal plasma at process temperature.

In addition, another novel device for on-line measuring of alkali metals in the gas phase will be used at LIT. The device and method, developed by Chalmers Technical University in Gothenburg

(Sweden), is suitable for determinations of trace alkali components in hot fuel gas. The technique is based on surface ionization of the alkali components and has been tested with pure alkali sources as well as with different biofuel with very encouraging results. Alkali concentrations in the range of 0.1 ppb to well above 1 ppm have been detected and measured. A setup was designed and constructed for the LIT test rig and preparation for measurement campaigns is presently in progress.

As a second main part of the EC project work at LIT, hot gas particulate removal is being studied in the LIT gasification test rig. The primary solid phase separation step is achieved by an internal axial cyclone that has shown a separation efficiency between 96-98% on a solid/gas phase ratio basis. A secondary step is performed by means of a single SiC-based candle filter with effluent gas dust concentration lower than 10 mg/Nm³. However, the operational time on the candle filter has so far been short to make adequate predictions regarding the suitability in biomass gasification.

Comparable filter test are additionally being carried out together with DMT in Germany where metallic filter are tested and evaluated for biomass gasification purposes. Advanced ceramic candle filters offer promising solutions and have good filtration efficiency but integrated in biomass gasification specific issues have to be covered before the technology can be fully accepted for biofuel based IGCC applications.

CONCLUSIONS

A growing interest in utilizing biomass and other so called alternative solid fuels is today seen among various countries in the European Community. Alternative solid fuels as a domestic resource for energy production is important not only for the energy supply but also for the potential benefits regarding the environment and rural and regional development[4].

Key issues in implementing the technology associated with sustainable biomass utilization for both power and heat production have been identified and are emphasized in different R&D programs sponsored by the European Commission. An important area is the integration of gas cleaning systems for IGCC and similar applications.

Dept. of Chem. Eng. II at LIT is involved in two so called Joule II research projects studying hot gas particulate removal and alkali reduction. In these studies particular interest is in hot gas solid phase separation including filtering systems suitable for biomass gasification processes. Additionally, research efforts have been made in investigating the effects from fuel alkali in the fluidized bed gasification process and studies including an assessment for the reduction or removal of alkali components in the gas phase. So far the preliminary results indicate that most of the alkali in the LIT test rig is adsorbed on the surface of the ash collected in the filter unit. Two individually developed systems for monitoring alkali species in hot fuel gas will be tested and evaluated.

REFERENCES.

1. A. Hallgren, I. Bjerle & L. Chambert, "PCFB Gasification of Biomass", paper presented and published in the proceedings to the 206th ACS National Meeting, Chicago, IL., Aug. 22-27, 1993
2. Minchner, A., "Integrated Hot Fuel Gas Cleaning for Advanced Gasification Combined Cycle Processes", project description Contract No. J0U2/CT93/0431, 1994.
3. A. Hallgren, "Hot Gas Particulate and Alkali Removal in PCFB Gasification of Biomass", paper presented and published in the proceedings to the AIAA 29th Intersociety Energy Conversion Engineering Conference, Monterey, August 7-11, 1994.
4. "Research and Technological Development Programme in the field of Non-Nuclear Energy (1990-1994) JOULE II; Project Synopses", European Commission, EUR 15893 EN, 1994.

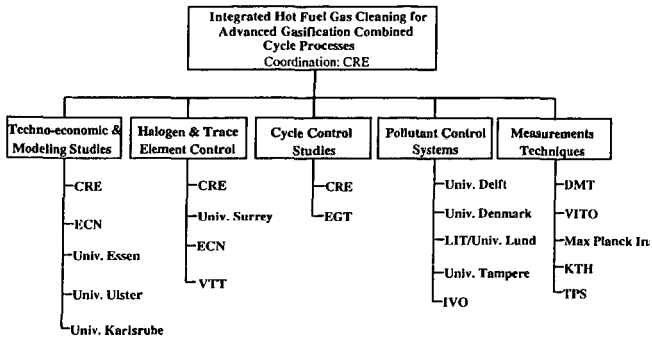


Figure 1. Project organization and activities

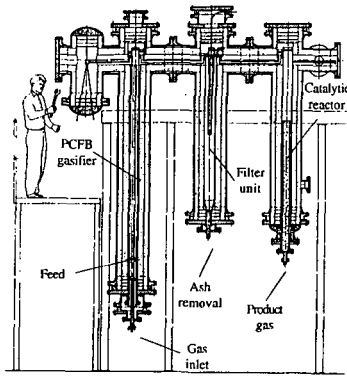


Figure 2. The PCFB biomass gasification test rig at LIT

**HIGH EFFICIENCY ELECTRICITY PRODUCTION IN THE
SUGAR INDUSTRY OF THE FUTURE:
THE PACIFIC INTERNATIONAL CENTER FOR HIGH TECHNOLOGY RESEARCH
PROJECT (>6 MW_e)**

Andrew R. Trenka
Pacific International Center for High Technology Research
2800 Woodlawn Drive • Honolulu, Hawaii 96822

Keywords: Sugarcane Bagasse, Electric Power, Gasification Demonstration

INTRODUCTION

The Pacific International Center for High Technology Research (PICHTR) is presently starting up a 100 tpd bagasse Renugas® gasifier which was developed under license from the Institute of Gas Technology (IGT).

For thousands of years, mankind has used biomass for energy, burning it first in campfires. In more modern times, combustion boiler systems were developed such as those fueled by coal. Through inefficient, these systems answered an increasing need for energy brought on by the industrial revolution. Yesterday's systems are being replaced with more efficient methods of energy conversion and extraction. Recognizing the untapped potential for biomass power to provide clean and efficient energy, the U.S. Department of Energy established the National Biomass Power Program in 1991. The State of Hawaii Department of Business, Economic Development & Tourism is collaborating in this national program to complement the development of its own sustainable resource program. As a key player in this program, PICHTR will design, construct, and operate a biomass gasification facility that will be the centerpiece of the nation's biomass gasification technology.

Current Power Generation by the Sugar Industry in Hawaii

Worldwide, the sugarcane industry has the potential to be a major generator of electric power for the electricity grid through the use of the by-product of sugarcane processing called bagasse as a fuel source. Initially, bagasse was used as a fuel solely for the evaporation of water in order to concentrate the sugar, since animal or hydropower was originally used to crush the cane. In time, the benefits of using steam power for in-plant power needs resulted in increased use of these by-products in energy production. The history of the industry in Hawaii was that although¹ some export of electricity to communities took place in the industry prior to 1970, the really major growth in generating capacity took place in the 1970s as the sugar industry consolidated its low pressure boilers into higher pressure units to produce more electricity. The passage of the 1978 Federal Public Utilities Regulatory Policies Act (PURPA) further stimulated the use of bagasse to the point where, in 1991, the industry burning bagasse in conjunction with fossil fuels supplied about 5.5% of the grid electricity. The generation in that year² was 495 TWh, down from a high of 681 TWh in 1988. Further, Biomass energy in Hawaii was provided in the form of energy recovered from the H-power plant in Honolulu, an ultra-modern Waste-to-Energy plant recovering steam and electricity from municipal waste generated on Oahu.

Global Sugarcane Power Potentials

The sugar industry worldwide offers the potential to produce about 500 TWh of electricity for export if significant energy-efficient gains could be made internally to the process of sugar production and advanced power generation technology was to be adopted along with increased residue collection from sugarcane growing³. To reach this output would require a power generation rate of 450-600 kWh/tc where tc is a tonne of cane processed. Table 1 shows the world cane production statistics from two viewpoints, the geographic area, and the development status. It can be seen that the majority of the sugarcane production is in developing countries.

¹ C.M. Kinoshita. *Cogeneration in the Hawaiian Sugar Industry*, Bioresource Technology. 35(3). pp 231-237. 1991

² DBEDT. *The State of Hawaii Data Book 1992*. A Statistical Abstract. Table 476, 477

³ R.H. Williams, and E.D. Larson. *Advanced Gasification based Biomass Power Generation in* Eds. T.B. Johansson, H. Kelly, A.K.N. Reddy, and R.H. Williams. *Renewable Energy: Sources for Fuels and Electricity*. Chapter 17, pp 729-785, Island Press: Washington, D.C. 1993

The current average rate of power generation from sugarcane in most developing countries is much less than 500 kWh/ton cane processed (tc)—typically less than 10 kWh/tc. Average values range from 15 to 25 kWh/tc in plants that do not require any fossil fuel input. This is barely sufficient to meet the internal needs of these sugarmills. Traditionally, the industry need has been for only sufficient electric power to meet the in-plant or factory demand, with the steam exhaust in balance with the thermal energy requirements. Essentially, the boilers are operated as a bagasse disposal unit since there is a need to maintain an equilibrium between bagasse production and utilization.

Additionally, the sugarcane industry does not normally operate on a year round basis—the cane harvesting and processing season in Hawaii can be quite long at 200 days, but in many places the season is less than 150 days. It is only when there is an incentive to sell power to the grid that the sugar industry can undertake the necessary investments in higher pressure steam boilers and turbogenerators along with energy efficiency improvements. In the Hawaiian industry (footnote 1) low pressure boilers were systematically replaced by higher pressure boiler systems of larger capacity in the period 1960 through 1980, with the average steam pressure and temperature increasing from 1.3 MPa and 210°C to 4.4 MPa and 380°C. Meanwhile, the net steam consumption in the mills decreased significantly from 600 kg/tc to about 300–400 kg/tc; resulting in a power output of about 60 kWh/tc on average, with the best mills reaching over 100 kWh/tc. The thermal efficiency to generate electricity is approximately 15%–20% in such combined heat and power arrangements. Increasing the power to heat ratio will require advanced technologies—such as the use of integrated gasification combined cycles (IGCC). The estimated steam that would be available from an IGCC is only 275 kg/tc and necessitate severe energy efficiency improvements in the sugar production process but would increase the electricity output in the sugarcane season to about 600 kWh/tc. For this to be produced on a year round basis would require additional fuels such as the tops and leaves from the sugarcane harvest (called *Barbojo* in Spanish-speaking countries) other Biomass fuels including wood and wastes or additional fossil fuel input.

PICHTR's development of the Renugas® gasifier is targeted towards this global market, as well as the needs of Hawaii. Recent studies of the profitability of using sugarcane and energy cane crops to increase the power output to the grid have shown that increasing both the power output and the power to heat ratio of the Pioneer Mill on the island of Maui will lead to a rate of return of 30% under a set of selling price assumptions that include sale of electricity at 5 c/kWh. A typical steam plant under the same conditions would not be profitable⁴. The typical performance and economic improvement according to NREL is given in Table 2.

The PICHTR Gasifier

The U.S. Department of Energy (DOE) and the State of Hawaii joined with PICHTR in this cost-shared cooperative project, with the objective of scaling up the process development unit (PDU) of IGT Renugas® pressurized air/oxygen gasifier to a 45–90 ton/day engineering development unit (EDU) operating at 1–2 MPa using bagasse and wood as feed. Other participants in the project are IGT, the Hawaii Natural Energy Institute (HNEI), the Hawaii Commercial and Sugar Company (HC&S), and the Ralph M. Parsons Company, the architectural and engineering firm for the project. The site is the HC&S sugar mill at Paia, Maui, Hawaii. The National Renewable Energy Laboratory is providing project oversight in addition to systems analysis.

The scaleup will be completed in several stages, as shown in Figure 1.

The first phase, which is now being commissioned, consists of the design, construction, and preliminary operation of the gasifier to generate hot, unprocessed gas. The gasifier is designed to operate with either air or oxygen at pressures up to 2.2 MPa, at typical operating temperature of 850°–900°C. In Phase 1, the gasifier will be operated for about four months at a feed rate of 45 ton/day at a maximum pressure of 1 MPa. Following the end of Phase 1 in late 1995, a hot-gas cleanup unit will be added and operated for a planned period of about 500 hours to generate design data and experience with third generation ceramic candle filters. In late 1997, a gas turbine will be added to the system

to generate 3 to 5MW of electricity. In this phase, the gasifier feed rate will be 90 ton/day, and the system will operate at pressures up to 2.2 MPa. In a projected but not yet funded Phase 3, the system will be operated in an oxygen-blown mode to produce a clean syngas for methanol synthesis in addition to producing electricity. Discussions are underway with interested commercial partners which could focus on a 1-2 MW power producing system.

A key element of the development in Hawaii will be to prove the suitability of ceramic barrier filters in gas turbine applications. PICHTR is working with Westinghouse, IGT, Gilbert Commonwealth, and the National Renewable Energy Laboratory to demonstrate this technology and have just completed short duration testing of a hot gas cleanup train on the Renugas® pressurized air-blown fluidized bed gasifier at IGT in Chicago. The tests in Chicago demonstrated that ceramic barrier filtration technology is effective in this application; however, the first generation ceramic filters used will not have a sufficiently long service life at the severity projected in this application. More advanced and more stable filters are now available for the following on testing at the BGF.

The project in Hawaii will establish the operational experience and broad data base needed to demonstrate full scale viability of the technology.

⁴ PICHTR Sustainable Biomass Energy Program, NREL LOI—Maui Project. Draft Report dated May 1995

Table 1. Sugarcane Production Statistics

WORLD CANE PRODUCTION

Source FAO—Agristat database 1990
Data in 1,000 tonnes (kt)

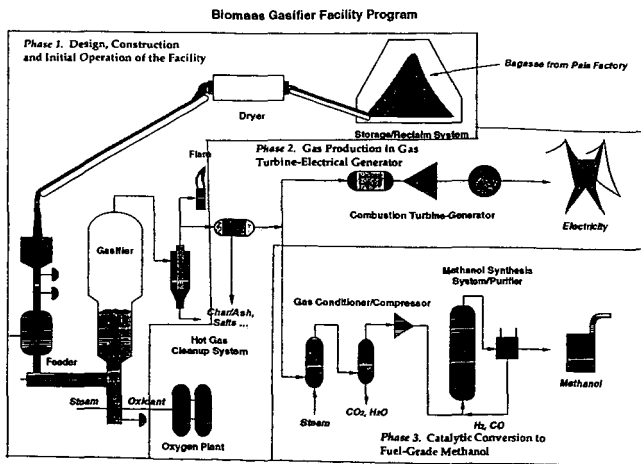
BY DEVELOPMENT CLASS		GEOGRAPHICAL DISTRIBUTION		
World	1,035,096			
Developed	72,193			
North America		24,575	N&C America	173,278
Europe		256	USA	24,576
Oceania		26,226	South America	332,016
Other		21,135	Africa	72,982
Developing	962,903		Asia	426,006
Africa		38,839	Europe	256
Latin America		480,718	Oceania	30,559
Near East		17,316		
Far East		421,698		
Other		433		
Least Developed		25,021		

Table 2. Comparison of Present Day Steam Generation With IGCC⁵

COST FACTORS (¢/kWh)	STEAM GENERATION	IGCC
Operations and Maintenance	0.5	0.5
Fuel Only Cost	3.6	1.6
Capital Recovery	4.2	3.0-3.5
Cost of Electricity	8.3	5.1-5.6

Notes to Table 2. Assuming a marginal cost of fuel of \$2/million Btu (or approximately \$40/tonne of dry Biomass), a load factor of 85% (base loaded), and a return on capital invested of 8%/year, it is possible to see the effect of the new technology. Both plants are approximately 50 MW_e capacity. The efficiency of the steam plant is about 20%, while the IGCC is estimated to have an efficiency of 45%. The capital cost of the steam plant is \$1.8/W, while that of the IGCC is expected to be in the range of \$1.3 to \$1.5/W.

Fig. 1



⁵ Table generated from systems studies by Kevin Craig and R.P. Overend, NREL

NUMERICAL MODELING OF A DEEP, FIXED BED COMBUSTOR

Kenneth M. Bryden, M.S., Graduate Student; and Kenneth W. Ragland, Ph.D., Professor
Department of Mechanical Engineering
University of Wisconsin - Madison
Madison, WI 53706 USA

Keywords: Computational Modeling, Biomass Combustion, Whole-Tree-Energy

INTRODUCTION

A steam power plant utilizing whole trees as the renewable fuel (Whole-Tree-Energy™) is being developed by Energy Performances Systems, Inc. of Minneapolis, MN [1]. Hardwood trees are grown and harvested on energy plantations, or harvested from inferior, over-aged standing trees, transported in trucks as whole trees, and stored in a large covered stack at the power plant site where the stack is dried with waste heat from the power plant. When dried to the desired moisture content, the whole trees are burned in a fixed bed boiler. This innovative system completed stacking, drying and combustion tests at a site near Aurora, MN in August, 1992 [2].

The advantages of the proposed system are 1) time, energy and processing costs are saved by not chipping the wood, 2) a 30 day supply of wood may be stored on site without degradation of the fuel, and 3) the combustion heat release per unit plan area is greater than with wood chips. The concept is envisioned for 25 MW to 400 MW Rankine cycle power plants.

In the WTE combustor a ram feeder located 6 m above a fixed grate injects batches of trees trimmed to 8 m in length (for a 100 MW plant) with trunks up to 20 cm in diameter. The fuel feed rate is set to maintain a fuel bed 3 to 5 m deep on a grate. Preheated air is blown upwards through the fuel bed such that the lower section of the bed has an oxidizing environment and the upper part of the fuel bed has a reducing environment. Combustion is completed by means of overbed air jets.

Tree sections are fed onto the top of a deep, fixed bed of reacting wood. These sections are dried further and pyrolyzed forming a char layer on the outside of the log. Pyrolysis products and moisture flow outward through the char layer. Typically the oxygen flux will be zero in the upper part of the bed, and the char will react with the carbon dioxide and water vapor. The surface of the char will be heated by the gaseous products and cooled by the reducing reactions of carbon dioxide and water vapor with the char. As the fuel moves downward in the bed, the char layer will grow in thickness as the inner core of the undisturbed wood is pyrolyzed more rapidly than the outer char surface is consumed. In the lower portion of the bed oxygen becomes available to react with the pyrolysis products. When the log is completely dried and pyrolyzed in the lowest portion of the bed the oxygen reacts directly with the char and the char is consumed rapidly, causing the entire bed to move downward. The overall bed heat release rate depends on the heat and mass transfer to the logs, the formation of the char layer, the reaction rate of the char with oxygen, carbon dioxide, and water vapor, and the nature and rate of reaction of the pyrolysis products.

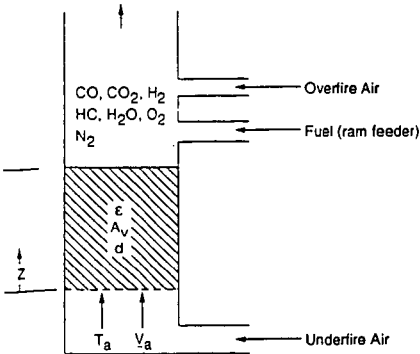


Fig. 1. Schematic of deep bed combustor.

DESCRIPTION OF THE MODEL

The model is a one-dimensional, steady state model for a top feed, updraft, packed bed combustor (Fig 1). It is assumed that the walls are adiabatic. The char reaction is assumed to be the rate limiting step and sets the pyrolysis rate [4]. An initial log diameter and a constant void fraction are used to characterize the pile, and the logs are assumed to be oriented across the gas flow. The surface area to volume ratio of the fuel is determined at each distance step in the bed as a function of diameter. As the log shrinks due to reaction with oxygen, carbon dioxide, and water vapor; moisture and wood volatiles are released

Table 1. Chemical Reactions Used in the Model.

Reaction #	Chemical Reaction	Heat of Reaction (kJ/kg)
1	$2 C + O_2 \rightarrow 2 CO$	9,211
2	$2 CO + O_2 \rightarrow 2 CO_2$	10,107
3	$C + CO_2 \rightarrow 2 CO$	-14,372
4	$C + H_2O \rightarrow H_2 + CO$	-14,609
5	$CH_{0.152}O_{0.028} + 0.867 O_2 \rightarrow 0.761 H_2O + CO$	17,473
6	$2 H_2 + O_2 \rightarrow 2 H_2O$	142,919

from the wood. For dry wood the ratio of wood consumed to char consumed is initially high at the top of the bed as the wood is rapidly pyrolyzed in the furnace environment and decreases as the diameter shrinks. When a 3 cm diameter is reached, the fuel remaining is assumed to be all char. The ratio is set based on data from the single log combustion tests performed in a specially designed furnace under conditions related to the WTE system [3]. The model solves the equations of conservation of mass and energy for the solid, conservation of mass and energy for the gas, and conservation of gas phase species. Seven gas phase species are considered; oxygen, nitrogen, hydrogen, water vapor, carbon dioxide, carbon monoxide, and nitrogen.

The gaseous species conservation equations in differential form are,

$$\frac{d(G_i)}{dz} = r_i \quad [1]$$

where G_i and r_i are the mass flux per unit area and chemical reaction rate per unit volume of species i , respectively, and z is the height of the combustor. The chemical reaction rate for each gaseous species is formed from the reactions shown in Table 1 as follows:

$$r_i = \sum_{j=1}^{N_r} b_{i,j} \dot{w}_j + y_i r_{wood} \quad [2]$$

where $b_{i,j}$ is the stoichiometric yield of species i in reaction j on a mass basis, \dot{w}_j is the rate of reaction j , y_i is the mass fraction yield of species i due to the pyrolysis of wood (Table 2), and N_r is the number of reactions ($N_r = 6$). The reaction rates include both chemical kinetics and diffusion. The consumption rate of char is

$$r_{char} = h_{char,1} \dot{w}_1 + h_{char,3} \dot{w}_3 + h_{char,4} \dot{w}_4 \quad [3]$$

The reaction rate of wood is

$$r_{wood} = r_{char} K_{wood} \quad [4]$$

where K_{wood} is the ratio of wood consumed to char consumed.

The mass flux of the gas is

$$G_g = \sum_{i=1}^{N_s} G_i \quad [5]$$

where N_s is the number species. Conservation of mass for the solid is

$$(1 - \epsilon) \rho_s \frac{dV_s}{dz} = r_s \quad [6]$$

where ϵ is the void fraction of the bed, ρ_s is the density of the solid, r_s is the net reaction rate per unit volume of the solid, and V_s is the downward solid velocity.

Conservation of energy for the gas is,

$$\frac{d(G_g h_g)}{dz} = \sum_{j=1}^{N_r} \Delta H_j \dot{w}_j - y_{H_2O} r_{wood} \quad (7)$$

where h_g is the enthalpy of the mixture and ΔH_j is the heat of reaction for reaction j . Conservation of energy for the solid is based on a surface energy balance,

$$A_s h_{conv} (T_s - T_g) = \Delta H_1 \dot{w}_1 + \Delta H_3 \dot{w}_3 + \Delta H_4 \dot{w}_4 + \dot{m}_r h_r - \dot{m}_p h_p \quad [8]$$

where h_{conv} is the convective heat transfer coefficient, A_s is the char surface area per unit bed volume, h_r is the enthalpy of the reactants, and h_p is the enthalpy of the products including pyrolysis products. The convective heat transfer coefficient is obtained from a correlation for non-reacting beds [5] with a screening factor to account for mass transfer [6].

Table 2. Mass Fraction Yield of pyrolysis products of dry, ash free wood [7].

char	0.200
water	0.250
hydrocarbons	0.247
carbon monoxide	0.183
carbon dioxide	0.115
hydrogen	0.050

The boundary conditions for the inlet air velocity, temperature, and the gas composition are specified at the grate ($z = 0$). The solid velocity of the fuel at the grate is zero. Log size and as-received moisture content are specified at the top of the bed. Eqs. 1 through 8 are solved by using a differential-algebraic implicit solver.

VALIDATION OF THE WTE COMBUSTOR/GASIFIER MODEL

Combustion tests were run at Aurora, MN in August 1992 using a 1.4 m by 2.6 m by 3.7 m deep bed of hardwood logs with an average top size of 20 cm and an average as-received moisture content of 31.6%. The fuel was supported by cooled steel tubes 6.4 cm diameter on 22 cm centers. The underfire air was preheated to approximately 275°C and the average air flow rate was 565 kg/min, which gave an inlet velocity under the bed of 3.8 m/s to 4.1 m/s. The average wood burning rate during the 2 hr test was 162 kg/min, and the average burning rate per plan area was 2670 kg/hr-m². The heat release rate per unit plan area was 10.1 MW/m², and the peak was 12.9 MW/m². These heat release rates are high compared to a coal-fired spreader-stoker because of the deep fuel bed and the high inlet air velocity.

The simulation model was run for the above conditions assuming a representative fuel size of

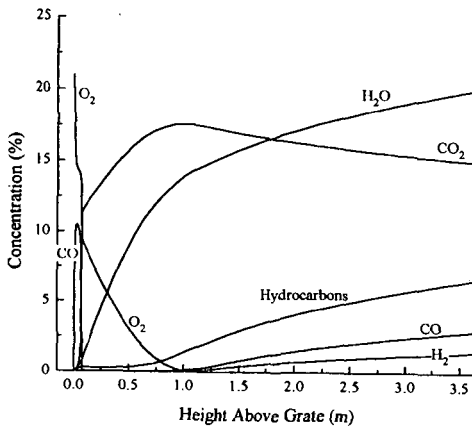


Fig. 2. Gas species concentration vs. height above grate. Inlet air preheat of 400°C, fuel moisture content of 23%, underfire inlet air velocity of 3.7 m/s, and bed height of 3.7 m.

17.8 cm, a bed void fraction of 0.60, inlet air temperature of 260°C, and an inlet air velocity of 3.95 m/s. The lowest portion of the fuel bed consists of small diameter char where the oxygen is rapidly consumed and the temperature rises rapidly. Above the oxidizing region is an extended reducing region where the logs slowly are dried and pyrolyzed and the char layer reacts with carbon dioxide and water vapor. The predicted burning rate per unit area for these conditions and assumptions is 2960 kg/hr-m², which compares well with the measured burning rate of 2670 kg/hr-m². Assuming a higher heating value of 19.1 MJ/kg for dried wood, the corresponding heat release rate is 10.7 MW/m², which is within 6% of the Aurora test.

SIMULATED PERFORMANCE OF THE WTE COMBUSTOR/GASIFIER

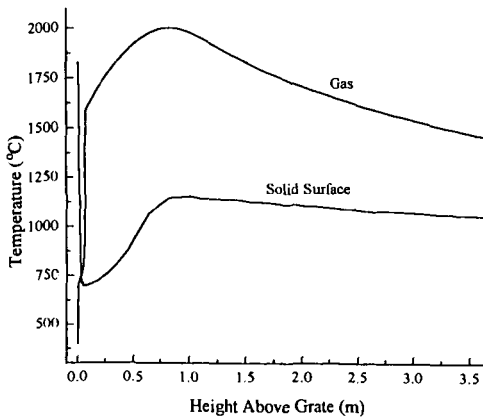


Fig. 3. Solid surface and gas temperature vs. height above grate. Inlet air preheat of 400°C, fuel moisture content of 23%, underfire inlet air velocity of 3.7 m/s, and bed height of 3.7 m/s.

The proposed design conditions for the combustor/gasifier for a 100 MWe WTE power plant specify a 4.3 m by 8.5 m by 3.7 m deep fuel bed of hardwood logs with an average top size of 20 cm diameter with 23% as-received moisture, and 400°C inlet air temperature. Keeping all the other model parameters the same as the validation run above, the predicted heat release rate is 9.5 MW/m² with an inlet air velocity of 3.2 m/s. Overfire air is needed to complete combustion, and the predicted overfire air to underfire air ratio is 0.85. The predicted gaseous species profiles in the fuel bed for the design case with an inlet air velocity of 3.7 m/s are shown in Fig. 2. The first 25% of

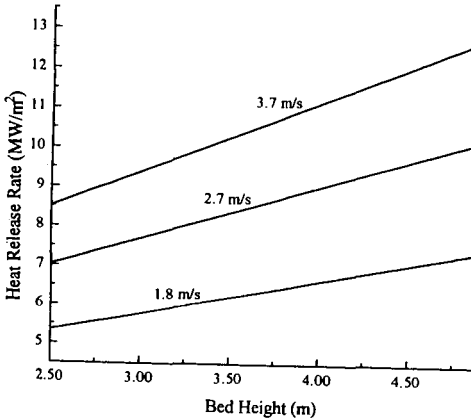


Fig. 4. Heat release rate vs. bed height and underfire air velocity. Inlet air preheat of 400°C and fuel moisture content of 23%.

fuel, the surface temperature is reduced rapidly, but then rises further above the grate due to heat transfer from the gaseous combustion products. At about 1 m above the grate the oxygen is consumed and the char reducing reactions gradually decrease the temperatures. The gas velocity at the top of the bed, prior to the overfire air, is 12.5 m/s when the inlet air is 3.2 m/s.

Several different options are available to the designer and operator to meet the goal of producing a given heat release rate to meet a given load. The underfire inlet air velocity may be changed by changing the air flow rate. The underfire air temperature may be changed by adjusting the air preheat. The fuel bed height may be increased or decreased by adjusting the fuel feed rate, and the fuel moisture content may be changed by adjusting the drying time. The impact of these is as follows:

1. Increasing the underfire air velocity causes a higher burning rate as the oxygen penetrates further into the bed. This consumes more char increasing the overall temperature, increasing the heat transfer to the fuel. This in turn increases the drying and pyrolysis of the fuel. However, excessive air velocity will cause higher pressure drop across the bed, more carry-over of partially burned fuel particles, and possible tube erosion. The predicted combined effect of increasing the inlet air flow and the bed height on the heat release rate is shown in Fig. 4.
2. Increasing the bed height lengthens the gasification zone and also increases the heat release rate, provided more overfire air is used.
3. Increasing the underfire air preheat decreases the fuel burning rate for a fixed underfire

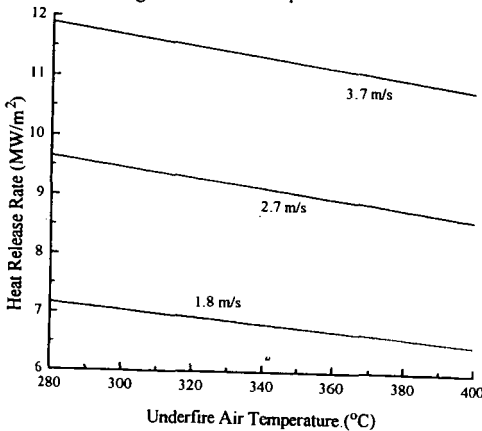


Fig. 5. Heat release rate vs. underfire air temperature and underfire air velocity. Bed height of 3.7 m and fuel moisture of 23%.

the bed (~1 m) is an oxidizing region in which the oxygen is completely consumed. The upper 75% of the bed is a reducing region in which the char-carbon dioxide and char-water vapor reactions dominate. The hydrocarbons, carbon monoxide, and hydrogen that are formed in reducing region, are burnt out in the overfire air region. The fuel is pyrolyzing in the upper 98% of the bed and pure char exists only in the lowest 2% of the bed. The predicted gas and solid surface temperatures are shown in Fig. 3. The solid surface temperature just above the grate is high because the high oxygen concentration is reacting with pure char. As the char surface reaction decreases and as the volatiles and moisture escape through the surface of the

air velocity, because less air mass flow is delivered to the fuel bed (Fig. 5). Although the chemical reaction rates tend to be increased by increased temperature, the reactions in the bed are more limited by mass transfer than kinetics.

4. Increasing the fuel moisture content decreases the pyrolysis rate because the temperatures are lowered, thus lowering the heat release rate, all else remaining constant (Fig. 6).

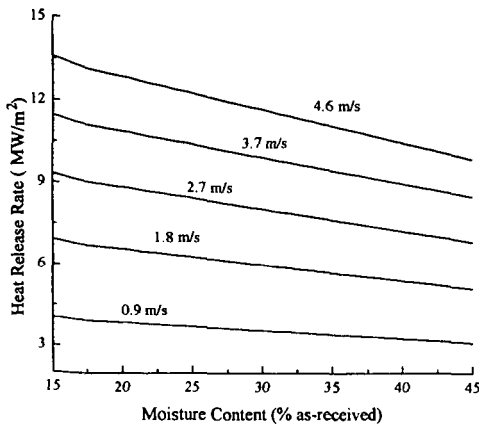


Fig. 6. Heat release rate vs. fuel moisture content and underfire air velocity. Inlet air preheat of 400°C and bed height of 3.7 m.

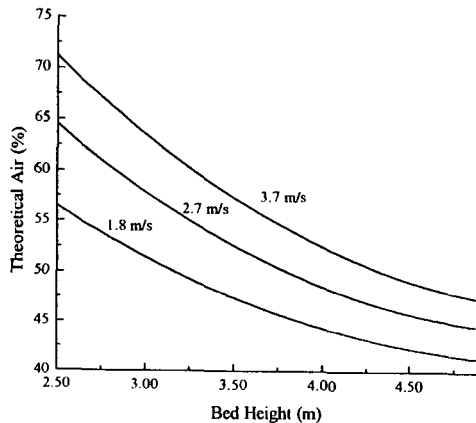


Fig. 7. % theoretical air vs. bed height and underfire air velocity. Inlet air preheat of 400°C and fuel moisture content of 23%.

The theoretical air required for complete combustion varies primarily with bed height and underfire inlet air velocity (Fig. 7). As the bed height is increased, more fuel is gasified, but a limit is reached because the gas temperature drops too low to support the reduction reactions and the carbon dioxide is consumed.

CONCLUSIONS

A computational model for the WTE combustor has been developed and adjusted to within 6% of heat output of 10.1 MW/m² of the Aurora, MN test run. The deep, fixed bed combustor obtains high energy release rates due to the high air velocity and extended reaction zone. The lowest portion of the bed is an oxidizing region and the remainder of the bed acts as a gasification and drying zone. For the 100 MW design case with 23% fuel moisture, inlet air preheat of 400°C, and underfire air inlet velocity of 3.2 m/s; the predicted heat output per unit bed area is 9.5 MW/m². The heat output of the combustor/gasifier can be changed by altering the underfire air flow rate, the bed height, the air preheat, and the fuel moisture.

ACKNOWLEDGMENTS

under contract RP3407-07 and directed by Evan Hughes, EPRI project manager.

This work is funded by the Electric Power Research Institute

REFERENCES

1. Lamarre, L., "Electricity from Whole Trees," *EPRI Journal*, 19(1):16-24 (1994).
2. Schaller, B. J., L. D. Ostlie, and R. E. Sundberg, "Program to Test Key Elements of the WTE™," EPRI Report TR-101564 (1993).
3. Bryden, K. M. and K. W. Ragland, "Burning Rate of Single Logs in a Controlled Convective Environment," Unpublished Paper (1995).
4. Ragland, K. W., J. C. Boerger, and A. J. Baker, "A Model of Chunkwood Combustion," *Forest Products Journal*, 38(2):27-32 (1988).
5. Wakao, N. and S. Kaguci, *Heat and Mass Transfer in Packed Beds*, Gordon and Breach, p. 292 (1982).
6. Kays, W. M. and M. E. Crawford, *Convective Heat and Mass Transfer*, McGraw-Hill, Third Ed., p. 507 (1993).
7. Ragland, K. W., D. Aertz, and A. J. Baker, "Properties of Wood for Combustion Analysis," *Biosource Technology*, 37:161-168 (1991).

MATHEMATICAL MODELLING OF STRAW BALE COMBUSTION IN CIGAR-BURNERS

Niels Bech
Department of Combustion Research
Risø National Laboratory
DK-4000 Roskilde
Denmark

Lars Germann
Danish Technological Institute
Teknologiparken
DK-8000 Århus C
Denmark

Lars Wolff
I/S VESTKRAFT
Vestkraftkaj 2
DK-6701 Esbjerg
Denmark

Keywords: Combustion, Mathematical Modelling, Straw

ABSTRACT

This paper describes a computer model for the calculation of the steady and non-steady behaviour of straw bales subject to surface combustion in cigar burners. The mathematical formulation is one-dimensional and the flow of gas through the straw bales is described by means of Darcy's law for flow through a porous medium. The computer model is able to predict flow rate, temperature and composition of gas and straw as function of axial length and time. Calculated results are compared to measurements of temperature- and gas composition profiles within the burning straw bales. It is observed that the straw bale temperatures as well as the outlet gas composition are predicted reasonably well. Calculations have been carried out in order to assess the implication of a straw bale feed stop in a 3 MW district heating plant fueled with Heston straw bales. The results indicate serious disturbances in the performance of the burner.

INTRODUCTION

A computer model, STRAW, has been developed for the calculation of the steady and non-steady behaviour of surface combusting straw bales¹. Paralleling the theoretical efforts experiments have been carried out with the purpose of measuring temperature and concentration profiles within the burning straw bales as well as in the furnace room²⁻³. The measurement have been used in the validation of STRAW.

The principle of surface combustion of straw bales is illustrated in figure 1 after Gundtoft⁴. The straw bales are fed from the left at a rate corresponding to the combustion rate in such a way that the burning bale front remains at a fixed position. The figure shows the different process areas. Due to diffusion and subsequent condensation of water vapour a zone of straw with a water content higher than that of raw straw may appear. As the temperature rises the straw is dried and after that it undergoes pyrolysis. The required heat is transported from the burning surface through thermal conduction and radiation. When the devolatilization of the straw is finished straw char remains. The burning of the char finally results in a layer of ash or slag. Primary air is injected for the combustion at the straw surface, while oxygen for the combustion in the furnace room of the remaining gases is provided by a secondary air stream.

THE COMPUTER MODEL STRAW

For a more detailed description of the mathematical model conf. reference 1.

Assumptions. The following assumptions are made:

1. The system is one-dimensional in space.
2. The cross sectional area of the straw bales is constant.
3. The gas is described as an ideal gas.
4. The flow of gas through the straw grid is described by means of Darcy's law for flow through a porous medium.

5. The velocity of the straw grid is constant in the axial direction (but not in time).
6. The porosity and the permeability of the straw grid depends upon time and the location in the bale.
7. Only water vapour diffusion is considered at the moment.
8. Straw-gas and gas-gas thermal radiation is neglected in the straw bales.

Basic Equations.

Mass conservation for component no. i in the gas phase:

$$\frac{\partial m_g^i}{\partial t} + \frac{\partial (m_g^i u_g)}{\partial x} = \Gamma^i + S_g^i \quad (1)$$

Mass conservation for component no. i in the straw:

$$\frac{\partial m_h^i}{\partial t} + u_h \times \frac{\partial m_h^i}{\partial x} = -\Gamma^i - S_h^i \quad (2)$$

Energy equation for the gas phase:

$$\frac{\partial e_g}{\partial t} + \frac{\partial (e_g u_g)}{\partial x} = Q_g + \sum_i (\Gamma^i h_p^i + S_{in_j}^i h_{in_j}^i) \quad (3)$$

Energy equation for the straw:

$$\frac{\partial e_h}{\partial t} + u_h \times \frac{\partial e_h}{\partial x} = Q_h - \sum_i \Gamma^i h_p^i + \frac{\partial}{\partial x} \left(\lambda_h^* \frac{\partial T_h}{\partial x} \right) \quad (4)$$

Momentum for the gas phase (Darcy's law):

$$u_g = u_h - \frac{K}{\mu_g} \left(\frac{dp}{dx} + g \cos \Theta \rho_g \right) \quad (5)$$

Symbols:

g	Acceleration of gravity [m/s ²]
K	Permeability of straw grid [m ²]
p	Gas pressure [Pa]
Q	Heat production per unit volume [W/m ³]
S	Mass source/sink [kg/m ³ /s]
T	Temperature [C]
u	Velocity [m/s]
Γ	Transfer of mass from straw grid to the gas phase per unit volume and time [kg/s/m ³]
h	Enthalpy [J/kg]
λ^*	Effective thermal "conductivity" of straw grid which takes into account heat conduction as well as thermal radiation [W/m/C]
μ	Dynamic viscosity of gas [kg/m/s]
ρ	Density of gas [kg/m ³]
Θ	Angle between x-axes and vertical [degrees]

EXPERIMENTAL DESIGN

A test facility for burning straw bales has been constructed (see fig. 2). It is capable of burning straw packed in small bales of 10-12 kg each by means of surface combustion, i.e. the bale is not torn up, but is burnt from one end to the other. Primary air is being injected directly to the straw surface by means of air nozzles. The remaining part of the air is being added in the main duct, giving an excess air ratio of about 1.7. Directly in front of the straw surface is an electrically heated zone giving a heat flux to the straw, and thereby illuding a combustion chamber with hot walls. By means of probes inside the straw bale, measurements of temperatures and gas concentrations during the whole combustion process have been performed. For a more detailed description see references 2 and 3.

COMPARISON TO MEASUREMENTS

Straw bales constitute a very inhomogeneous fuel. Fig. 3 shows measured temperatures for four "near identical" experiments. The calculated temperatures are shown as well. The burning straw bale surface is located where the temperature reaches its first maximum around 1000 centigrade (around $x = 230$ mm in the figure). It is seen that the rise in straw bale temperature close to the burning surface as well as the temperature at the surface are predicted reasonably well.

The measured concentrations at the burning surface shown in table 1 are averages for the four experiments. It is seen that the gas concentrations of CO_2 , CO and C_xH_y are also predicted reasonably well although the amount of C_xH_y is slightly underestimated. The gas composition inside the straw bale close to the burning surface (which is not shown here) is not predicted well enough. This is believed to be due to the fact that the model does not account for turbulent diffusion of the gas phase components. In the calculation it has been assumed that 80 % of the primary air is available for combustion at the straw bale surface.

CALCULATED FEED STOP IN CIGAR BURNER

One event which is known to cause problems in a cigar burner in terms of a deterioration of the combustion and increased pollution is the stop in the straw bale feeding which occurs in some plants in connection with the delivery of a new straw bale. Calculations have been carried out in order to assess the implication of a straw bale feed stop in a 3 MW district heating plant fueled with Heston straw bales.

The straw bale feed and air injection are interrupted for 60 seconds and then continued from $t = 75$ sec. at the previous rates. In fig. 4 are shown the inlet and exit mass flow rate of straw carbon W_{in}^C and W_{hex}^C respectively. The amount fed at the inlet drops to nil after 15 sec. and increases to the initial rate at 75 sec. The exit value is zero initially at the normal operating conditions. This means that all the straw carbon is burned at the straw surface. It is seen however, that when the feeding starts again at $t = 75$ sec then W_{hex}^C becomes positive for a short period of time (≈ 5 sec). In other words, unburned straw carbon falls into the combustion chamber when the straw feeding is restarted. The reason is that the temperature at the straw surface drops about 200 degrees during the feed stop, conf. fig. 5.

SUMMARY AND CONCLUSIONS

A computer model, STRAW, has been developed for the calculation of the steady and non-steady behaviour of surface combusting straw bales. Model predictions have been compared to measurements of temperature- and gas composition profiles within the burning straw bales and calculations have been carried out in order to assess the implication of a straw bale feed stop in a 3 MW district heating plant fueled with Heston straw bales.

Comparisons between calculated and measured results show that:

- The rise in straw bale temperature close to the burning surface as well as the temperature at the surface are predicted reasonably well.
- The concentrations of CO_2 , CO and C_xH_y in the exit gas are also predicted reasonably well although the amount of C_xH_y is slightly underestimated.
- The gas composition inside the straw bales close to the burning surface is not predicted well enough probably because the model does not account for turbulent diffusion of the gas phase components.

It has been shown that an interruption of the feed for 60 sec causes violent disturbances in the computed performance of the burner. Unburned straw carbon is pushed into the combustion chamber when the straw feeding is restarted. In order to maintain good burner performance it is essential to avoid this behavior. This can be done by introducing a continuous feeding system which maintains the straw bale feeding rate at the operating value.

ACKNOWLEDGEMENTS

The work which has been supported by the Danish Ministry of Energy's energy research programme EFP-92 has been carried out in cooperation with the Department of Energy Technology at the Danish Technological Institute in Aarhus and Vølund R & D Center in Kolding.

REFERENCES

1. Bech, N. "Modelling of the Vølund Cigar Burner by means of the Computer Model STRAW", Risø-R-817, Risø National Laboratory, Roskilde, Denmark, 1995.
2. Wolff, L. "Forsøgstopstilling til forbrænding af halmballer ('Pyrolyseforsøg)", Risø-R-721 (DA) Forskningscenter Risø, december 1993.
3. Wolff, L. and Bech, N. "Surface combustion of straw bales, a test facility for pyrolysis investigations", 8th European Conference on Biomass for Energy, Environment, Agriculture and Industry, Vienna, 3-5 October, 1994.
4. Gundtoft, S. "Forbrænding af halm i mindre anlæg", Jysk Teknologisk, august 1989.

	O ₂	CO ₂	CO	C _x H _y
Measured	0.04	0.14	0.14	0.015
Calculated	0.04	0.15	0.14	0.011

Table 1: Comparison of measured and calculated concentrations in the gas at the burning straw bale surface

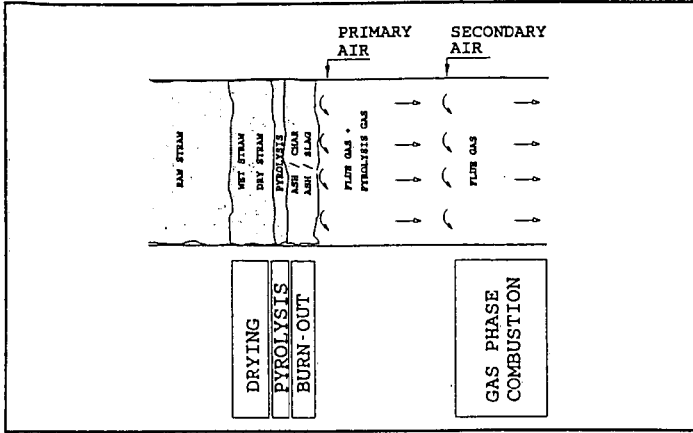


Figure 1: Surface combustion of straw. Definition of processes and zones.

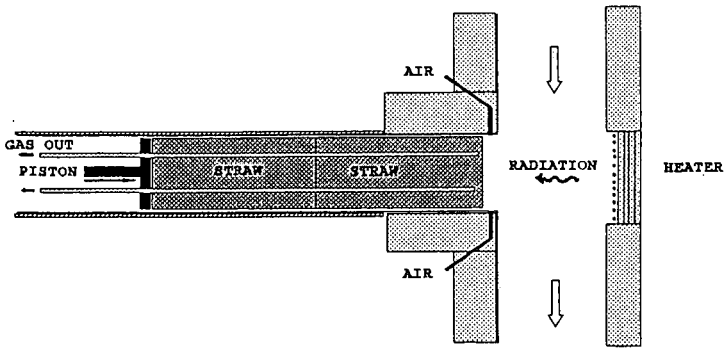


Figure 2: Experimental setup.

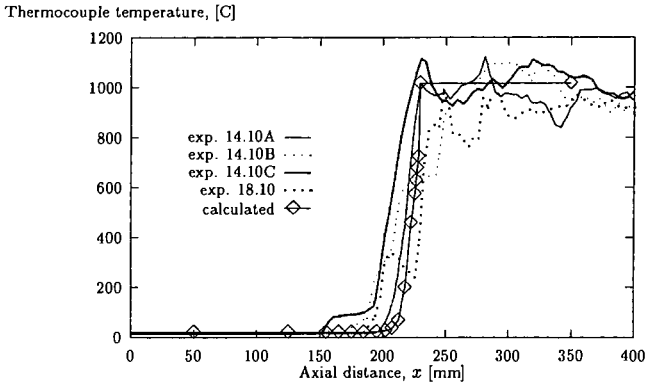


Figure 3: Comparison of measured and calculated thermocouple temperatures

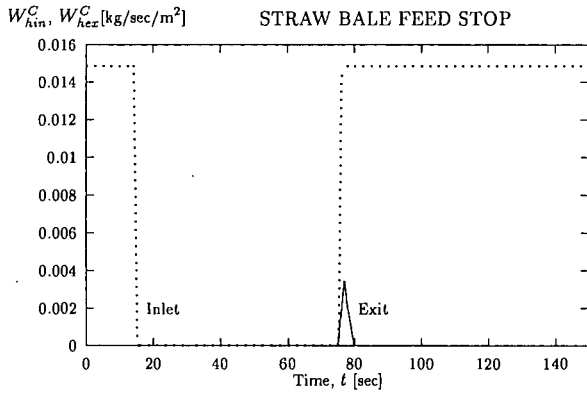


Figure 4: Inlet and exit mass flow rate of straw carbon for straw bale feed stop

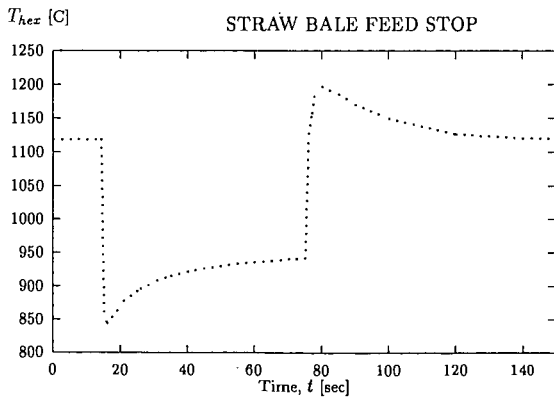


Figure 5: Calculated exit straw temperatures for straw bale feed stop

ORGANIC EMISSIONS FROM COMBUSTION OF PLYWOOD AND PARTICLEBOARD

Jeffrey M. Hoerning, Michelle A. Evans, Danny J. Aerts, and
Kenneth W. Ragland
Department of Mechanical Engineering
University of Wisconsin-Madison, Madison, WI 53706

Keywords: wood combustion; volatile organic emissions

INTRODUCTION

Large amounts of wood, wood waste and manufactured wood products are burned on grates to produce process heat and electricity in industrial boilers. Industrial combustion chambers generate high temperatures for relatively long residence times, however emissions of volatile organic substances are of concern if the residence time, temperature and turbulence are inadequate. The typical industrial plant does not measure volatile organic emissions, but does measure oxygen and carbon monoxide concentrations. With sufficient excess O₂ and low enough CO, the organic emissions are thought to be acceptably low. For example, the Wisconsin Department of Natural Resources specifies good combustion practice as CO less than 600 ppm corrected to 7 % oxygen plus temperatures greater than 675°C for 1.0 s. The purpose of this project was to determine the adequacy of this criteria with respect to volatile organic emissions for selected wood and manufactured wood products in a laboratory combustor.

Manufactured wood products contain wood, wood fiber, and non-wood additives such as adhesives, wood preservatives and fire retarding chemicals. Secondary manufacturing processes can add plastic overlays, paints, varnishes, lacquers, fillers, strength additives, and dyes. Primary wood products include lumber, plywood, composition board, and pulp and paper. Primary residue is in the form of edge trimmings, sawdust, sander dust, shavings, and fiber sludge, which could be used to replace fossil fuels for steam generation at the industrial site. Eventually the manufactured products are discarded, and rather than going to a landfill, the wood products may be burned in a boiler.

Particleboard is made from sawdust and contains 6% phenol-formaldehyde resin solids. Because of the phenol formaldehyde resin, there is concern that the formaldehyde emissions may be higher than in pure wood. Formaldehyde is considered a hazardous air pollutant by the 1990 Clean Air Act. Under proper operating conditions a wood-fired, spreader-stoker boiler has low formaldehyde emissions, however when the temperature and/or excess oxygen are too low, the formaldehyde emissions can be high [1].

TEST SETUP

The combustor is a 13 cm i.d. by 5 m long chamber made from low density Ceraform ceramic risers which are 13 cm i.d., 30 cm o.d. by 30 cm long. The insulation tubes were force fit into a long steel tube assembly which was hung vertically from a fixed platform as shown in Fig. 1. A propane burner was fitted into the bottom of the combustor for startup, and a mullite honeycomb grate was mounted 60 cm above the burner. Two underfire air opposed jets were located 20 cm below the grate and two overfire air opposed jets were located 40 cm above the grate. The fuel feeder was mounted in a stainless steel tee at the top of the combustor. The combustor exhaust flowed to a wet scrubber and induced draft fan.

Single 11 mm pine plywood cubes were fed at constant rate into the top of the combustor and fell quickly by gravity onto the grate. The cube feed rate must be very constant to maintain constant combustion conditions. The cube feeder consisted of a vibrating hopper feeding the cubes onto a stainless steel, Teflon coated chute. Cubes were held at the bottom of the chute until a rod driven by a pneumatic cylinder, pushed the cube into the combustor. A solenoid turned the air to the cylinder on and off. A pulse generator controlled the timing of solenoid and a counter, which gave the time between pulses, indicated the feed rate of the cubes.

The untreated southern pine cubes had a density of 0.55 g/cm³ and contained about 8% moisture. The particleboard, which was

southern pine with 6% phenol-formaldehyde based resin, had a density of 0.80 g/cm³. The plywood was made of southern pine and had a density of 0.65 g/cm³.

MEASUREMENT METHODS

For detection of aromatic compounds during combustion, a known volume of sample gas was drawn through a collection tube which was connected to the side of the combustor through a 200 mm long, 3 mm id. stainless steel transfer line. To obtain an accurate sample volume of gas, a graduated sealed 3 liter acrylic tube was filled to a known level with water. During the sampling process the water was pumped out of the tube at a known rate. Displacing the water in the tube was the sample gas that was drawn through the adsorbent tube. The difference in volume from the initial and final level of water in the acrylic tube indicated the exact volume of gas that passed through the adsorbent tube. Two types of collection tubes were used. The first was a glass lined thermal desorption tube packed with 250 mg of Tenax-GR adsorbent. The second was a solvent desorption tube, ORBO-32 standard charcoal tube (Sulpelco).

The thermal desorption system was attached to the injection port of a Hewlett Packard 5890 Series II GC using both a 5971 Mass Selective Detector and a Flame Ionization Detector. The desorption heater was maintained at 300°C for the 10 min. desorption process. The sample was then cryo. focused at the injector end of the GC column. The peaks were identified with the Wiley NBS library using Hewlett Packard Chemstation software. The GC capillary column is a 30 meter 0.53 mm i.d., 0.88 µm film thickness HP-5 Column (Hewlett Packard). A short 0.5 m by 0.53 mm i.d. deactivated fused silica guard column was used on the injection port end of the capillary column to provide an area for cryo focusing and to protect the capillary column. For solvent desorption, NIOSH method 1501 was used. After a known amount of sample gas was drawn through the desorption tube, the contents of the tube were added to 1 ml of carbon disulfide. A 1 µL sample was taken from this solution and injected into the same GC and column described above.

Single point calibration was performed every day for aromatic compounds being analyzed using certified calibration test mixes. For the thermal desorption, a known amount of calibration mix was added to the desorption tube through a special fitting (from Scientific Instruments) while passing He gas through the tube for 30 min. The tube was then analyzed in the typical manner. For solvent desorption a known amount of test mix was injected into the desorption tube, then the tube was capped and let stand overnight. The tube was then analyzed in the usual solvent desorption way.

CO, CO₂ and O₂ were continuously monitored during each run at the same sample point in the combustor that the GC sample was taken. These meters were calibrated daily with certified gas mixes.

TEST RESULTS AND DISCUSSION

Some tests were run using both underfire and overfire air, and some were run using extra nitrogen to lower combustor temperatures. However, the best operation was obtained using only underfire air, which is the condition reported here. Air flow was varied from 0.3 m³/min. (std) to 0.9 m³/min. (std) (1 m/s to 4 m/s). Residence time was varied from 0.5 s to 3 s by adjusting the air flow and by changing the sampling location. Sample ports were located at 1.9 m and 3.8 m above the grate. Fuel flow rate was varied to control combustor temperature and ranged from 15 g/min. to 70 g/min. The combustor required about 10 min. to warm up with the propane burner and about 10 min. to reach steady state with the wood cubes feeding. Combustor gas temperatures were measured at the centerline of tube at 0.9 m, 1.9 m, 2.5 m and 3.8 m above the grate. The vertical temperature drop above the first thermocouple was 50°C/m to 100°C/m depending on the conditions. The emissions data was correlated based on the gas temperature at the point of sampling.

The emissions of volatile organic compounds from the wood cubes depended on the excess oxygen, the gas temperature, and the residence time. Under fuel rich conditions high concentrations

of benzene, PAH's and formaldehyde were observed, with major abundances of benzene, naphthalene, acenaphthylene and anthracene. (Fig. 2). With high excess oxygen in the combustion products, polynuclear aromatic compounds were not observed, but benzene, and toluene were observed unless the temperatures were above 650°C. When excess oxygen was greater than 6 %, benzene concentrations ranged from undetected to 2 ppm, and toluene concentrations ranged from undetected to 0.4 ppm as the temperature was decreased.

The wood feed rate and the ppm concentration data were converted to an emission factor basis of $\mu\text{g/g}$ wood. The results are plotted versus temperature at the sampling point, for two groups of residence times and for excess oxygen above 4% in Figs. 3 and 4 for benzene and toluene. For a residence time of 0.5 s to 1.5 s benzene emission factor averaged $7 \pm 5 \mu\text{g/g}$ wood for temperatures above 600°C, whereas below 600°C the emissions increased rapidly. When the residence time was increased to 2 s to 3 s, the emissions did not increase until the temperature dropped below 400°C. Toluene exhibited a similar behavior but the emissions were lower by a factor of 2. Carbon monoxide concentrations were below 1000 ppm when the temperature was above 650°C for residence times of 0.5 s to 1.5 s, and above 450°C for residence times of 2.0 s to 3.0 s. The CO increased rapidly for temperatures below these values. A cross plot of the benzene emissions versus CO concentration (Fig. 5) shows that the benzene is below 20 $\mu\text{g/g}$ wood when the CO is below 4000 ppm. As the CO rises above 4000 ppm, the benzene emissions increase rapidly. Toluene shows a similar behavior.

Formaldehyde concentrations are plotted versus temperature at fuel rich conditions and 3% O_2 for particleboard (Fig. 6). Under rich combustion conditions, as the average temperature is reduced below 700°C the formaldehyde increased rapidly. At 3% oxygen the formaldehyde was less than 25 ppm. For pine plywood, concentrations of formaldehyde plus acetaldehyde were tested with O_2 at 15% and residence times of 0.9 sec. Tests were made using Kitagawa gas detector tubes. At 460°C 11 ppm (500 $\mu\text{g/g}$) of formaldehyde plus acetaldehyde was detected and at 530°C 3 ppm (130 $\mu\text{g/g}$) was detected at CO levels of 5000 - 6000 ppm.

Hubbard [1] measured benzene and formaldehyde emissions from a 20 million Btu/hr wood fired stoker boiler at a lumber and veneer plant. Benzene emissions ranged from 1 to 11 $\mu\text{g/g}$ and formaldehyde ranged from 1 to 6 $\mu\text{g/g}$, and CO levels were between 200 and 700 ppm during the tests. Fritz and Hubbard [2] measured CO emissions from six wood fired boilers with a heat capacity of 7 to 20 million Btu/hr and found many exceedances above 600 ppm with some levels above 10,000 ppm. They suggest an upper CO limit of 1080 ppm in addition to an 8 hr ave. limit of 600 ppm for CO to give low VOC emissions. Fig. 5 indicates that benzene emission increase rapidly when the CO exceeds 4000 ppm. Low formaldehyde emissions require CO levels below several hundred ppm.

REFERENCES

1. Hubbard, J., Encouraging Good Combustion Technology at Wood-Fired Facilities in Wisconsin, National Biofuels Conference, Newton, MA, 1992.
2. Fritz, R.A. and Hubbard, A.J., Control of Hazardous Air Emissions from Wood-Fired Boilers, Bioenergy 94, pp. 335-341, 1994.

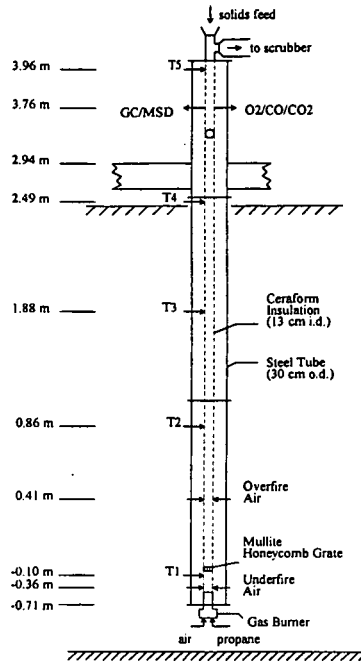


Fig 1. Fixed Bed, Up-Draft Combustor

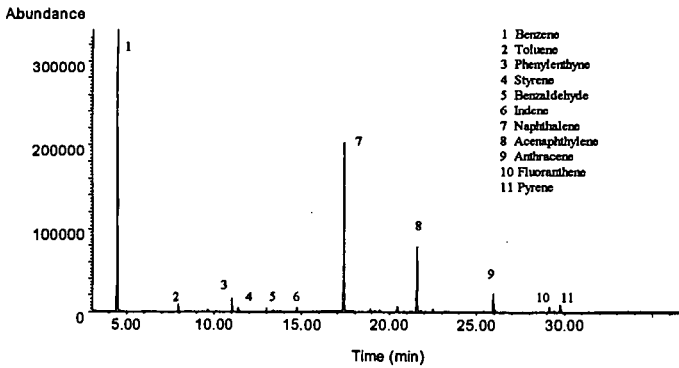


Fig 2. Chromatogram of rich fuel conditions

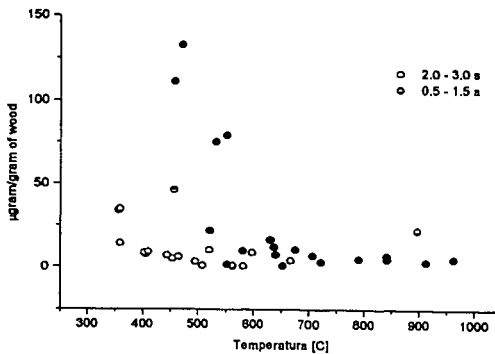


Fig 3. Benzene emission vs. temperature for 2 different residence times

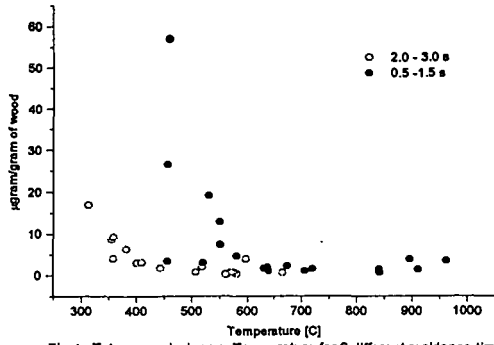


Fig 4. Toluene emission vs. Temperature for 2 different residence times

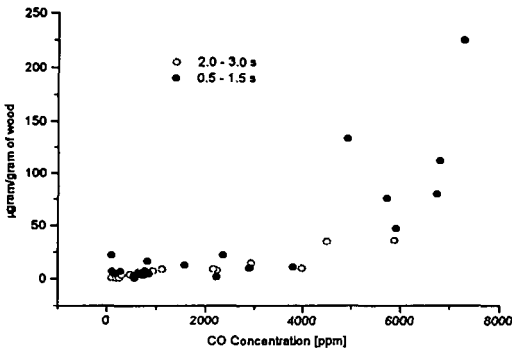


Fig 5. Benzene emission vs. CO concentration for 2 different residence times

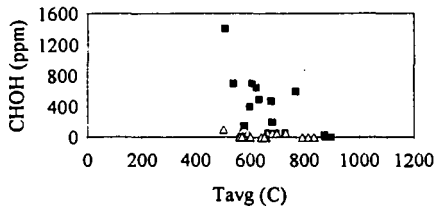


Fig 6. Formaldehyde Concentration vs. Average Temperature for Particleboard
Solid squares indicate rich combustion and open triangle indicates 3% O₂

PRODUCT ANALYSIS FROM THE OPERATION OF A 10 TON/DAY, DIRECT, FLUIDIZED BED, BIOMASS GASIFIER AND HGCU SYSTEM

Matthew A. Ratcliff^a, Michael Onischak^b, David A. Gratson^a, Joseph A. Patrick^a,
Richard J. French^a and Benjamin C. Wiant^c

a) NREL, Golden, CO, 80401 b) IGT, Chicago, IL, 60632 c) Westinghouse, Orlando, FL, 32826

Keywords: Gasifier Products, Hot Gas Cleanup, Molecular Beam Mass Spectrometry

Introduction

A principal goal of the DOE Biomass Power Program is the development of advanced high efficiency electric power generating cycles, such as integrated gasifier-gas turbine-generator systems. A key technical development required to economically produce electric power with an integrated gasifier-turbine system is the ability to remove chars and alkali metals from the gasifier product gas stream, to protect the turbines, and do so at high temperature and pressure. Westinghouse hot gas cleanup (HGCU) technology, based on ceramic membrane candle filters, has been selected for validation in this application [1]. The HGCU system was tested at the 10 ton/day scale, using a direct, pressurized, fluidized bed gasifier [2]. Two tests were conducted at the Institute of Gas Technology (IGT) RENU GAS process development unit (PDU) in Chicago, IL, during the weeks of October 31-November 5, 1994 and February 5-11, 1995.

The overall objective of the Westinghouse/IGT HGCU performance test program was to evaluate the performance of the hot gas filters with a dust-laden product gas generated from the gasification of bagasse in the RENU GAS PDU. This filter performance information will be used to determine the HGCU operating conditions for subsequent extended testing of the hot gas filters installed in a slipstream from the 100 ton/day bagasse demonstration gasifier in Hawaii [3]. Initially there was concern that tars produced in the gasifier would undergo coking reactions within the ceramic candles, leading to irreversible plugging of the filters. Consequently, a tar-cracking reactor was designed and installed ahead of the HGCU to remove the tars.

In order to characterize the tars and the performance of the process, the National Renewable Energy Laboratory's (NREL) Transportable Molecular Beam Mass Spectrometer (TMBMS) was interfaced with the PDU to monitor the performance of the RENU GAS gasifier, tar-cracker and candle filter unit operations. The development of a comprehensive, on-line, process monitoring capability has been a long term goal of NREL's Industrial Technologies Division. We have realized that goal with the successful demonstration of the TMBMS during the Westinghouse/IGT tests.

Experimental

The design and construction details of the TMBMS have been covered elsewhere [4]. In this application the instrument was interfaced with the PDU by a heat traced sampling system that permitted manual selection of three sampling ports with high temperature ball valves, as shown schematically in Figure 1. The sample ports A, B and C were installed at the tar-cracker inlet, tar-cracker outlet, and HGCU outlet, respectively. The sampling system incorporated the following functions. Particulate was removed from the gas samples with stainless steel filters at process pressure (nominally 300 psig) and at a temperature $\geq 300^\circ\text{C}$. The designed sample flow rate was 18.4 lb/h or 1% of the nominal process stream mass flow rate. The sample pressure was let-down in two stages with critical flow orifices (CFO1 and CFO2). The first stage caused the largest pressure drop from process conditions. A regulating valve between the CFO's was manually adjusted to maintain the pressure upstream of CFO2 at 20 psig by diverting most of the sample flow to vent. CFO2 dropped the pressure to 2-3 psig. The two stage CFO/diverted flow design of the sampling system enabled rapid detection of process fluctuations due to the dynamic nature of the sample flow.

The sample gas was then diluted 1:4 with preheated N_2 from a mass flow controller and a small amount of argon was blended (via mass flow controller) with the diluted sample as an internal standard. The sample then flowed through heat traced 0.5 inch stainless steel transfer lines to the TMBMS, while a constant temperature of 300°C was maintained. The diluted gas volumetric flow rate was measured by an orifice plate flow meter, just ahead of the TMBMS. This flow rate signal was recorded with the mass spectral data. The total diluted flow was directed past the TMBMS sampling orifice before being exhausted outside the building.

A port was provided in the sampling system for standards injection into the low pressure N_2 stream ahead of a static in-line mixer (see Figure 1). Multi-level calibration solutions of benzene, naphthalene, anthracene and pyrene were prepared. The standards were injected into the sampling system with a syringe pump several times each day, alone and as standard additions to sampled process gas.

IGT's sampling procedures for the PDU included product gas sampling at two points: downstream of the

gasifier and downstream of the tar-cracker. Gases, condensable liquids and entrained solids were collected from these points with iso-kinetic sampling systems, then separated for off-line analysis. The gases were analyzed with a Carle GC equipped with TCD and FID detectors. Immediately after the HGCU a Westinghouse alkali probe was installed. The product gas stream from this port was condensed and depressurized. The aqueous phase of the condensable liquids was analyzed for sodium and potassium. A breakthrough dust detector probe was installed at this same location. Solids collected on this probe were weighed but not analyzed because the quantity was too small. No gas or organic liquid analyses were performed from this third sample stream.

Results

The product gas composition measured by IGT, exiting the PDU gasifier is shown in Table 1. This raw gas composition reflects the non-optimized input of steam to the PDU and also nitrogen purges that are greater than would be used commercially. The condensed tar components collected after the gasifier measured 1.7 wt% of the bagasse feed on a moisture and ash free basis.

In the case of the TMBMS on-line measurements, tars are defined here as hydrocarbons with molecular weights starting with benzene on up. The TMBMS was programmed to scan to 350 amu (skipping masses 18 and 28 for H₂O, N₂ and CO to avoid saturating the detector) every 10 or 20 seconds. Figure 2 shows the total ion current vs. time trace for a 1 hour sampling period where we cycled through all of the sampling ports. Each point in the trace represents the acquisition of a complete mass spectrum. Thus the TMBMS is essentially a multi-channel on-line chemical analyzer. Figure 3 is the mass spectrum of the tars exiting the gasifier (sample port A), averaged over a six minute period starting at 2:00am (refer to Figure 2). The mass spectrum is representative of the tars produced in the gasification of bagasse in the IGT gasifier. They are of a tertiary nature, dominated by benzene ($m/z = 78$) and naphthalene ($m/z = 128$), along with smaller amounts of polycyclic aromatic hydrocarbons (PAH's) such as anthracene ($m/z = 178$) and pyrene ($m/z = 202$). Multi-level calibration of the TMBMS with standards allowed quantitative measurement of these species as shown in Figure 4. These data are from the first HGCU performance test and demonstrate that the tar-cracker was destroying about 75% of the tars and the HGCU was not removing much tar from the gas stream (< 10% of the raw tar). During the second test the tar-cracker was operated at a lower temperature and with different fluidizing media. In that test the TMBMS measured no significant change in tar concentration across either the tar-cracker or the HGCU.

The feeder system for the RENUGAS process was originally designed for wood chips. The change to bagasse in these tests forced numerous modifications to be made to the feeder system, many of which were anticipated and implemented before the first test. Further modifications to the feed injection screw, including water cooling and serrated threads, were made before the second test. In the field, analysis of the TMBMS data revealed some unexpected chemical behavior occurring in the process, which eventually lead to a new understanding of the importance of accurate feed level control in maintaining stable gasification.

The TMBMS monitored the concentrations of the various gases and vapors, which varied in a regular periodic fashion, during stabilized PDU operation. Figure 5 shows this behavior for just three of the numerous species monitored simultaneously: carbon dioxide ($m/z = 44$), benzene ($m/z = 78$) and methane ($m/z = 16$), sampled at port A. We observed that this cyclical behavior was correlated with the operation of the bottom feed lock-hopper valve and had a period of approximately 5 minutes. The feed lock-hopper was slightly over-pressurized with nitrogen, relative to the gasifier, to prevent back-flow of gasification product gas containing combustibles and steam. For this reason part of the concentration variation was probably due to nitrogen dilution of the products when the bottom gate valve opened. However, because the relative magnitude of the concentration drops were not the same for all products, we deduced that there were more complex effects of the lock-hopper operation on the gasification process than product dilution.

The concentration variation was not due to process pressure fluctuations because our sample gas flow meter, an orifice plate/differential pressure meter, was stable through this monitoring period. Sampling system artifacts such as distillation or chromatography in the sample transfer lines are largely ruled out by the fact that the variation magnitude was approximately the same for hydrocarbons from benzene through pyrene and only slightly less for methane. The swing effect was attenuated for tar compounds above mass 202, and this may be due to sampling artifacts because of the 300° C temperature of the transfer lines and the relatively low vapor pressures of the higher molecular weight species.

Our explanation for the product concentration swing is a momentary upset of the residence time of the bagasse in the gasifier when the bottom lock-hopper valve opens. At that moment, we believe that bagasse distributed along the feed injection screw was blown into the gasifier at an uncontrolled rate by the over-pressurized nitrogen from the lock-hopper. This was followed by a brief period during which no fresh bagasse was injected into the gasifier, as the feed injection screw grooves refilled. Thus, the bagasse residence time in the gasifier was disrupted causing the product concentrations to drop then return to normal.

Tars and methane are formed early in the gasification process, by pyrolytic mechanisms from the volatile components in the fresh bagasse [5,6]. Their residence time in the gasifier is short, being controlled by the steam and gas flow rate. In contrast, char has a longer residence time in the gasifier and distributes throughout the fluidized bed. Char continues to react with steam producing CO₂, CO and H₂ long after the volatile tars have left the reactor, explaining the less pronounced concentration drop for CO₂ than for tars and methane.

During the second test the TMBMS detected the effects of a feed interruption and change in feeder system operation, while monitoring port C. An overheating tar-cracker forced an interruption in bagasse feeding to permit the tar-cracker to cool down. Mechanical problems with the feed lock-hopper began as feeding was restarted. These problems took about 30 minutes to resolve, and when feeding recommenced the TMBMS made it apparent that the gasifier product concentrations were no longer varying during lock-hopper operation. Figure 6 shows the HGCU outlet concentrations of CO₂, benzene and methane before, during and after the feeder problems, starting at 9:14pm. These observations with the TMBMS were carefully correlated with events in the PDU control room. During the sample time frame of 10-24 minutes we see the concentration swing behavior characteristic of the PDU operation with bagasse to that point. At 24 minutes the PDU operator interrupted feeding to cool down the tar-cracker. The TMBMS detected this interruption as, for example, the drop in benzene concentration to baseline. It remained there until 33 minutes, and the methane behaved similarly, yet the CO₂ concentration remained high. A partial batch of fresh feed was delivered into the gasifier at 33 minutes, when the concentrations of all three products rise. Then the upper lock-hopper valve jammed at about 34 minutes. The TMBMS again detected this as the precipitous drop in methane and benzene concentrations and the more gradual drop in CO₂.

We presently do not have an explanation for the sudden unilateral rise in CO₂ at 46 minutes, but by 54 minutes the feeding problems were resolved and all the product concentrations were near normal by 10:09pm. The TMBMS monitoring of port C was interrupted between 10:09pm and 10:10pm and then sample dilution nitrogen was measured for background for 3 minutes. By 10:14pm the TMBMS was back on-line with port C, and we observed that the average product concentrations were roughly equivalent to those prior to the feed interruption, however, the periodic concentration swings were gone. The TMBMS detected the back-pulse of the HGCU at 104 minutes. The cause of the concentration spike for benzene and methane at 88 minutes has not been determined.

The reason for the improved chemical stability was that the PDU operator had made an operational change that increased the inventory of bagasse in the feeder section between the bottom lock-hopper valve and the injection screw. This change was made possible because the feed level sensor had spontaneously begun to operate in a satisfactory manner, during the correction of the feeder system mechanical problems in the previous half hour. (The capacitance-type feed level sensor had been reliable with wood chips but not with the bagasse up to this point). The higher feed level effectively sealed the gasifier from the pressure bursts associated with the lock-hopper operation. Thus, the actual bagasse feed rate into the gasifier was stabilized, the residence time of the feed in the gasifier was no longer disturbed and the product concentrations stabilized.

Conclusions

A Molecular Beam Mass Spectrometer was successfully interfaced with a high temperature/pressure, PDU scale biomass gasifier, hot gas conditioning and cleanup unit operations. We demonstrated the instrument's ability to continuously sample from the process and measure multiple products simultaneously. Statistical analysis of the calibration standards data demonstrated that the TMBMS response to the analytes was linear and very precise over the range of 10-1000 ppm. Excellent instrument calibration stability was achieved over a period of five days and the standard addition tests revealed no sample matrix effects on the calibration of the TMBMS for these analytes.

The identification and explanation of the process fluctuations and the feeder system operational change described above, as well as other transient phenomena, was facilitated by the on-line multi-species detection capabilities of the TMBMS. The TMBMS process gas measurements showed that the HGCU was not affecting the tar species concentrations, implying that coking would not be a problem. Analysis of the candle filters at Westinghouse showed no evidence of carbon deposition within the filters, confirming our conclusion.

The sampling experience with the TMBMS during transient feeding upsets demonstrated that chemical channels leading to the formation of benzene (and the other PAH's) and methane shut down rapidly in the absence of fresh feed. Thus, these compounds appear to be very sensitive indicators of feeding and gasification stability. Continuous measurement of one or more of these species would be very beneficial to process control.

References

- 1) NREL sub-contract No. XAZ-3-12092-01-106794, "Hot Gas Cleanup for Operation of a Gas Turbine with a Fluidized Bed Air Blown Biomass Gasifier" awarded to Westinghouse Electric Corporation, in progress.
- 2) Final report for PNL sub-contract No. B-C5821-A-Q, "Development of Biomass Gasification to Produce Substitute Fuels" details the IGT gasifier, 1987.
- 3) In progress, joint project with DOE, Hawaii and the Pacific International Center for High Technology Research (PICHTR) to scale up the IGT RENGAS gasifier.
- 4) Ratcliff, M. A. "Design and Construction of a Transportable Molecular Beam Mass Spectrometer, and its Application to the Analysis of Diesel Exhaust", Masters Thesis T4606, Colorado School of Mines 1994.
- 5) Evans, R. J.; Milne, T. A. *Energy and Fuels* 1987, 1, pp. 123-137.
- 6) Evans, R. J.; Milne, T. A. *Energy and Fuels* 1987, 1, pp. 311-319.

Acknowledgments

The authors are grateful to the numerous people who participated in these tests. Special thanks go to David Dayton, Steve Deutch, Robert Meglen, Steve Phillips, Ralph Oyerend and Tom Milne from NREL, and Rick Knight, Bob Schlusser, Ken Kozlar, Dave Parham and Jim Wangerow from IGT. This project was funded by the DOE's Solar Thermal and Biomass Power Program directed by Gary Burch. The NREL program manager was Rich Bain.

Table 1. Gasifier Product Gas Composition^a (vol. %, wet)

H ₂	4.23	CH ₄	3.81
H ₂ O	56.14	C ₂ H ₄	0.14
N ₂	17.58	C ₂ H ₆	0.06
CO	6.83	C ₃ H ₆	0.00
O ₂	0.07	C ₃ H ₈	0.00
CO ₂	10.91	C ₆ H ₆	0.23 ^b

^a Reflects non-optimized steam input and nitrogen purges.

^b Includes benzene from condensate.

Figure 1

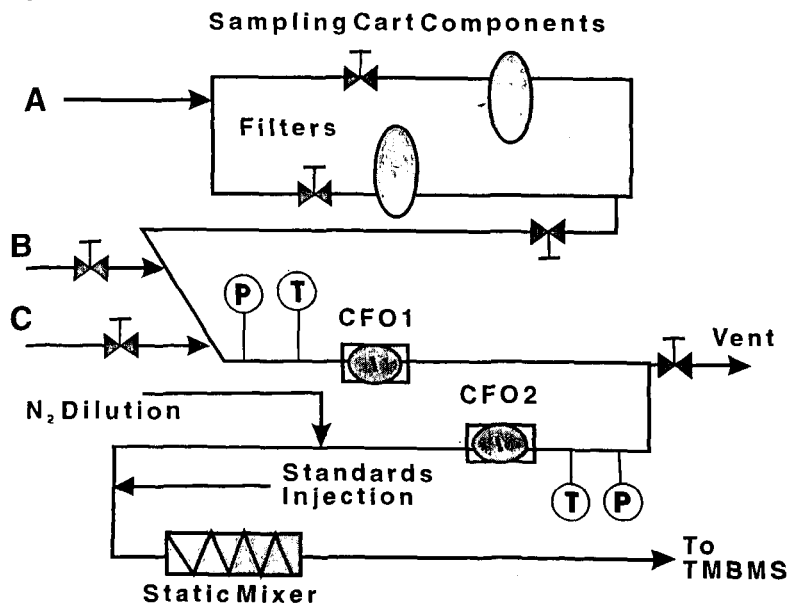


Figure 2

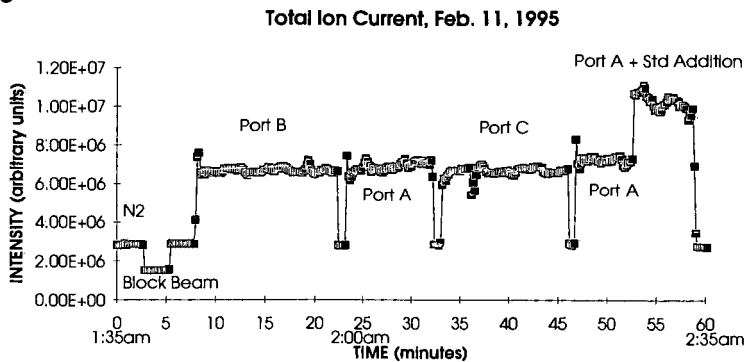


Figure 3

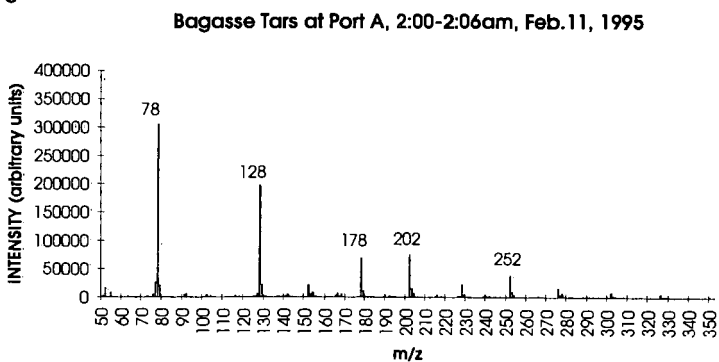


Figure 4

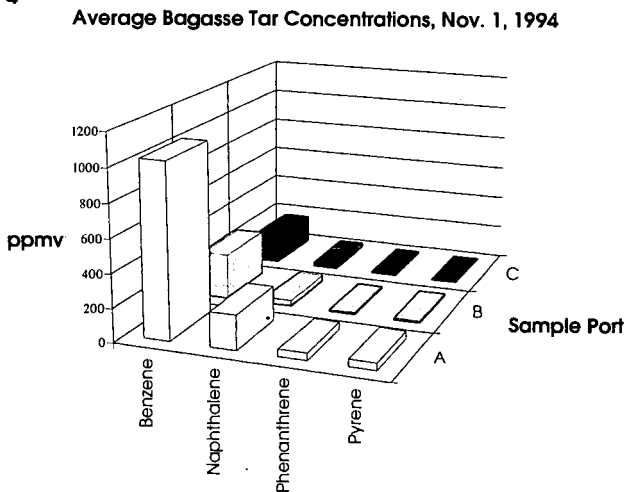
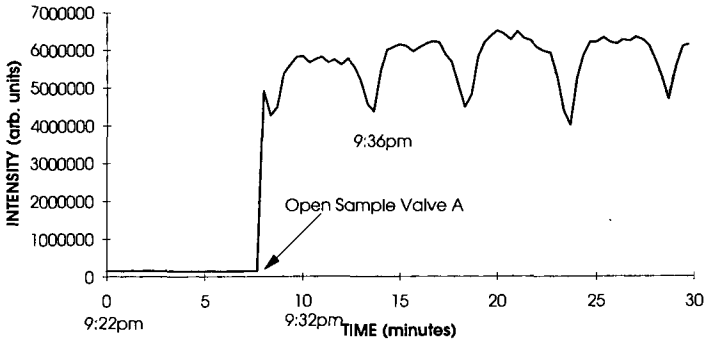
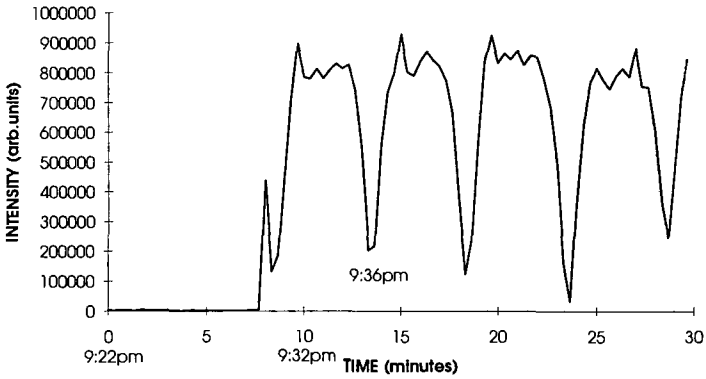


Figure 5

CARBON DIOXIDE at Port A: Tar-Cracker Inlet, Nov. 1, 1994



BENZENE at Port A: Tar-Cracker Inlet, Nov. 1, 1994



METHANE at Port A: Tar-Cracker Inlet, Nov. 1, 1994

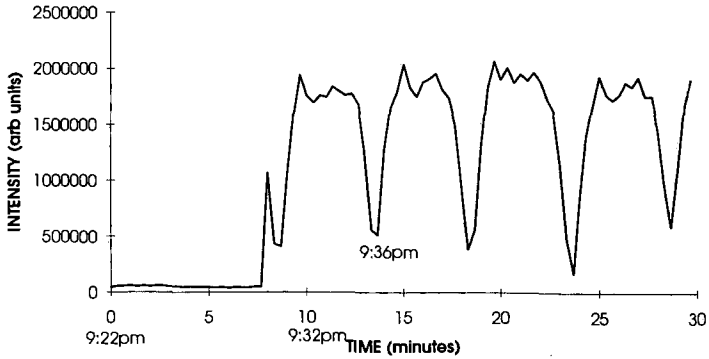
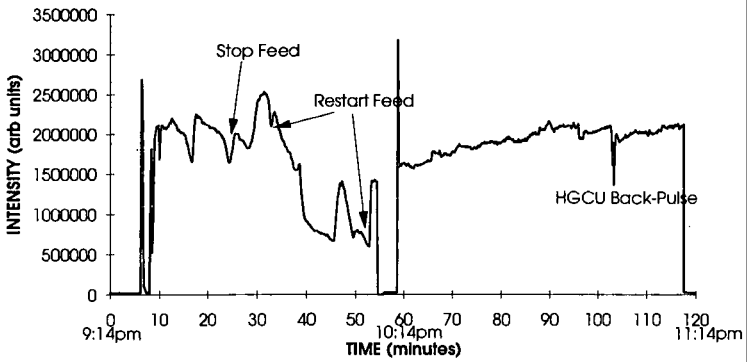
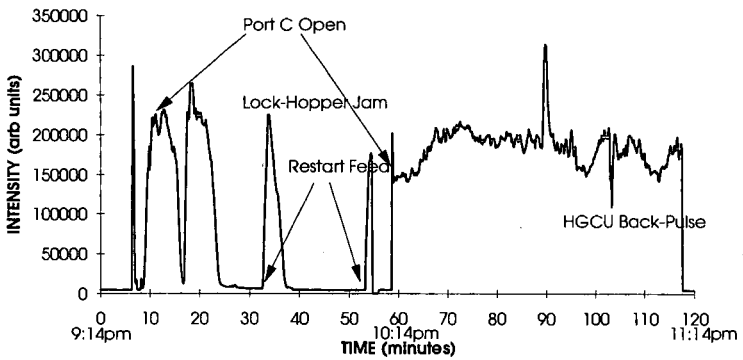


Figure 6

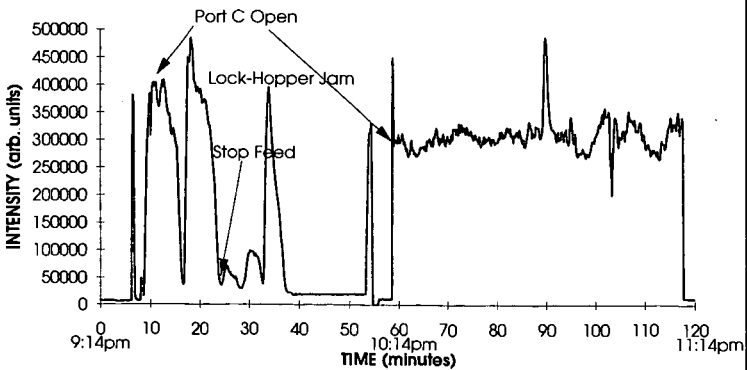
Carbon Dioxide at HGCU Outlet, Feb. 10, 1995



Benzene at HGCU Outlet, Feb. 10, 1995



Methane at HGCU Outlet, Feb. 10, 1995



GASIFICATION REACTIVITIES OF SOLID BIOMASS FUELS

Antero Moilanen, Esa Kurkela
VTT Energy, P.O.Box 1601, FIN-02044 FINLAND

Keywords: Biomass, gasification, reactivity

INTRODUCTION

The design and operation of the biomass based gasification processes require knowledge about the biomass feedstocks characteristics and their typical gasification behaviour in the process. In this study, the gasification reactivities of various biomasses were investigated in laboratory scale Pressurised Thermogravimetric apparatus (PTG) and in the PDU-scale (Process Development Unit) Pressurised Fluidised-Bed (PFB) gasification test facility of VTT (Figure 1).

EXPERIMENTAL

In PTG, the effects of individual process parameters (relevant to pressurized fluidised bed gasification) on gasification rate were studied using following parameter ranges: gasification agent (CO_2 , H_2O), temperature (700 - 1 000°C), pressure (1-30 bar). With some samples, also the effect of product gas on gasification rate was tested.

The characteristics of the samples are presented in Table 1. The selected samples are part of a biomass sample collection analysed in the EU-project (European Union) belonging JOULE II Program /1/.

The gasification rate measurements were carried out in the pressurised thermobalance (PTG), which is presented schematically in Figure 1. A more detailed description of its operation has been presented in /2/. The tests were carried out isothermally by lowering down the sample of about 50 mg in size to the reactor with the winch system equipped in the PTG. During this time, the sample was pyrolysed when it heated up to the reaction temperature at an estimated rate of above 10K/s. The weight change, which was recorded during this approximately 60 seconds period, was due to, mainly, the pyrolysis of the sample and the buoyancy phenomena. After this period, the weight change due to the gasification (and eventual postpyrolysis) was monitored.

In the fluidized-bed gasification tests, air and a small amount of steam were used as gasification agents. The feedstock and dolomite were fed into the lower part of the bed and part of the fines elutriated from the fluidized-bed were separated in the primary cyclone and recycled back to the bed. The fines separated by the secondary cyclone and the ceramic filter unit were collected, weighed and sampled. The main variable in the tests was the gasification temperature, which was controlled by changing the air-to-fuel ratio.

The carbon conversion data for three biomass fuels are presented together with data for two bituminous coals and Rhenish brown coal. The feedstock analyses are shown in Table 2. Examples of the operation conditions and process data for the different fuels are presented in Table 4.

RESULTS

The gasification rates obtained from the PTG measurements are shown in Table 3 as a function of CO_2 and H_2O pressure measured at 850°C. The gasification rate denoted as r'' is indicated as an instantaneous gasification rate, i.e. mass change rate divided by residual ash-free mass (%/min). The conversion used indicates the burn-off of the whole fuel including the mass loss due moisture and pyrolysis release. In Figure 2, the conversion behaviour, i.e. r'' vs. conversion, is given for the fuels which were gasified also in the PFB.

The PTG tests show that there are great differences in gasification rates between various fuels. The preliminary correlations between gasification rates and ash composition indicated that, especially,

the rates at higher fuel conversions seemed to decrease with increasing silica content in the fuel. This indicates that catalytically active ash components can lose their activity due to reactions with silica, or due to sintering behaviour. Also, adding a product gas component to the gasification gas decreased radically the gasification rate. For example, the gasification rate (r'') of wheat straw decreased from 27 %/min to 10%/min when CO was added 10% to CO₂ at 30 bar pressure.

The carbon conversions of the PFB tests shown in Table 4 are calculated from the material balances. The great differences between the gasification behavior of the five feedstocks used in PFB measurements can be clearly seen by comparing the data shown in Figure 3. Only the two bituminous coals seemed to behave more or less similarly and a strong and clear correlation was found between carbon conversion and equivalence ratio (or temperature). With these fuels it took several hours to reach steady state char inventory in the bed and also in the freeboard and in the recycling loop.

The three different biomass fuels had also clearly different gasification behavior. In gasification of pine sawdust, very high carbon conversions could be achieved already at relatively low temperatures, while bark and straw were more difficult to be completely gasified. In the case of straw gasification high conversion efficiencies could be achieved at above 850°C, but unfortunately sintering of the straw ash caused severe operational problems. Pine bark did not have problematic ash sintering behavior, but has a clearly lower reactivity than wood or straw. Consequently high gasification temperatures and efficient recycling of elutriated fines are required with pine bark to reach high conversion efficiencies.

Rhenish brown coal is an excellent feedstock for fluidized-bed gasification and over 95 % carbon conversion could be reached already at about 900 °C temperature. This fuel has also a high reactivity measured in PTG /3/.

The results of this study shows that gasification reactivities of the biomasses can differ greatly from each other. The comparison of the results between PTG and PFB shows that the gasification rates measured in PTG have the same order as the reactivities in PFB based on achieved carbon conversion calculations.

REFERENCES

1. Wilén, C. et al. The feasibility of electricity production from biomass by gasification systems - Fuel analyses. EU-Joule II Program Contract No. JOU2-CT92-0226, ENEL, VTT, IVO, DMT, Final report. To be published 1995.
2. Saviharju, K, Moilanen, A., van Heiningen, A.R.P., New High Pressure Gasification Rate Data on Fast Pyrolysis of Black Liquor Char. Preprints 1995 International Chemical Recovery Conference TAPPI, April 24-27, 1995, Toronto, Canada, pp. A237-243.
3. Mühlen, H.-J., Sowa, F., van Heek, K.H., Comparison of the gasification behaviour of a West and East German brown coal. Fuel Proc. Tech., 36(1993), pp. 185-191.

Table 1a. The characteristics of the feedstock samples, wt%, dry basis

Sample	V.M. %	F.C. %	Ash, %	C, %	H, %	N, %	C _{fixed} , %	S, %
Pine saw dust	83.1	16.8	0.1	51.0	6.0	0.1	42.8	nil
Pine bark	73.1	25.3	1.7	52.5	5.7	0.4	39.7	0.03
Forest residue (pine)	79.3	19.4	1.3	51.3	5.8	0.4	40.9	0.02
Salix	79.9	18.9	1.2	49.7	6.1	0.4	42.6	0.03
Wheat straw	77.7	17.6	4.7	47.5	5.9	0.6	41.5	0.07
Barley straw	76.1	18.0	5.9	46.2	5.7	0.6	41.5	0.08
Reed canary grass	73.5	17.6	8.9	45.0	5.7	1.4	38.9	0.14
Miscanthus	78.5	18.2	3.3	47.9	6.0	0.6	41.6	0.6
Sweet sorghum	77.2	18.1	4.7	47.3	5.8	0.4	41.7	0.1
Kenaf	79.4	17.0	3.6	46.6	5.8	1.0	42.8	0.1

V.M.: Volatile Matter Content, F.C.: Fixed Carbon

Table 1b. The ash compositions of the samples.

Sample	Ash composition, %									
	SiO ₂	Al ₂ O ₃	Fe ₂ O ₃	CaO	MgO	K ₂ O	Na ₂ O	TiO ₂	SO ₃	P ₂ O ₅
Pine saw dust	8.3	4.0	3.7	41.8	11.8	24.6	0.5	0.12	1.9	10.5
Pine bark	1.3	10.6	0.6	40.6	4.5	15.2	1.0	0.12	2.0	9.6
Forest residue (pine)	38.5	9.4	7.4	15.4	4.0	16.6	0.7	0.5	1.6	6.4
Salix	0.4	0.6	0.4	30.8	5.1	53.0	0.5	0.02	3.0	22.9
Wheat straw	59.9	1.6	1.1	7.3	1.8	33.7	0.9	0.04	1.1	4.5
Barley straw	62.0	0.4	0.3	4.5	2.2	38.5	1.0	0.02	1.4	5.0
Reed canary grass	89.8	2.8	2.3	3.5	1.5	6.3	0.3	0.05	1.1	8.2
Miscanthus	42.8	1.0	0.8	7.6	4.8	50.6	1.3	0.03	2.1	10.5
Sweet sorghum	57.8	1.3	1.1	9.0	2.7	16.4	3.0	0.05	3.0	6.0
Kenaf	6.6	3.6	2.4	30.8	6.0	26.5	2.5	0.08	5.7	5.5

Table 2. The analyses of the feedstock materials used in the fluidised bed tests.

	Polish coal	Colombian coal	Rhenish brown coal	Wheat straw	Pine sawdust	Pine bark
Moisture content, wt-%	3.6-6.7	7.6	11.5-12.2	6.1	6.1-16	5.6-6.7
<u>Proximate analysis, wt-% d.b.</u>						
Volatile matter	31.8	34.7	53.0	75.8	83.1	71.8
Fixed carbon	59.9	53.2	42.7	18.2	16.8	26.7
Ash	8.34	12.1	4.3	6.1	0.08	1.6
<u>Ultimate analysis, wt-% d.b.</u>						
C	75.5	71.9	63.8	46.1	51.0	53.9
H	4.7	4.9	4.6	5.6	6.0	5.8
N	1.3	1.5	0.8	0.52	0.08	0.35
S	0.7	1.0	0.3	0.08	< 0.01	0.03
O (diff.)	9.5	8.6	26.2	41.6	42.8	38.4
Ash	8.3	12.1	4.3	6.1	0.08	1.6

Table 3. The instantaneous gasification rates of the samples at the minimum and at the conversion value of 95% measured at 850°C.

Sample	1 bar CO ₂		30 bar CO ₂		1 bar H ₂ O		30 bar H ₂ O	
	r" min.	r" at X=95%	r" min.	r" at X=95%	r" min.	r" at X=95%	r" min.	r" at X=95%
Pine saw dust	27	39	22	43	25	25	50	71
Pine bark	9	16	7	13	7	13	44	71
Forest residue (pine)	18	20	na	na	na	na	na	na
Salix	29	42	23	50	30	130	60	225
Wheat straw	16	19	25	42	13	17	46	58
Barley straw	19	22	na	na	na	na	na	na
Reed canary g.	3	3	10	15	15	19	na	na
Miscanthus	18	25	26	59	24	45	na	na
Sweet sorgh.	20	23	26	51	29	62	na	na
Kenaf	50	83	55	103	67	83	na	na

Table 4. Operational data on typical set points with different fuels.

	Polish Coal	Colombian coal	Rhenish brown coal	Wheat straw	Pine sawdust	Pine bark
Equivalence ratio	0.47	0.49	0.44	0.3	0.39	0.34
Fuel feed rate, g/s	5.33	5.49	11.50	13.30	10.67	11.45
g/s-daf	4.70	4.50	9.70	11.70	9.00	10.40
Air feed rate, g/s	23.67	23.66	35.03	21.2	21.15	23.56
kg/kg-fuel(daf)	5.04	5.26	3.61	1.81	2.35	2.27
Steam feed rate, g/s	4.06	4.50	1.90	3.6	1.77	1.23
kg/kg-fuel(daf)	0.86	1.00	0.20	0.31	0.20	0.12
Purge N ₂ feed rate, g/s	3.3	3.4	1.2	4.6	2.1	2.6
Dolomite feed, g/s	0.45	0.45	0	0	0.7	0.39
Pressure, MPa	0.5	0.5	0.5	0.5	0.5	0.5
Bed temperature, °C	1 001	980	824	772	831	871
Freeboard temperature, °C	1023	1014	910	848	968	978
Carbon conversion, wt%						
to gas (C1)	85.0	86.2	95.9	83.4	94.6	87.7
to gas+tars (C2)	85.3	86.7	96.2	93.9	100.3	90.0
incl.dolomite input (C3)	84.2	85.5	96.2	93.9	98.6	89.3
Carbon losses, wt-% of input, Bottom ash	0.5	0.2	0.1	0	0.1	0
Cyclone dust	2.3	3.4	2.4	2.1	0	2.5
Filter dust	13.0	11.1	1.1	2.5	0.8	8.3
Carbon balance closure output, wt % of input	100.0	100.2	99.8	98.5	99.5	100.1
Gas composition, vol%						
CO	8.7	6.9	16.4	9.0	8.8	12.0
CO ₂	10.6	10.8	10.0	11.5	13.8	12.8
H ₂	8.4	8.1	12.0	4.0	7.8	9.0
CH ₄	0.7	0.9	1.1	3.6	3.8	3.1
C ₂ hydrocarbons	0.00	0.00	0.02	0.78	0.15	0.20
H ₂ O	15.6	18.3	7.3	23.9	17.2	12.6
NH ₃	0.12	0.14	0.19	0.15	0.026	0.13
H ₂ S	0.039	0.058	0.017	0.014	0.005	0.009
N ₂ (+Ar)	55.8	54.8	53.0	47.1	48.4	50.2

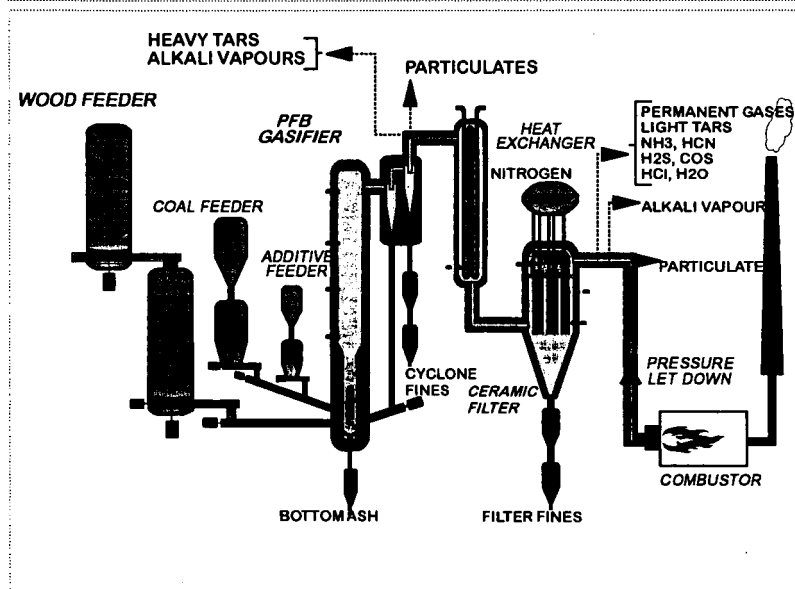
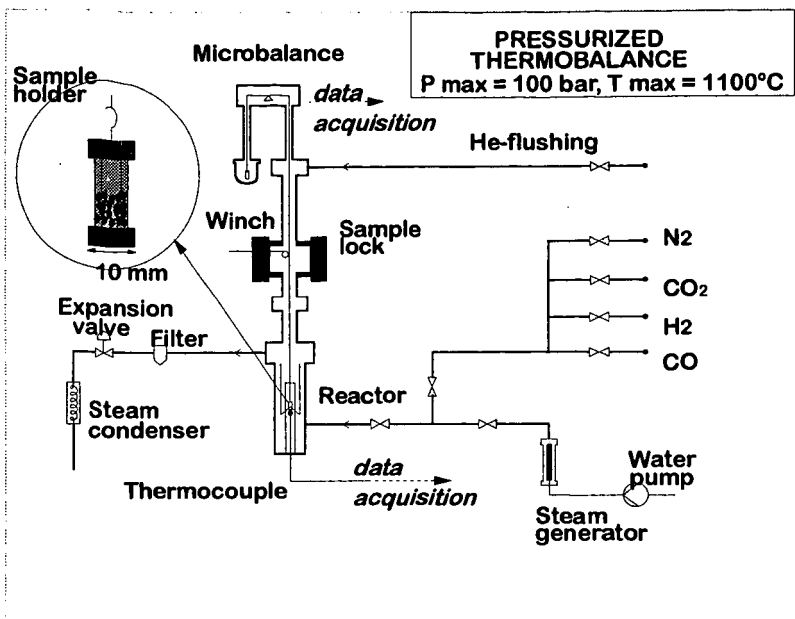


Figure 1. The pressurized thermogravimetric apparatus and pressurized fluidized-bed gasification test facility used in the study.

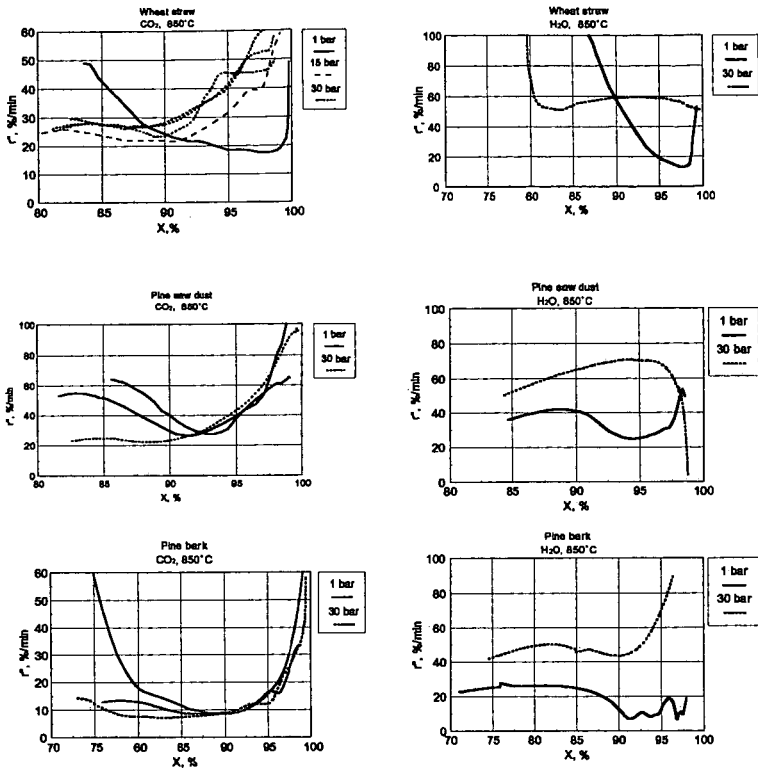


Figure 2. The gasification rate r'' vs. fuel conversion X of CO_2 and H_2O gasification in 1 and 30 bar pressures and at 850°C .

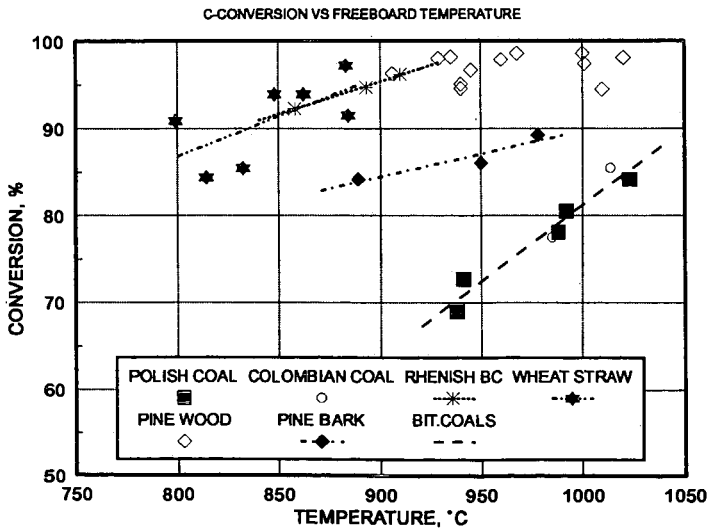


Figure 3. The achieved carbon conversions as a function of freeboard temperature in the PFB.

COMPARISON OF BIOMASS AND COAL CHAR REACTIVITIES

Sidney P. Huey, Kevin A. Davis¹, Robert H. Hurt², and Mary J. Wornat³

Sandia National Laboratories
Combustion Research Facility
Livermore, CA 94551-0969

¹Current Address: Reaction Engineering International
77 West 200 South, Suite 210
Salt Lake City, UT 84121

²Current Address: Brown University
Division of Engineering, Box D
Providence, RI 02912

³Current Address: Princeton University
Department of Mechanical & Aerospace Engineering
Princeton, NJ 08544

Keywords: biomass, char reactivity, extinction behavior

ABSTRACT

Char combustion is typically the rate limiting step during the combustion of solid fuels. The magnitude and variation of char reactivity during combustion are, therefore, of primary concern when comparing solid fuels such as coal and biomass. In an effort to evaluate biomass' potential as a sustainable and renewable energy source, the change in reactivities with the extent of burnout of both biomass and coal chars were compared using Sandia's Captive Particle Imaging (CPI) apparatus. This paper summarizes the experimental approach used to examine biomass and coal char reactivities and extinction behaviors and presents results from CPI experiments.

The reactivity as a function of extent of burnout for six types of char particles, two high-rank coal chars, two low-rank coal chars, and two biomass chars, was investigated using the CPI apparatus. Results indicate that both of the high-rank coal chars have relatively low reactivities when compared with the higher reactivities measured for the low-rank coal and the biomass chars. In addition, extinction behavior of the chars support related investigations that suggest carbonaceous structural ordering is an important consideration in understanding particle reactivity as a function of extent of burnout. High-rank coal chars were found to have highly ordered carbon structures, where as, both low-rank coal and biomass chars were found to have highly disordered carbon structures.

INTRODUCTION

Char combustion is typically the rate limiting step during the combustion of solid fuels. Incomplete combustion of solid fuels in utility boilers has long been an important concern for power generation facilities [Hottel and Stewart, 1940]. The result of incomplete combustion is a high level of unburned carbon in a boiler's flyash. This, in turn, causes a number of deleterious effects, including, a significant decrease in combustion efficiency, an adverse effect on heat transfer and electrostatic precipitator operation, and a greater difficulty marketing the flyash for recycling (i.e., for carbon contents greater than 3 to 6 percent). Determining the relative level of unburned carbon from burning coal and biomass fuels in boilers motivates this investigation.

This paper concentrates on biomass chars produced from the pyrolysis of two biomass feedstocks—a soft wood, Southern Pine; and an herbaceous material, switchgrass. The biomass chars were formed by pyrolyzing pine and switchgrass particles in a vortex reactor at 625 °C, described elsewhere [Diebold and Scahill, 1988]. Previous work on biomass chars has focused on (1) structural and compositional changes [Wornat *et al.*, 1995] and (2) quantitative measurements of global reactivity at early and intermediate levels of combustion under pulverized-fuel conditions [Wornat *et al.*, 1994]. This paper focuses on the reactivity of chars during the late stages of combustion, which is critical to unburned carbon in flyash.

In practice, the level of unburned carbon in the flyash is related to the fuel's rank. Coal rank is a measure of volatile matter contained in the coal and is generally considered an indicator of its geologic

age. Our earlier work [Hurt, 1993; Hurt and Davis, 1994; Davis *et al.*, 1995] indicates that the carbonaceous structure of young materials (biomass and low-rank coal chars) is less susceptible to the structural ordering process that bituminous and high-rank coals can undergo. The more amorphous nature of the younger materials during the latter stages of combustion should maintain their initially high level of reactivity throughout the entire combustion process, insuring lower levels of unburned carbon in the flyash.

Bituminous and high-rank coals produce high levels of unburned carbon, whereas, low-rank coals produce lower levels of unburned carbon. Biomass, with a very high volatile matter content, high oxygen content, and a correspondingly low heating value, is thermochemically similar in many respects to a low-rank coal. Given the thermochemical similarity of low-rank coals and biomass chars, we expect both fuels to exhibit comparable reactivities and to produce similarly low levels of unburned carbon. This paper presents an investigation of char reactivity as a function of burnout for biomass chars and compares them to our observations for coal chars of various ranks.

A relationship exists between a char's reactivity and extinction behavior and its temperature-time profile [Hurt, 1993]. Temperature-time profiles of chars provide the relative magnitude of reactivities for different chars, where as, normalized temperature-time profiles of chars are best suited to illustrate and compare the extinction behavior of different chars. Because maximum temperatures and extinction times vary greatly for different types of chars, temperatures and times were normalized to allow for a comparison of extinction behaviors for various types of chars.

EXPERIMENTAL METHODS

The high-temperature reactor in Sandia's Coal Combustion Laboratory (CCL) was used to measure the temperature-time profiles during combustion of two high-rank coal chars (Illinois #6 and Pocahontas #3), two low-rank coal chars (Beulah and Dietz), and two biomass chars (pine and switchgrass). Data were obtained with the Captive Particle Imaging (CPI) diagnostic system that has been discussed in previous reports [Hurt and Davis, 1994]. Figure 1 presents a schematic of the CPI. The system provides optical access for high-resolution video imaging of complete particle combustion for individual 100 μm to 200 μm char particles in a well-controlled combustion environment. Particles are placed on an alumina fiber bed supported by fine platinum wires. The particles are oxidized in a laminar flow of vitiated air with 6 mole-% excess oxygen at a temperature of approximately 1600 K. The particle is positioned along the reactor centerline at the focal point of a long-focal-length microscope. During the positioning process a water-cooled coil surrounding the particle holder provides local cooling and therefore prevents premature reaction of the particle. This microscope is connected to a video system capable of simultaneously imaging both reflected light and near infrared (IR) emission from the reacting particles. The IR images can be used for determination of radiance temperatures. Radiance temperature is defined as the temperature of a hypothetical black body emitting the same radiative power as the real object (particle) in the wavelength range of interest (here 700 to 1000 nm). For particles that have undergone low to intermediate extents of burnout, emissivities are approximately 0.8 [Baxter *et al.*, 1988] and true particle temperatures will be approximately 20 K greater than the reported radiance temperatures.

For the temperature-time profiles, the radiance temperatures are normalized to their corresponding maximum temperatures (i.e., normalized temperature equals the actual temperature divided by the maximum temperature). The temporal data are normalized by the time at which near-extinction (in the case of the higher rank coals) or extinction (in the case of lower rank coals and biomass chars) of the combustion process occurs. These extinction (and near-extinction) times correspond to the inflection point in the temperature-time profile that occurs after the peak temperature.

Using the CPI, normalized temperature-time profiles of several coal chars and solid biomass-derived fuels were determined for at least 20 particles of each type. Figures 2, 3, and 4 present the normalized temperature-time profiles for bituminous and high-rank coal chars (Illinois #6 and Pocahontas #3), low-rank coal chars (Beulah and Dietz), and biomass chars (pine and switchgrass), respectively. The figures show that for all the chars the particle temperature increases to a maximum and decreases to the reactor temperature, nominally 1400 to 1500 K. Table 1 summarizes the overall reactivity for various char particles [Wornat *et al.*, 1994].

RESULTS AND DISCUSSION

The general shape of a temperature-time profile is an indicator of a char's reactivity as a function of extent of burnout. A gradual decrease in temperature occurring after a char's peak temperature indicates that the reactivity of that char is decreasing with the extent of burnout, as shown for bituminous and high-rank coals in Figure 2. Chars that remain at or near their peak temperature for a

significant period during combustion then display a sudden decrease in temperature at the end of oxidation are believed to have relatively high reactivities that do not decrease with extent of burnout. Figures 3 and 4 show examples of chars with high reactivities that do not decrease with extent of burnout. These results show that the time or conversion dependence of reactivity for low-rank coal chars and biomass chars are very similar, the reactivities for both types of chars are relatively high, and the reactivities do not decrease with extent of burnout.

In addition to the information regarding extinction behavior, the CPI technique allows one to qualitatively compare the magnitude of the global reactivities of the various chars. Peak temperatures and burnout times obtained from these experiments suggest global reactivities qualitatively similar to the earlier quantitative work of past work [Wornat *et al.*, 1994]. The relative overall reactivities of chars are in the following order.

lignite chars > biomass chars > high-volatile bituminous coal chars

Table 1 lists the quantitative results obtained in the CCL over the past several years. The slightly higher reactivities of the biomass chars under CPI conditions may be a result of the somewhat lower temperatures used for the CPI compared to the CCL.

CONCLUSIONS

Based on our previous work on carbon reactivity and ordering of the carbon structure during coal and char combustion [Davis *et al.*, 1995], the current results for the biomass chars are not surprising. High-rank coals are observed to undergo a significant decline in reactivity with increasing burnout. This is a consequence of carbon structural ordering in the char during exposure to the high-temperature combustion environment. Highly ordered carbon structures offer fewer active sites for heterogeneous surface oxidation, which, therefore, decreases the reactivity of the carbon particle. In our related work on biomass chars [Wornat *et al.*, 1995], short-range ordering of the biomass char carbon is observed in carbon-rich portions of the chars. However, the high levels of oxygen content in biomass fuels favors cross-linking of the carbon chains that inhibits further carbon ordering during combustion. This persistence of disorder in the carbon structure during biomass char oxidation is also observed for the high-oxygen-content chars of low-rank coals. We believe that the disorder in the carbon structure is responsible for the high reactivities found in both the low-rank-coal and biomass chars throughout their combustion lifetime. A consequence of this high char reactivity is that the particle temperature remains high for these chars through the entire burnout. In summary, the combustion behavior of biomass chars was found to be similar to that of low-rank coals—high reactivity with no evidence of a decrease with extent of burnout.

REFERENCES

- Baxter, L.L., Fletcher, T.H. and Ottesen, D.K. (1988). *Energy and Fuels* 2:423.
- Davis, K.A., Hurt, R.H., Yang, N.Y.C. and Headley, T.H. (1995). *The Evolution of Char Chemistry, Crystallinity, and Ultra-fine Structure during Pulverized-coal Combustion*, *Combustion and Flame* 100:31
- Diebold, J. and Scahill, J. (1988). *Pyrolysis Oils from Biomass: Producing, Analyzing, and Upgrading*, *ACS Symposium Series 376* (E.J. Soltes and T.A. Milne, Eds.), The American Chemical Society, Washington, D.C., pp. 31-40
- Hottel, H.C. and Stewart, I.M. (1940). *Space requirement for the combustion of pulverized coal*, *Ind. Eng. Chem.* 32:719.
- Hurt, R.H. and Mitchell, R.E. (1992). *Unified High-Temperature Char Combustion Kinetics for a Suite of Coals of Various Rank* *24th International Symposium on Combustion*, The Combustion Institute
- Hurt, R.H. (1993). *Reactivity distributions and extinction phenomena in coal char combustion*, *Energy and Fuels* 7:721.
- Hurt, R.H. and Davis, K.A. (1994). *Near-Extinction and Final Burnout in Coal Combustion*; *25th International Symposium on Combustion*, The Combustion Institute
- Wornat, M.J. (1993). *Combustion Studies of Pyrolysis Oils and Chars — November to February*; Sandia National Labs Quarterly Progress Report, Case No. 4317.000

Wornat, M.J., Hurt, R.H., and Yang, N.Y.C. (1994). *The Combustion Reactivity of Biomass Chars, Proceedings from the Eastern States Section Meeting of the Combustion Institute*, The Combustion Institute

Wornat, M.J., Hurt, R.H., Yang, N.Y.C. and Headley, T.H. (1995). *Structural and compositional transformations of biomass chars during combustion, Combustion and Flame* 100:131

Table 1. Overall Reactivities of Various Chars

Fuel Name	Fuel Type	Rate [†] (g of Cl/cm ² ·sec)
Southern Pine Char ¹	woody	0.0037
Switchgrass Char ¹	herbaceous	0.0041
Beulah ²	lignite	0.0065
Lower Wilcox ²	lignite	0.0056
Smith-Roland ²	subbituminous	0.0065
Dietz ²	subbituminous	0.0061
Hiawatha ²	high-volatile bituminous	0.0059
Blue #1 ²	high-volatile bituminous	0.0045
Illinois #6 ²	high-volatile bituminous	0.0033
Pittsburgh #8 ²	high-volatile bituminous	0.0024
Lower Kittanning ²	low-volatile bituminous	0.0021
Pocahontas ²	low-volatile bituminous	0.0012

[†] rates are calculated from global kinetic parameters at gas conditions of 1500K & 6 mole-% O₂, the value 0.0065 is the diffusion-limited maximum for these conditions

¹ Wornat, Hurt, and Yang (1994)

² Hurt and Mitchell (1992)

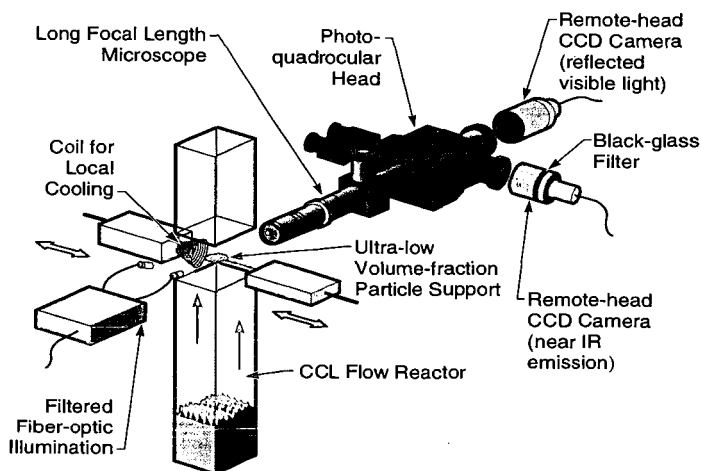


Figure 1. Schematic of the Captive Particle Imaging System

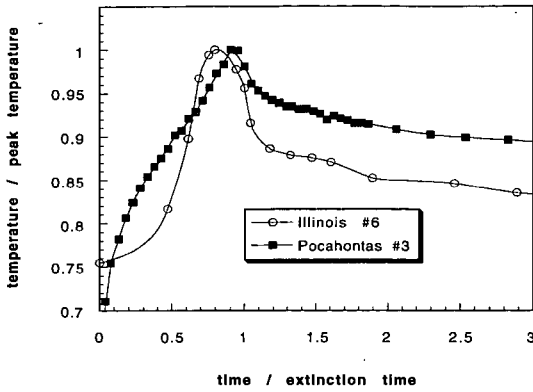


Figure 2. Normalized Temperature versus Normalized Time for Bituminous and High-Rank Coals

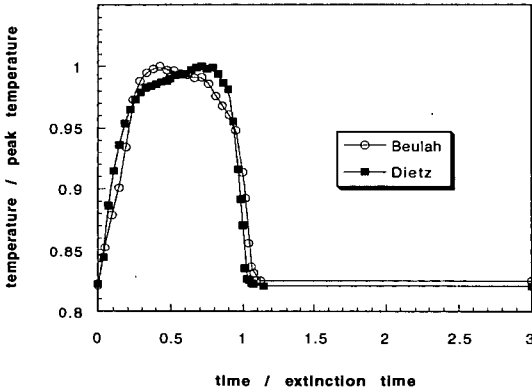


Figure 3. Normalized Temperature versus Normalized Time for Low-Rank Coals

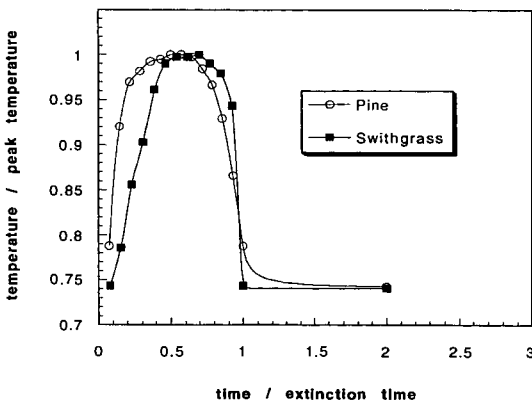


Figure 4. Normalized Temperature versus Normalized Time for Biomass Chars

ALFALFA STEM FEEDSTOCK FOR IGCC POWER SYSTEM FUEL

by

Dr. Max M. DeLong, Northern States Power Company

Dr. Michael Onischak, The Institute of Gas Technology

Michael Schmid, Tampella Power Corporation

Benjamin Wiant, Westinghouse Electric Corporation

Professor Ervin Oelke, University of Minnesota

Keywords: IGCC, alfalfa, gasification

ABSTRACT: A feasibility study was completed for an integrated gasification combined cycle (IGCC) electric power generation plant to operate in conjunction with an alfalfa processing plant that provides the gasification feedstock and a mid-level protein animal feed co-product. Alfalfa stem material was evaluated as a gasification feedstock. The leaf material was evaluated as a mid-level protein animal feed supplement. The alfalfa leaf-stem separation and power generation operations have dual and/or synergistic functions which contribute to a technically and economically compatible combination.

The pressurized biomass gasification process selected is the IGT RENUGAS™ system licensed to Tampella Power Corp. Adaptation of the air-blown gasification process to alfalfa stems results in low-Btu fuel gas suitable for combustion turbines. The gasification process is expected to obtain very high carbon conversion with low tar production, overcome ash agglomeration, and provide for control of volatile alkali species. A hot gas clean-up system removes particulate matter with a ceramic filter system. The collected ash residues are expected to be returned to the land that grew the alfalfa.

The physical and chemical properties of the alfalfa feedstock were evaluated for the gasification process. The alfalfa char carbon-steam reaction, which is the slowest step in the complete conversion of biomass to gases, was measured and the char proved to have a high reactivity. Ash components were measured and evaluated in terms of agglomeration within the gasifier. Using this information, the alfalfa gasification conditions were predicted. A subsequent preliminary gasification test confirmed the alfalfa gasification conditions. To complete the engineering design of the IGCC system, additional testing is required, but the results to date are positive for a successful process.

INTRODUCTION: In response to a solicitation by USDOE, through the National Renewable Energy Laboratory (NREL), with co-sponsorship by the Electric Power Research Institute (EPRI), Northern States Power Company (NSP) formed a team with the University of Minnesota, The Institute of Gas Technology, Tampella Power Corp. and Westinghouse Electric Corp. to perform a feasibility study of alfalfa crop production coupled to a gasifier/hot gas clean-up/gas turbine/steam turbine power generation system. Figure 1 presents a block diagram of the combined electrical power and alfalfa co-product concept. In accordance with the solicitation by NREL, the study investigated economic development through biomass systems integration, and emphasized: 1) sustainable biomass energy crop production, 2) efficient power generation, and 3) co-product value from alfalfa-leaf meal.

This system concept uses alfalfa from a dedicated feedstock supply system (DFSS); namely, biomass material planted specifically for an energy production facility. The proposed cropping plan involves planting alfalfa in a seven year cycle with 4 years of alfalfa followed by 2 years of corn and one year of soybeans. This seven year rotation is in contrast to the often used current rotation system of corn and soybeans being continuously alternated. Alfalfa is a crop that can be grown on a long term basis by a group of farmers with coordination through a closed-end cooperative arrangement (i.e., membership is offered only to producers). The co-op carries on a value added processing and marketing function for the farmer.

Alfalfa provides real benefits for other agricultural crops in the rotation and the land. These benefits result from the inclusion of a perennial (nitrogen-fixing) legume in the crop rotation. The need for external inputs of fertilizers, fossil fuels, herbicides and insecticides are reduced while distinct environmental benefits including reduced soil erosion, improved soil tilth, increased soil organic matter levels, and reduced potential for nitrate leaching are realized. Alfalfa was chosen as a feedstock because it has been successfully grown in NSP's service territory including the region surrounding the plant site of the feasibility study, NSP's Minnesota Valley Generating Plant at Granite Falls, MN. Additional acreage of the crop would enhance the regions ability to continue progress towards achieving a sustainable agricultural (i.e., preservation of long term productivity and no adverse environmental impact). The knowledge base, expertise and production capability for producing the crop is well established in the region.

ALFALFA FRACTIONATING PROCESS: The alfalfa fractionating (separating) plant diagram shown in Figure 2 receives sun-cured alfalfa in a conventional round bale package; reduces the particle size of the alfalfa material; dries it to a suitable moisture content for fractionation, storage or further processing. A dual air path (radially and axially) hammermill separates the leaf from the stem material. The separation of leaf from stem enhances the quality of the stem material as fuel, because the leaf fraction has the higher proportion of ash, fuel bound nitrogen and sulfur. Also, the stem material after fractionation has lower particle-to-particle friction and a higher bulk density than a mixture of the two fractions. The leaf fraction benefits from separation because the resulting crude protein concentration is raised, and the subsequent power for pelletizing is reduced as a result of the removal of the fibrous stems. Gas turbine exhaust heat can be used to assist in drying the incoming alfalfa. Low grade steam from the power cycle can be used to roast the leaf fraction to improve the digestibility and value of the crude protein.

ALFALFA FEEDSTOCK PROPERTIES: The alfalfa stem feedstock was analyzed chemically and physically. The analyses were compared with similar biomass feedstocks, namely bagasse and wood chips that have been successfully gasified in the RENUGAS™ fluidized-bed gasifier. The initial results were positive. The alfalfa stem feedstock is expected to be as good as the bagasse feedstock, in terms of gasification operating conditions and feed handling operations.

Important physical properties of alfalfa include its particle shape, particle size distribution, and bulk density. Handling characteristics relate to biomass particle-to-particle friction and biomass particle-to-wall friction factors that are important in solids handling considerations. Tests showed that sized and dried alfalfa should handle and feed well.

Also included with the physical properties is an assessment of the tendency of the ash constituents to combine and form agglomerates within the gasifier or in downstream equipment. Alkali elements such as potassium and sodium can combine with silica to form agglomerates in the gasifier. Unlike woody biomass feedstocks, which tend not to form agglomerates, alfalfa contains amounts of potassium, sodium, and silica that may form a eutectic mixture with a melting point near the expected gasification temperature. Furthermore, alkali compounds may exit the gasifier with the product gases as aerosols. These could potentially pass through the barrier filter and eventually deposit on the blades of the combustion turbine.

The important chemical properties of alfalfa include its moisture level, ultimate analysis, calorific value, and the elemental composition of the ash. Another chemical property important for gasification is char reactivity with steam. Reactivity of the biomass char carbon with steam is a measure of the slowest reaction step in the complete conversion of biomass into gases. After the very rapid devolatilization step, about 5% to 15% of the initial biomass weight remains as char carbon. The char carbon reacts with steam in the gasifier to complete the gasification process forming additional carbon monoxide and hydrogen. The rate of this reaction determines the char residence time in the fluidized bed, hence, is related to the size of the gasifier. Figure 3 shows the measured char reactivity or the steam-char gasification rate for the char of alfalfa stems compared to chars measured previously from a similar agricultural residue, namely, corn stover, and a silvicultural residue, maple wood chips. Also shown in comparison to the three biomass species are the slower char gasification rates measured for peat and bituminous coal. The base carbon entity plotted in the figure is the weight of char carbon that remains after completion of the rapid devolatilization step minus the weight of the ash in the material.

The char reactivity measurements were made in a pressurized thermobalance operating at expected gasification conditions of 1600°F and 300 psig. The composition of the gas in the thermobalance was representative of the gasifier product gas with respect to steam and hydrogen: namely, 45% steam, 5% hydrogen, and 50% nitrogen. Hydrogen is a product of the steam-char reaction, thus the design char gasification rate is measured under similar hydrogen concentration.

As seen in the Figure 3, the alfalfa char reacted at essentially the same rate as the corn stover and the maple chars under similar conditions. Therefore, it is expected that the alfalfa char should gasify at least at the same rate as char from wood chips that have been successfully gasified. In terms of the process design, the alfalfa throughput rate over the same cross-sectional area of the gasifier should be at least equal to that of the maple wood chips, which have been extensively tested in the PDU.

ALFALFA EVALUATION RESULTS: The moisture, ultimate analysis, and heating value results for the alfalfa feedstock are presented in Table 1 for samples of alfalfa obtained from three counties with different soil classifications surrounding the Granite Falls plant site. The alfalfa samples received were separated into stem and leaf fractions and were analyzed individually. The alfalfa stems are intended to be the gasification feedstock. The leaves are to be separated and processed into value-added leaf meal products, although the gasifier system does not preclude the leaves being sent to the gasifier along with the stem material.

The alfalfa compositions shown in Table 1 are within the expected range of most biomass feedstocks considered for gasification. The major distinctions seen in Table 1 are that the leaf fraction has more ash and also a higher nitrogen content than the stems. The higher nitrogen content of the leaves is related to the animal protein feed value. If the leaf fraction is to be gasified along with the stems, then the higher ash and fuel-bound nitrogen levels have to be considered in the design of the plant.

Table 2 presents the ash analyses of the stem and leaf fractions of alfalfa from the three county samples. The leaf fraction is up to 47 wt % of the dried alfalfa plant. The amounts of potassium, sodium, and silicon are important. These elements can combine to form a eutectic that have a melting temperature below the normal gasification temperature. Possible combinations of the oxides of these elements are well known in coal combustion systems and in iron-making. The presence of these species is a concern in combustion boilers with an oxidizing atmosphere which favors the formation of agglomerates that foul the boiler internals. There is a concern that even at lower temperatures and in the reducing atmosphere of a fluidized-bed gasifier these agglomerates may form.

A coal agglomeration test used at IGT was modified for biomass agglomeration to assess the degree of agglomeration under non-oxidizing conditions (the IGT boat test). The general test procedure involves reducing the size of the biomass to 200 mesh and then pyrolyzing the mass in a 3/8-inch by 3-inch ceramic boat under nitrogen at 1800°F followed by cooling under nitrogen to room temperature. The residue is then evaluated in terms of agglomeration strength. The mass of biomass char carbon and ash that remains in the boat after cooling is described in terms of varying degrees of agglomeration ranging from a very strong adhesive mass to completely free-flowing particles.

The boat test conducted with the alfalfa stems alone showed a very weakly agglomerated mass of char and ash. Just the weight of a pencil point could break up the mass and it also could not be extracted intact from the boat. It was weakly held together by the adhesion due to some tar pyrolysis products and ash components. The bagasse feedstock that was successfully gasified in the RENUGAS process development unit (PDU) at IGT showed a more strongly agglomerated mass in the boat test compared to the alfalfa. However, the subsequent PDU bagasse gasification test at 1600°F (871°C) did not show any evidence of agglomeration with the agitation and mixing with the inert material in the fluidized-bed gasifier. Bagasse, however, is washed of most of the potassium and sodium elements in the sugaring process, so a precaution is recommended for initial alfalfa gasification tests.

One possibility for preventing agglomeration in the gasifier is to add small amounts of certain additives that contain magnesium, which is known to combine with alkali and prevent the formation of the lower melting temperature agglomerates. Two such additives were tested in the boat tests. These additives were magnesium oxide and a high magnesium carbonate content dolomite. The amount of these materials that were added to the alfalfa was kept to a minimum and was calculated as a one-to-one weight ratio of the amount of potassium that was measured in the ash of the samples, i.e., 4 wt % magnesium oxide and 8 wt % dolomite.

All of the boat tests conducted with these two additives showed that the char-ash residue became completely free flowing, just like dry sand. Hence, if the alfalfa fluidized-bed gasifier is designed to operate with dolomite as the fluidized-bed media, then alfalfa ash agglomeration will be controlled and not a concern. Furthermore, conditions for alkali capture or removal from the product gas stream should be enhanced with the collection of the dolomite fines by the hot gas filter.

BASIC GASIFICATION PROCESS CONDITIONS: The specification of the basic conditions for the air-blown, fluidized-bed gasification process include the gasification temperature and pressure, and to a lesser degree, the acceptable limits for feed moisture and the amount of steam addition to the fluidized bed. The gasification temperature is the most important operating variable in terms of achieving the highest carbon conversion efficiency, namely, conversion of the feed carbon to gases along with the lowest amount of oil and tar species in the product gas. The incoming feed moisture will affect the amount of air needed to maintain a selected gasification temperature. Hence, the heating value of the product gas is affected due to feed moisture and the additional air that is required to maintain the gasification temperature.

Based on data in Figure 3 from the thermobalance test of the alfalfa char gasification rate at pressure and 1600°F, and from the previous gasification test experience in the IGT RENUGAS™ 10 ton per day process development unit (PDU) with the Hawaiian bagasse feedstock at 1580°F, which yielded 96% bagasse feed carbon conversion, it is expected that an alfalfa gasification temperature near 1600°F should yield similar or greater feed carbon conversions.

PDU TESTS WITH ALFALFA: In a concurrent DOE program, the IGT RENUGAS process development unit (PDU) gasifier system was modified to evaluate the hot gas cleanup for the 100

ton per day bagasse demonstration gasifier being built in Hawaii. One alfalfa gasification test was conducted in that program. The alfalfa was successfully reduced in size with a forage harvester with an increase in the bulk density to about 10 lbs per cubic foot and fed smoothly to the PDU gasifier at the rate of 7.7 tons per day for an 8-hour test duration. The entire alfalfa plant was gasified, including the leaves and stems.

The PDU gasifier results showed that the alfalfa carbon conversion to gases and condensable liquids at the 1470°F gasifier temperature was about 98%, and the product gas composition was similar to bagasse gasification. The alfalfa test in the PDU was conducted with about 8 wt % dolomite added with the alfalfa to the fluidized bed of the inert alumina bead material used for alfalfa gasification. However, in this limited test, the test conditions were not optimized for the alfalfa according to the conditions identified in this feasibility study, but overall, the test indicates alfalfa can be successfully gasified. Additional alfalfa gasification performance testing at the PDU or larger scale is needed to obtain detailed engineering design information. Alfalfa exhibits some variation in the amount and type of ash components between the stem and leaf fractions and also between the different growing regions around the proposed plant site. It is expected that these differences will not impact the proposed alfalfa gasification scheme, but this also needs to be evaluated with gasification tests. The gasification of alfalfa stems in a fluidized bed of dolomite is expected to control ash agglomeration tendencies.

Table 1. ALFALFA ANALYSIS: FROM THREE COUNTIES NEAR THE PLANT SITE

County	Olivia		Montevideo		Clarkfield		Average	
Moisture and Ash Analysis, wt %	Stems	Leaves	Stems	Leaves	Stems	Leaves	Stems	Leaves
Moisture	9.99	6.65	8.40	6.91	9.73	6.42	9.37	6.66
Ash	5.18	11.01	4.62	7.37	4.69	9.03	4.83	9.14
Ultimate Analysis, wt %								
Ash	5.65	11.43	4.98	7.68	5.14	9.48	5.26	9.53
Carbon	47.15	47.11	47.47	48.22	46.96	47.02	47.19	47.45
Hydrogen	5.84	5.89	5.94	6.10	5.93	5.92	5.90	5.97
Nitrogen	2.14	4.76	2.07	4.80	1.98	4.53	2.06	4.70
Sulfur	0.08	0.29	0.08	0.28	0.08	0.21	0.08	0.26
Oxygen (by diff.)	39.14	30.52	39.46	32.92	39.91	32.84	39.5	32.09
Total	100.00	100.00	100.00	100.00	100.00	100.00	100.00	100.00
Higher Heating Value, Btu/lb (dry)	8030	8230	8140	8660	8080	8360	8083	8417

Table 2. ELEMENTAL ASH ANALYSIS OF ALFALFA: THREE COUNTIES NEAR THE PLANT SITE

County	Olivia		Montevideo		Clarkfield		Average	
Ash Element, wt % of Ash	Stems	Leaves	Stems	Leaves	Stems	Leaves	Stems	Leaves
Silicon	0.23	0.56	0.26	0.25	0.80	1.21	0.43	0.67
Aluminum	0.00	0.00	0.00	0.00	0.00	0.00	0.00	0.00
Iron	0.00	0.00	0.00	0.00	0.00	0.00	0.00	0.00
Manganese	0.00	0.00	0.00	0.00	0.00	0.00	0.00	0.00
Titanium	0.00	0.00	0.00	0.00	0.00	0.00	0.00	0.00
Phosphorus	0.95	0.76	1.84	1.13	1.57	1.93	1.45	1.27
Calcium	5.67	5.77	6.33	11.40	13.80	11.20	8.60	9.46
Magnesium	1.46	1.18	2.09	1.69	1.65	2.29	1.73	1.72
Sodium	0.56	0.49	0.70	0.37	0.32	0.42	0.53	0.43
Potassium	10.50	7.40	12.60	9.59	6.23	10.50	9.78	9.16
Sulfur	0.52	0.50	0.62	1.24	2.04	1.54	1.06	1.09

Figure 1 Power And Co-Product Plant Concept

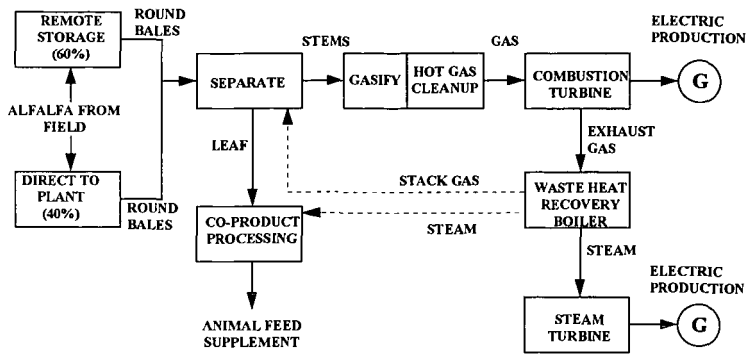


Figure 2 Processing Plant

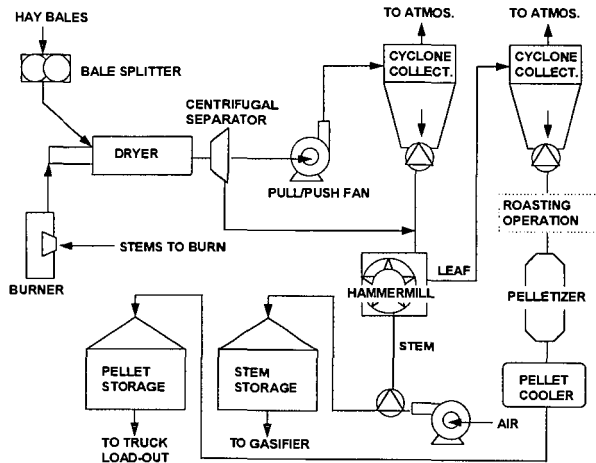
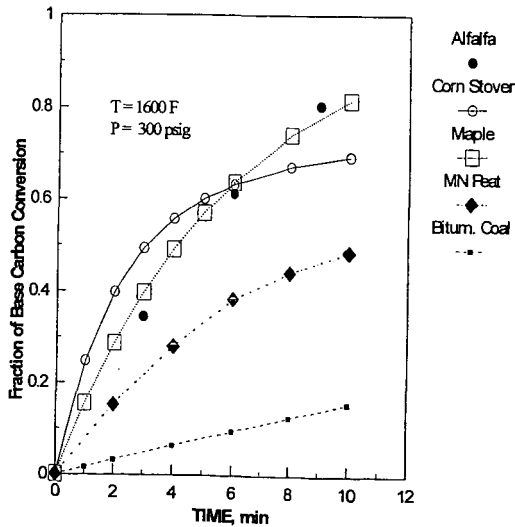


Figure 3. Comparison of Char Gasification Rates



PRESSURIZED THERMOGRAVIMETRIC REACTIVITY STUDY OF WHEAT STRAW COMBUSTION AND CO₂-GASIFICATION.

Ole Rathmann and Jytte B. Illerup
Department of Combustion Research
Risø National Laboratory
DK-4000 Roskilde, DENMARK.

Keywords: Wheat-straw biomass, Pressurized, Gasification reactivity.

Abstract.

Biomass fuel reactivity is interesting since biomass, as e.g. wheat straw, is a relevant fuel for advanced pressurized power plants due to the CO₂ neutrality. In this study combustion- and CO₂-gasification reactivities of pulverized wheat straw char up to 40 bar were investigated by isothermal thermogravimetric analysis, and the results were compared to a typical subbituminous coal. A recently built pressurized thermogravimetric analyzer of the horizontal type, with operating conditions at least up to 1200°C, 45 bar, was used. In the study the effects of temperature and partial pressure of the reactants O₂ and CO₂, respectively, were seen, for gasification also the inhibition effect of CO, whereas a distinct total pressure effect could not be observed. Also the effect of using non-pulverized straw pieces was investigated.

INTRODUCTION

The use of biomass fuels for power generation and heat production has a number of advantages with the CO₂ neutrality and saving of depletable fossil fuels among the most obvious. In addition, national legislation in Denmark urge to use locally available biomass as e.g. wood waste and straw. Considering the future, characterization of biomass fuel will thus be relevant in relation to combustion and gasification for high efficiency pressurized power plant types (as IGCC). As a result, research groups in Scandinavia and elsewhere have been active in characterizing the biomass fuels relevant in their respective countries, and main issues have been influence of pressure, temperature and gas composition on the reaction rate.

Especially wood, straw and black liquor char gasification reactivities at moderate reaction rates have been studied using large-sample vertical Pressurized ThermoGravimetric Analyzer (PTGA) instruments. Blackadder & Rensfelt (1985) studied pyrolysis of wood, cellulose and lignine up to 800 °C at 1 to 40 bar. Moilanen et al. (1993) investigated atmospheric steam gasification of chars of wood, peat and black-liquor in comparison with coal and brown-coal, while Whitty et al. (1993b) investigated pyrolysis and char CO₂-gasification of coarsely pulverized wood and peat at 850°C at 1-20 bar. Stoltze et al. (1993) studied atmospheric steam gasification of large samples of barley straw char at 750°C-950°C. Black liquor char was investigated by Backman et al. (1993) and by Whitty (1993) regarding pressurized CO₂- and steam gasification in presence of CO at 650-800°C and 1-30 bar. The following overall picture is seen: In pyrolysis, wood char yield increases clearly with increasing pyrolysis pressure, while the reactivity displays a weak decrease. Wood char reactivity is similar to that of peat and brown coal and about 1 order of magnitude faster than for coal, black liquor displays a reactivity 2 orders of magnitude faster than wood, and gasification with steam has a reactivity about 4 times faster than with CO₂. The reactivity increases strongly with increasing temperature and as seen for coal. Increase in total pressure at constant gas percentage composition has a weak, enhancing effect for wood while for black liquor the effect is directly reducing, attributed to inhibition by CO or H₂ inside the char pores.

In this work we have investigated combustion and CO₂-gasification reaction rates of straw as this fuel is expected to be one of the important biomass fuels in future advanced Danish power/heating stations. The work was performed under contract with and the Danish utility associations Elsam and Elkraft within the European Union APAS programme, and was supported by the Danish Ministry of Energy.

EXPERIMENTAL

The fuel samples were prepared from wheat straw normally used in Danish electrical-power/district-heating stations. Entire straws were ground to pulverized, average straw samples with a particle diameter smaller than 200µm. Char of pulverized straw, straw inter-node pieces, straw nodes and grains were produced in a furnace by a 7 minutes 900 °C pyrolysis heat treatment at atmospheric pressure without oxygen access. The raw fuel compositions given in table 1 indicate rather similar proximate compositions while ash compositions differ, especially with respect to K₂O and P₂O₅.

The PTGA-instrument used for the study (fig.1) is a modified DuPont thermogravimetric analyzer of the horizontal type, recently built at RISØ. The fuel sample is placed on a small 1cm diameter Platinum tray hanging on a horizontal balance arm, situated in a reaction tube together with thermocouples. The reaction tube is heated from outside by a heater element, and the entire thermobalance arrangement is placed inside a 35 l pressure vessel. Pressure and flow control are performed by a number of valves and gas mass flow controllers. The test gas, selectable from either an inert gas (N₂) source or a premixed reactive gas source, is supplied to the rear end of the reaction tube with a filler element to heat the test gas to operating temperature. A test gas rate corresponding to a linear velocity in the reaction tube of about 1 cm/s at 1000 °C is used giving a switching time for the gas composition at the sample position of about 100 s. The balance system is the original DuPont component, while reaction tube, oven and all external systems are new. The PTGA can operate up to 45 bar and 1200°C simultaneously. Samples up to about 150 mg can be investigated, but for low density fuels the practical limit is set by the fuel volume and may be 5 to 10 mg. Data logging is performed once per 2 seconds.

Pyrolysis experiments were performed in an inert test gas with a ramped temperature. The combustion and gasification reactivity experiments were performed isothermally with the operating temperature established in inert test gas after which the reactive test gas (N₂/O₂ or N₂/CO₂/CO mixture) was selected. The maximum conversion rate that could be measured was set by the test gas switching time and the maximum diffusion rate of reactant to the sample and within the sample.

The experimental weight signals were compensated for bouyancy and balance arm length expansion, based on calibration tests. For the reactivity experiments a transformation then followed of the compensated weight to a conversion degree X and a reactivity R(= reaction rate per remaining char)

$$X = (m_{c0} - m_c) / m_c \quad (1)$$

$$R = -dm_c/dt / m_c = dX/dt / (1-X) \quad (2)$$

where m_c and m_{c0} are the instantaneous and initial char mass on dry and ash free basis, respectively. Each reactivity experiment was characterized by the reactivity at 50% conversion, $R_{0.5}$, and the variation of R with conversion X was, as an approximation, described by a single normalized reactivity profile $f(X)$ (normalized to 1.0 at $X=0.5$) for each of the reaction types, i.e. $R(X) \approx R_{0.5} f(X)$. An estimate of the reaction time to a certain conversion degree could then be calculated as

$$t_X \approx 1/R_{0.5} \int_0^X \frac{f(X')}{(1-X')} dX' \quad (3)$$

RESULTS

A minor number of pyrolysis experiments were performed on raw, pulverized straw samples to see the influence of heating rate and pressure in the temperature range 150-1000°C. At 20 bar, heating rates of 10, 30 or 50°C/min had no effect on char yield. With a heating rate of 30°C/min the char yield seemed to increase weakly with pressure: 15%, 20% and 22% char yield (2.5% uncertainty) for 1.5, 20 bar and 40 bar, and the maximum pyrolysis rate occurred in a narrow range from 342°C to 355°C. More accurate experimental results are necessary to quantify the pressure effect on the char yield. As these results showed little effect of pyrolysis pressure it was assumed that the atmospheric pyrolysis pressure was of no importance for the resulting char.

Combustion reactivity was measured at temperatures from 300°C to 410°C, pressures from 1.5 bar to 40 bar and O₂ pressures from 0.08 bar to 0.8 bar. The results for $R_{0.5}$ are shown in fig.2. The reactivity increased with increasing conversion degree, with values at $X=0.2$ and $X=0.8$ about 0.6 and 1.7 times the value at $X=0.5$, respectively. While results at such low temperatures are not directly applicable to practical conditions they permit comparison to corresponding reference coal data. At 400°C and 0.26 bar O₂, the reactivity was found to be about 0.002s⁻¹, about 30 times higher than the reactivity for the reference coal. The dependence on temperature and O₂ partial pressure corresponds to an activation energy of 110 kJ/mole and a reaction order of 0.61. The activation energy is similar to that of the reference coal but the reaction order is a little lower. No significant effect of the total pressure was observed.

CO₂ gasification reactivity was measured in the fluidized-bed relevant temperature range 850°C-1050°C at 20 bar and with 3 different gas compositions, including one with the inhibitor-component CO, as shown in fig.3. A few of these experiments were repeated at 4 and 40 bar total pressure with unchanged CO₂/CO partial pressures. At 1000°C the reactivity R_{0.5} was found to be about 0.006s⁻¹ in 0.7 bar CO₂ and no CO. The reactivity increased with conversion degree, with values at X=0.2 and X=0.8 about 0.6 and 2 times the value at X=0.5, respectively. The present straw reactivity is about 16 times faster than for the reference coal and 1.5-2 times faster than for the wood reactivity as measured by Whitty et al.(1993a). The results for R_{0.5} could be interpreted in terms of Langmuir-Hinshelwood kinetics (see e.g. Laurendeau (1978)):

$$R_{0.5} = k_1 P_{CO_2} / (1 + aP_{CO} + bP_{CO_2}),$$

where k₁, a, and b have Arrhenius temperature dependence, for a and b, however, with negative activation energies. In spite of some unsystematic variation in the experimental data, saturation (described by the 'b' parameter) was clearly observed as the reactivity increased less than proportionally to the increase in CO₂ pressure from 0.7 to 2.2 bar in absence of CO. Also, the clear decrease in reactivity from 1.5 to 5 times, when changing from a 2/0 bar to a 2/2 bar CO₂/CO test gas, indicates clearly inhibition (described by the 'a' parameter) at the test temperatures. Both the saturation and inhibition effects showed an expected reduction with increasing temperature. The present results are too scarce to permit an unambiguous determination of kinetic parameters, but as shown in fig.3, a Langmuir-Hinshelwood representation could be obtained using a- and b-parameters from the reference coal in combination with a fitted k₁-parameter. However, the value of this k₁-parameter in dependence of temperature is strongly dependent on the applied values of the a- and b- parameters. The measurements suggest a moderate reactivity reduction with increasing total pressure, may be up to 2 times when the pressure is increased from 4 to 40 bar at constant CO₂ and CO partial pressures. In contrast to black liquor reactivity, the present data suggest an increasing reactivity when increasing the pressure at constant gas percentage composition.

The reactivity of char of non-pulverized 'straw particles' was measured at 900-1000°C with 20 bar pressure and 2/2 bar CO₂/CO partial pressure. Relative to the char of average, pulverized straw the inter-node particles showed a reactivity more than 2.5 times faster, node-particles showed a reactivity 2 times slower at 900°C while at 950°C and 1000°C it was more than 3 times faster than for pulverized straw. Grains showed a reactivity about 2.5 times slower than pulverized straw. The surprising faster reactions of inter-node and node particles may be due to the non-packed structure of the sample, but for the nodes this behavior may also be due to the higher concentration of the catalyst K₂O in the ash (see table 1).

DISCUSSION AND CONCLUSION

The present PTGA instrument has proved to be a valuable instrument for biomass fuel reactivity analysis at moderate reaction rates, in the present study of wheat straw.

Pyrolysis of pulverized straw suggested a small increase in char yield with increasing pressure. Pressurized combustion and gasification reactivity of straw char samples, pyrolyzed at low heating rate, was investigated up to 40 bar but with the main part of the investigations at 20 bar.

The combustion reactivity at low temperature (around 350°C) with 0.08 to 0.8 bar O₂ was somewhat more than one order of magnitude higher than for a reference coal and with the same relative temperature dependence. The dependence on O₂ partial pressure was weaker, and no significant dependence on total pressure (at constant partial pressure) could be observed.

CO₂-Gasification reactivity was investigated around 950°C at CO₂ and CO pressures around 1 bar. The results, displaying both CO₂-saturation and Co-inhibition, could be understood in terms of Langmuir-Hinshelwood kinetics, but more accurate measurements are necessary to actually determine the kinetic parameters. In absolute magnitude the straw char reactivity was found to be an order of magnitude higher than for the reference coal and also a little higher than for wood biomass. Char of non-pulverized 'straw-particles', including grains, displayed reaction rates moderately scattering above (3 times) and below (2 times) that of the pulverized samples, presumably as a combined result of size effect, compactness and composition of the non-pulverized particles. The pulverized fuel reactivity results displayed a moderate decrease with total pressure, but more accurate measurements are needed to tell whether this is a significant effect. Also, experiments with chars pyrolyzed at high heating rates at various pressures would be relevant to distinguish between the effects of total pressure through pyrolysis and through char gasification.

REFERENCES

- Backman,R., Frederick,W.J. and Hupa,M., *Basic Studies on Black-Liquor Pyrolysis and Char Gasification*. Bioresource Technology **46** (1993) pp 153-158.
- Blackadder, W., Rensfelt,E. (1985). *A pressurized thermobalance for pyrolysis and gasification studies of biomass, wood and peat*, in: Fundamentals of Thermochemical Biomass Conversion, edited by R.P. Overend et.al., Elsevier (1985).
- Laurendeau,N.M.(1978). *Heterogeneous Kinetics of Coal Char Gasification and Combustion*. Prog.Energy Combust. Sci. **4** (1978), pp 221-270.
- Moilanen,A., Saviharju,K. and Harju,T. (1993). *Steam gasification reactivities of various fuel chars*, in: Advances in Thermochemical Biomass Conversion, pp.131-141, edited by Bridgwater, A. V., Blackie Academic & Professional (1993).
- Stoltze,S., Henriksen,U., Lyngbech,T. and Christensen,O. (1993). *Gasification of straw in a large-sample TGA*. Nordic seminar on solid fuel reactivity, Gothenburg, Nov. 24th 1993.
- Whitty,K.J. (1993a). *Gasification of black liquor with H₂O under pressurized conditions*. M.Sc. thesis. Report 93-4, Dept. Chem.Engin. Åbo Akademi, Finland.
- Whitty,K.J., Sorvari,V., Backman,R.,and Hupa,M.(1993b). *Pressurized pyrolysis and gasification studies of biomasses*. Åbo Akademi, Department of Chemical Engineering, Report 93-7, IFRF Swedish-Finnish Flame Days 1993.

TABLES AND FIGURES

*Table 1. Fuel proximate-ultimate analysis.
Most relevant species and compounds are included.*

w% in dry non-pyrolyzed fuel	Pulv. straw (average)	Straw-nodes	Grain
Ash	6.4	9.0	1.6
Volatiles	77.3	75.1	83.2
Hydrogen	5.8		6.8
Carbon	47.2		44.6
w% in ash			
SiO ₂	62	2.7	1.4
CaO	8.1	11	3.7
MgO	1.8	3.4	11
Na ₂ O	0.4	0.2	0.2
K ₂ O	14	55	34
P ₂ O ₅	2.4	2.0	45

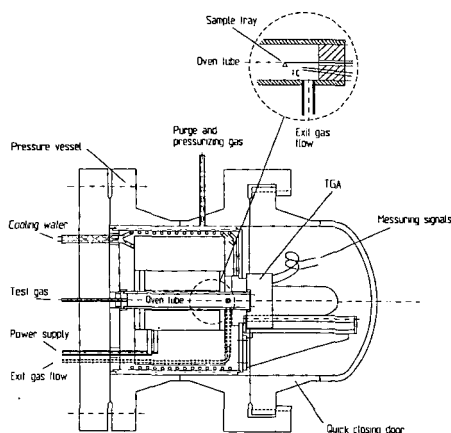


*Fig 1. Recently built Pressurized Thermogravimetric Analyzer instrument used in this study.
All electrical connection fit-throughs are placed in the rear flange (left side) of the pressure vessel.*

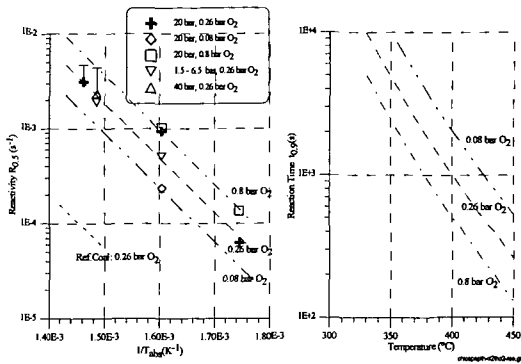


Fig.2. Straw char combustion reactivity experimental results.

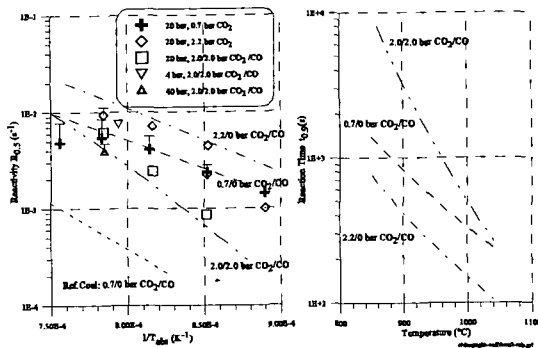


Fig.3. Straw char CO₂-gasification reactivity experimental results.

In both fig.2 and fig.3 representative Langmuir-Hinshelwood kinetic model values are shown by dashed and dash-dotted lines. Error bars indicate uncertainty due to large instrument diffusion limitation. The over-all accuracy is 10-15%. Preliminary results from a reference pulverized coal char (Colombian Cerrejón) are included. Predictions of conversion times to a conversion degree of 0.9 are shown in the right part of the figures.

PYROLYSIS AND COMBUSTION OF PULVERIZED WHEAT IN A PRESSURIZED ENTRAINED FLOW REACTOR

Jan Fjellerup, Erik Gjernes and Lars K. Hansen
Department of Combustion Research
Risø National Laboratory
DK-4000 Roskilde, Denmark

Keywords: Straw, pressurized, reactivity

INTRODUCTION

During recent years there has been an increasing interest for pressurized combustion and gasification of solid fuels in power plants due to the potential for high efficiency. The utilization of new types of solid fuels for pressurized combustion and gasification depends on the reactivity at relevant conditions. Risø's pressurized laboratory was established in 1992 with the aim of studying pressurized pyrolysis, combustion and gasification of solid fuels. At present the laboratory comprises a Pressurized Entrained Flow Reactor (PEFR) and a Pressurized Thermogravimetric Analyzer (PTGA) for the study of reactivity of solid fuels at high pressure. In the present paper the PEFR facility is presented and pyrolysis and combustion of pulverized straw at elevated pressure are shown.

EXPERIMENTAL

The PEFR facility

Pyrolysis and combustion of pulverized wheat were performed in a PEFR [1]. The reactor is operated differentially, which means that the reactant gas flow is large compared to the particle flow. This implies that during combustion or gasification of solid fuels, the bulk concentration and temperature are well controlled. The system layout of the facility is seen on Figure 1. The main components are the gas mixing system, pressure vessels, furnace, moveable probe, gas outlet and conditioning system. The systems consists of a vertical cylindrical furnace fed with a reaction gas of a specified composition. The furnace consists of three parts; a gas preheater section and two half cylinder reactor sections each with Super Kanthal heating elements which can give a maximum reactor temperature of 1500°C.

The fuel is fed pneumatically by the primary gas through a narrow ceramic tube and enters near the top of the reaction tube. The fuel tube is mounted through the centre of the gas preheater and cooled by water to avoid reaction of the fuel in the preheating section. The reactor tube is approximately 7 cm ID and 2 m long. The probe can be positioned to collect particles at various distances and thereby various residence times. The probe is water cooled and nitrogen quench gas is added to the top of the probe to stop the chemical reaction instantaneously as soon as the particles enter the probe. The collected particles are trapped on a filter, and they are analyzed for moisture, volatiles and ash content in the TGA. The conversion of the particles is determined using the ash tracer technique.

The furnace is built into a 100 bar pressure vessel. The reaction gas is a mixture of various gases N_2 , O_2 , H_2 , CO_2 , CO , CH_4 and H_2O (as steam). The reaction gas is added to the top of the furnace after being preheated to the furnace temperature. The flow is estimated to give the wanted gas velocity in the furnace at the actual furnace temperature and pressure. An average gas velocity of 0.3 m/s is used in all experiments. Assuming a laminar parabolic velocity distribution, the 0.3 m/s average gas velocity corresponds to a gas velocity of 0.6 m/s centrally in the reactor.

The performance of the facility is listed in table 1.

Fuel selection and preparation

The biomass selected for this study was Danish wheat, which were pulverized [2] and sieved with an Alpine sieve. The size distribution based on mass can be seen in Table 2, while the proximate and ultimate analysis are shown in Table 2 and 3, respectively [3].

RESULTS AND DISCUSSION

In the PEFR experiments samples were taken out at five different locations representing a residence time of 0.5 to 2.5 s. The residence time is based on a velocity of 0.6 m/s. All samples have been double analyzed for ash percentage in the TGA, and the conversion is calculated using the ash tracer technique. The results are presented as m/m_0 , which is the collected DAF (Dried and Ash Free) mass divided by the initial DAF mass.

Pyrolysis

The pyrolysis experiments were performed at 10 bars total pressure in an atmosphere of pure nitrogen, and at temperatures of 700, 800, 900 and 1000°C. Figure 2 shows the m/m_0 value plotted versus time for the 1000°C case. The experiments resolved a mass loss profile showing that the m/m_0 value is decreasing towards the end point at 2.5 s. The final values for the 700 to 1000°C experiments were 0.14, 0.12, 0.10 and 0.11. For the 900 and 1000°C cases approximate constant m/m_0 values were found at the last three probe positions which corresponds to a residence time of 1.2, 1.6 and 2.5 s. By averaging the results from these three probe positions the m/m_0 value became 0.10 for both cases. The proximate analysis gave a pyrolysis yield of 81.5%, while in the present experiments the yield is increased to 90%.

Combustion

Combustion experiments were performed in an atmosphere of nitrogen and oxygen at 800°C and 10 bar and at 1000°C using both 10 and 20 bars total pressure. The mass loss profile for the experiments at 800°C is shown in Figure 3 and the pyrolysis level found above is indicated by a solid line. Figure 3 shows that for a residence time of 0.5 s the m/m_0 is below the pyrolysis level, which means that the straw has started to burn. For a residence time of 1.2 s the particle has burned more than 98% (pyrolysis+combustion), and the conversion remains constant with residence time. Figure 4 shows that at 10 bar and 1000°C the pulverized straw has burned 95% at 0.5 s residence time. The final conversion at 2.5 s residence time is 99.5%, which is higher than the 800°C case. At 20 bars pressure the conversion at 0.5 s residence time is only 80% compared to 95% at 10 bars pressure, even though, the oxygen partial pressure is higher for the 20 bars experiments. The final conversion at 2.5 s residence time is 97%. Thus the general trend is that the combustion reactivity is decreased with increasing total pressure.

CONCLUSION

The pyrolysis experiments show that the pulverized straw pyrolysis 90 % of DAF in the PEFR at 1000°C and 10 bars pressure, which is above the volatile yield from the proximate analysis (81.5% of DAF). The pyrolysis in the reactor at 900-1000°C reaches its final values in about 1 s.

The combustion experiments show a high reactivity with oxygen, at 10 bar and 1000°C the pulverized straw has burned 95% at a residence time of 0.5 s. Increasing the absolute pressure from 10 to 20 bar for similar temperature and oxygen partial pressure reduces the conversion of the pulverized straw.

ACKNOWLEDGMENTS

This work has been performed within the European Union APAS Clean Coal Technology Programme for the Danish utility associations Elsam and Elkraft and for the Danish Ministry of Energy under the EFP91 programme.

REFERENCES

1. Hansen, L.K., Fjellerup, J., Stoholm, P. and Kirkegaard, M. (1995). *The Pressurized Entrained Flow Reactor at Risø. Design Report. Risø-R-822(EN)*.
2. Wenzel, W. et al. (1994). *Versuche zur Grosskornvergasung von Stroh in der Versuchsanlage Freiberg* (in German). NOELL Energie- und Entsorgungstechnik GmbH, Freiberg.
3. Illerup, J.B. and Ethelfeld, J. (1995). *Combustion and Gasification of Coal and Straw under Pressurized Conditions. Task 1: Preparation and characterization of fuels. Risø-R-809(EN)*, Risø National Laboratory, Denmark.

Table 1. The performance of the PEFR facility

Pressure	0.1 - 80 bar
Primary gas flow	0.3 - 6.0 Nm ³ /hr
Reaction gas flow	1.5 - 30 Nm ³ /hr
Reaction gas preheating	600 - 1500°C
Reactor temperature	600 - 1500°C
Fuel (coal or biomass) up to 10mm	10 - 300 g/h
Optical ports (Used at moderate pressures)	10 (2 in two levels) (3 in two levels)

Table 2. Size distribution based on mass (sieve method) and proximate analysis of pulverized wheat (wt%)

Size (µm)	wt %
> 1000	0
500 - 1000	0.2
250 - 500	6.2
125 - 250	25.0
63 - 125	14.7
32 - 63	9.5
< 32	44.4

	Dry	DAF
Fixed Carbon	17.5	18.5
Volatiles	77.3	81.5
Ash	5.2	---

Table 3. Ultimate Analysis, wt

C	H	N	S	Cl	Na	K	O
47.2	5.8	0.7	0.17	0.17	0.034	0.70	45.2

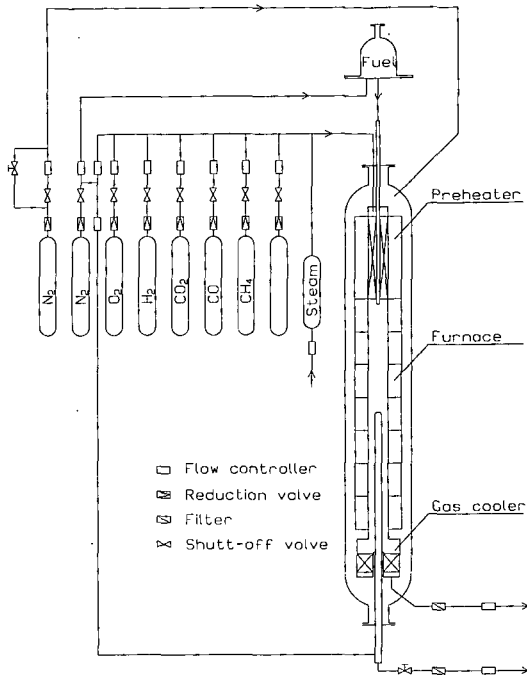


Figure 1. PEFR system layout

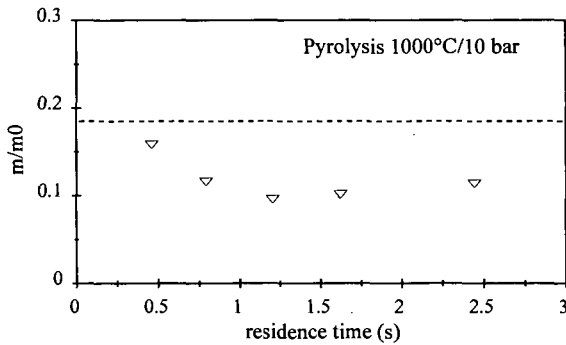


Figure 2. Pyrolysis of pulverized straw at 10 bar and 1000°C. Collected DAF mass divided by the initial DAF mass (m/m_0) is plotted versus residence time. The line indicates proximate pyrolysis level.

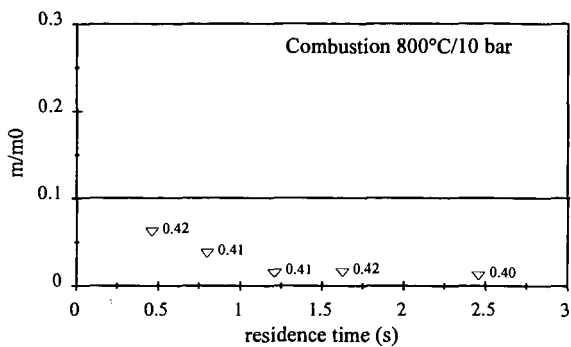


Figure 3. Combustion of pulverized straw at 10 bar and 800°C. Solid line indicates pyrolysis level, and partial pressure of oxygen in bar is written at each point.

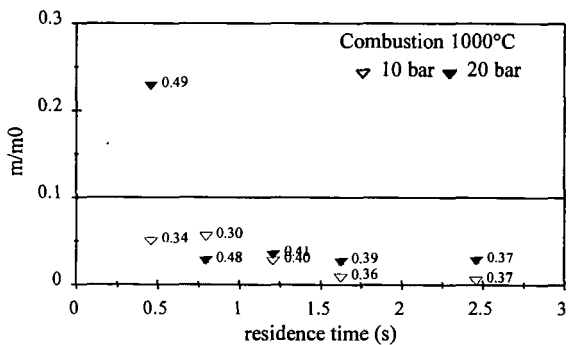


Figure 4. Combustion of pulverized straw at 10 and 20 bar and 1000°C. Solid line indicates pyrolysis level for the 10 bar case, and partial pressure of oxygen in bar is written at each point.

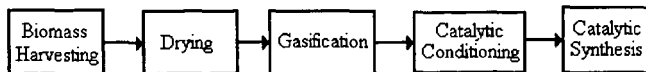
LIFETIME TESTING OF CATALYSTS FOR CONDITIONING THE PRODUCTS OF A BIOMASS GASIFIER

W. A. Jacoby, S. C. Gebhard and R. L. Vojdani
National Renewable Energy Laboratory
1617 Cole Boulevard
Golden, CO 80401

Keywords: synthesis gas, hot-gas conditioning, biomass gasification

INTRODUCTION

The National Renewable Energy Laboratory, in collaboration with its industrial and academic partners, is engaged in a project with the goal of developing and facilitating the commercialization of safe, cost-effective, and environmentally benign technologies for the production of transportation fuels from biomass via thermal gasification. The block diagram below illustrates the steps involved.



The research presented in this paper focuses on the catalytic conditioning step, also referred to as hot-gas conditioning. The product of biomass gasification is crude synthesis gas, a mixture of hydrogen (H_2), carbon monoxide (CO), carbon dioxide (CO_2), methane (CH_4), steam, and higher molecular weight hydrocarbons and oxygenates (referred to as tar). The goals of synthesis gas conditioning are threefold: 1) reduce the concentration of tar by catalyzing steam reforming reactions; 2) reduce the concentration of methane by catalyzing steam reforming reactions; 3) increase the hydrogen/carbon monoxide ratio from the value of 0.7 (representative of crude syngas from a biomass gasifier) to about 2 (desirable for production of syngas or H_2) by catalyzing the water-gas shift reaction.

Previous investigations have focused on developing catalysts or disposable solids to achieve hot-gas conditioning. The most promising materials identified in recent work have been commercial supported nickel (Ni)-steam reforming catalysts and dolomite.¹⁻⁷ Dolomite is only moderately effective for tar destruction. The primary issue with Ni-based steam reforming catalysts is lifetime. When exposed to the high molecular weight aromatic hydrocarbon and oxygenated compounds found in biomass gasifier tar, supported Ni catalysts deactivate on a time scale that is unacceptable for commercial use.

EXPERIMENTAL METHODS

The experimental apparatus is illustrated in Figure 1. It includes a vaporizer enclosed in a single zone furnace. A high pressure, positive displacement liquid pump feeds water to the vaporizer for steam generation. A second identical pump supplies a mixture of aromatics (benzene, toluene, and naphthalene) to simulate the tar found in syngas from a biomass gasifier. The liquids are vaporized in a stainless steel tube packed with stainless steel balls. Hydrogen and a 3:1:1 mixture of CO, CO_2 , and CH_4 , are also metered into the vaporizer through mass flow controllers. This model crude syngas solution is fed into a catalytic reactor operating in down-flow mode and heated by a three zone furnace equipped with microprocessor temperature control. Reactors are fabricated from stainless steel with aspect ratios appropriate for catalyst loads between 0.5 grams and 30 grams. Catalyst particles are ground and sieved to 16-20 mesh size (0.841 mm to 1.19 mm). Two basic reactor/catalyst configurations are tested, a commercial Ni-based steam reforming catalyst alone and Ni catalyst in conjunction with an upstream high-temperature water-gas shift co-catalyst in a dual bed reactor. The Ni catalysts are reduced overnight (15 hrs) prior to use in a stream of 14% H_2 in steam and He at 600°C. The composition of the feed and product mixtures is monitored by two computer controlled, on-line gas chromatographs; one for the permanent gases (Carle Refinery gas analyzer) and one for tar (Hewlett Packard 5890II with a DB-5 capillary column). The apparatus is automated and equipped with safety features that allow it to operate unattended during extended lifetime tests.

RESULTS AND DISCUSSION

Supported Ni catalysts will catalyze steam reforming of methane and tar compounds. Figure 2 illustrates the performance of United Catalysts Inc. (UCI) G90B Ni catalyst in treating the model crude syngas mixture with a steam mole fraction of 0.5. The simulated tar solution introduced into the vaporizer was comprised of 5 mole percent naphthalene in benzene. The composition of the effluent gas was monitored hourly. The observations reported were made under steady state conditions more than 60 hours into the run. We observed near complete conversion of tar and a high conversion of methane by steam reforming; however, the effluent mixture did not achieve equilibrium with respect to water-gas shift and CO hydrogenation.

The issue of catalyst lifetime was addressed during a subsequent experiment run under similar conditions. The UCI G90B remained active for 585 hours (the experiment was stopped at this time when a feed line plugged). A significant build up of coke was observed in and around the catalyst bed and many of the catalyst particles had been reduced to a fine powder. The steam content of the syngas produced during biomass gasification can be as low as 0.3-mole fraction¹, therefore the performance of the catalyst at lower steam to carbon ratios is of interest. Figure 3 shows that reducing the steam mole fraction in the feed

shortens catalyst lifetime. Thus, the use of supported nickel catalyst alone may not be practical for the synthesis gas conditioning application.²⁻⁴ In all cases in Figure 2, steam is in excess over that required by stoichiometry for both steam reforming of tar and the water-gas shift reaction. The large effect of steam concentration in this case supports previous assertions that the water adsorption rate is important for these reactions.⁸

Alumina will catalyze the water-gas shift reaction at high temperatures⁹. Figure 4 illustrates this activity for χ -alumina at 815°C. Near equilibrium concentrations of CO, H₂, and CO₂ were observed with and without steam pretreatment (50% steam in He for 10 hours at 850°C) and in the presence and absence of a model tar compound (1 mole percent toluene). In separate experiments, an η -alumina also catalyzed the water-gas shift reaction. Coke was not formed to a significant extent on either of the aluminas.

The combined effect of the alumina and nickel catalyst would fulfill the syngas conditioning objectives if their performance characteristics were additive. Figure 5 shows the results of an experiment addressing this possibility. The primary bed containing Imperial Chemical Industries (ICI) 46-1, K-promoted supported Ni catalyst was combined with an upstream co-catalyst bed of χ -alumina. The ICI catalyst was used in this initial proof of concept run because it has been shown to be active for conditioning of the effluent of a biomass gasifier and is resistant to deactivation.¹⁰ Later experiments involved UCI G90B because it was expected that this catalyst would be more susceptible to deactivation in this application, increasing the sensitivity of investigation of the efficacy of the alumina bed.¹¹ This dual bed reactor was fed with a model crude syngas mixture containing a 0.5-mole fraction steam and a 0.01-mole fraction toluene. Figure 5 shows that both toluene and methane steam reforming and water-gas shift are achieved simultaneously. Thus, the dual bed concept provides the catalyst activity needed to effectively condition biomass gasifier synthesis gas, but questions of catalyst lifetime remain.

The function of the upstream, co-catalyst bed is to catalyze the water-gas shift reaction. This is postulated to improve the lifetime of the downstream Ni steam reforming catalyst by increasing the concentration of hydrogen adsorbed on the surface of the Ni crystallites. An increased surface hydrogen atom coverage could inhibit coke formation if the rate of hydrogenating adsorbed coke precursors is greater than the rate of precursor polymerization. Table I outlines a 2² factorial designed to test this hypothesis. The primary response is the elapsed time until the "end of useful life". This transition corresponds to a loss of tar and methane reforming activity, i.e., when gas chromatographic peak areas for methane and tar compounds rose to within experimental error of the areas of the same peaks during control runs.

Table 1 also summarizes the results of the 2² factorial subset of this experimental work that has been completed to date. In this work, the model crude syngas mixture contained 0.3-mole fraction steam and a 0.03-mole fraction of tar solution comprised of 5 mole percent naphthalene in benzene. Based on the results of previous work, the total gas flow rates and the amounts of UCI G90B and alumina were chosen to give a gas hourly space velocity (GHSV) of 170,000 h⁻¹ for the Ni catalyst, and a GHSV = 2,000 h⁻¹ for the alumina catalyst. The response reported for the 2² factorial experiment is the loss of tar reforming activity. In some cases, the loss methane of reforming activity occurred more quickly than the loss of tar reforming activity, but our conclusions regarding the use of the alumina co-catalyst bed are not altered.

This 2² experimental design investigated the main effects of the presence or absence of an upstream alumina co-catalyst bed and the temperature of the reactor. It shows that the co-catalyst bed significantly increases the lifetime of the Ni catalyst (B = +55 hours). Figure 6 illustrates this effect; increased lifetime was observed with respect to methane, benzene, and naphthalene steam reforming. Data analysis also revealed that the temperature and temperature-co-catalyst interaction are less important (T = +13 hours and B x T = +23 hours). When the entire 2² design matrix has been completed, it will be possible to estimate the standard error in the response based on the magnitude of third and fourth order interactions and tests of significance will be performed.

CONCLUSIONS AND FUTURE WORK

Our results show that a dual bed configuration using alumina as a co-catalyst upstream of a conventional Ni-based steam reforming catalyst provides appropriate activity and can increase the catalyst lifetime for catalytic conditioning of a model biomass gasifier product gas. The full experimental design also addresses main effects and interactions involving steam mole fraction and reactor temperature, as well as a comparison of the UCI G90B catalyst and an experimental catalyst (Ni/Al₂O₃ promoted with oxides of chromium, magnesium, and lanthanum). The results of a comprehensive catalyst characterization effort will be reported and the use of mixed metal oxides with perovskite structures as the co-catalyst are also planned. Finally, the optimal configuration identified in the laboratory experiments will be tested with syngas generated in a pilot scale biomass gasifier currently under construction at NREL.

ACKNOWLEDGEMENTS

This work was funded by the Department of Energy's Biofuels Systems Division through the NREL Biofuels Program. The authors would also like to thank Esteban Chornet, Ralph Overend, Robert Evans, and Helena Chum for useful discussions.

REFERENCES

1. Furman, A. H., Kimura, S. G., Ayala, R. E., and Joyee, J. F. Biomass gasification pilot plant study. AEERL-748, 3R, 6/8/93. Prepared for the U. S. Environmental Protection Agency, Office of Research and Development, Washington, DC.

- Aznar, M. P., Corella, J., Delgado, J., and Lahoz, J. Improved steam gasification of lignocellulosic residues in a fluidized bed with commercial steam reforming catalysts. *Ind. Eng. Chem. Res.* 32, 1-10 (1993).
- Baker, E. G., Mudge, L. K., and Brown, M. D. Steam gasification of biomass with secondary catalysts. *Ind. Eng. Chem. Res.* 26, 1335 - 1339 (1987).
- Donnot, A., Magne, P., and Deglise, X. Method of determining catalyst lifetime in the cracking reaction of tar from wood pyrolysis. *J. Anal. and Appl. Pyrolysis*, 22 39 - 46 (1991).
- Simell, P. A. and Bredenberg, J. B. Catalytic purification of tarry fuel gas. *Fuel* 69, 1219 - 1225 (1990).
- Simell, P. A., Leppälähti, J. K., and Bredenberg, J. B. Catalytic purification of tarry fuel gas with carbonate rocks and ferrous materials. *Fuel* 71, 211-218 (1992).
- Vassilatos, V., Taralas, G., Sjöström, K., and Björnbom, E. Catalytic cracking of tar in biomass pyrolysis gas in the presence of calcined dolomite. *J. Canadian Chem. Eng.* 70, 1008 - 1013 (1992).
- Rostrup-Nielsen, J. R. Activity of nickel catalysts for steam reforming of hydrocarbons. *J. Catal.* 31, 173-199 (1973).
- Amenomiya, Y. Active sites on solid acid catalysts, II. Water-gas conversion on alumina and some other catalysts. *J. Catal.* 55, 205 - 212 (1978).
- Zhou, J. Catalytic tar reforming for gasified biomass. Masters Thesis, University of Hawaii, 1994.
- Mudge, L. K., Baker, E. G., Brown, M. D., and Wilcox, W. A. Bench scale studies on gasification of biomass in the presence of catalyst. Report PNL-5669, Pacific Northwest Laboratories, Richland, WA, 1987.

Table 1: 2⁴ Experimental Design and Initial Results

Factors				Variable	Levels	
B	T	S	K		-	+
-	-	-	-	B = Co-catalyst Bed	no	yes
+	-	-	-	T = Temperature	750°C	800°C
-	+	-	-	S = Steam Mole Fraction	30%	40%
+	+	-	-	K = Ni Catalyst	UCI G90B	Exp.
Initial Results: 2² Design						
+	-	+	-			
+	+	+	-			
-	+	+	+			
-	-	-	+			
+	-	-	+			
-	+	-	+			
+	+	-	+			
-	-	+	+			
+	-	+	+			
-	+	+	+			
+	+	+	+			

Figure 1: Schematic of Experimental Apparatus

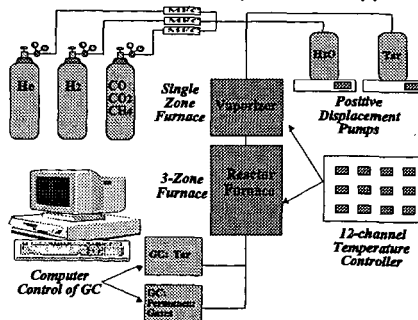


Figure 2: Activity of UCI G90B Catalyst

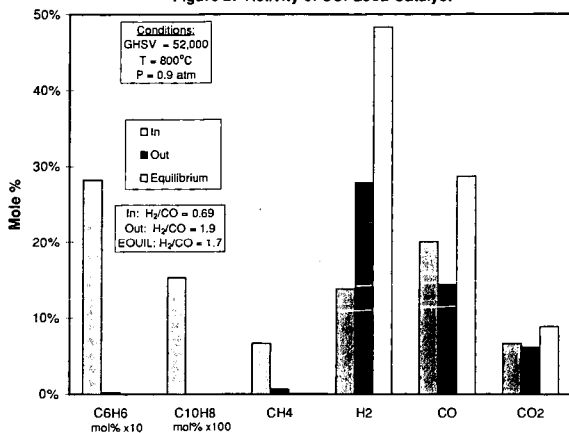


Figure 3: Effect of Steam on Time to Complete Deactivation for UCI G90B

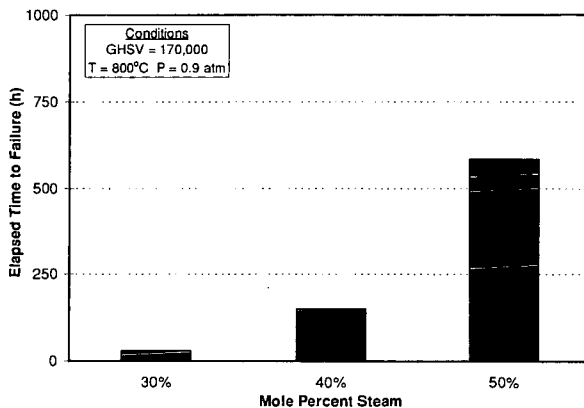


Figure 4: Water Gas Shift Activity of γ -Alumina Catalyst

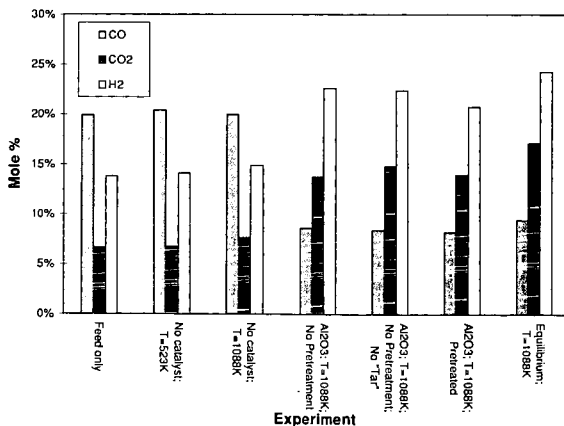


Figure 5: Activity of Dual Bed System with ICI 46-1 and γ -Al₂O₃

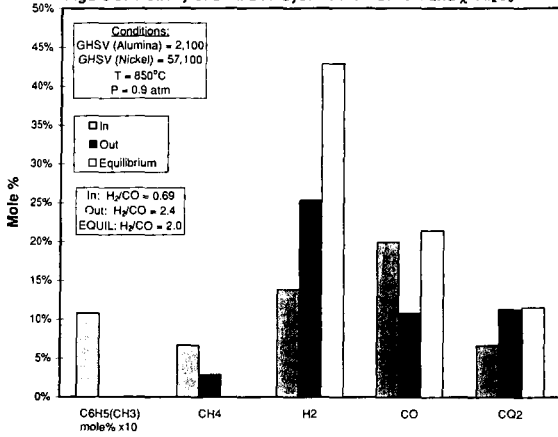
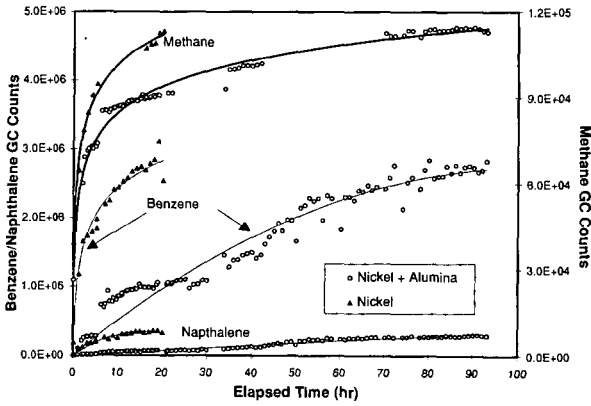


Figure 6: Steam Reforming Activity vs. Elapsed Time



INDIRECT LIQUEFACTION OF BIOMASS: A FRESH APPROACH

J.L. Cox, A.Y. Tonkovich, D.C. Elliott, E.G. Baker
Pacific Northwest Laboratory
Richland, Washington 99352

E.J. Hoffman
P.O. Box 1852
Laramie, Wyoming 82070

Keywords: gasification, liquefaction, biomass

INTRODUCTION

A variety of gaseous products for use as synthetic fuels and chemicals are produced by gasifying biomass. The actual product composition depends on the biomass composition and the reaction conditions. Several different gasification approaches have been investigated, at rather small scale, and reported in the literature (1,2). Many of these methods have their roots in coal gasification, including the work on catalytic gasification presented by Baker and Mudge (3) and Cox et al. (4). Catalytic gasification takes advantage of catalysts to serve two primary functions: 1) to increase the yield of gases, at the expense of tar and char, at lower temperatures than are possible without catalysts, and 2) to catalyze secondary reactions to produce the specific product desired. Sufficiently high rates can be achieved to allow operation at lower temperatures so that oxygen is not needed as a co-reactant, thus eliminating the need for an oxygen plant.

One catalytic approach to producing synthetic fuels and chemicals is indirect liquefaction of biomass, which entails gasifying the biomass to create a synthesis gas consisting of hydrogen and oxides of carbon. These materials, in turn, are converted to the desired liquid fuels and/or chemicals by suitable choice of catalyst, synthesis gas composition, and reaction conditions. This type of approach has been extensively investigated where coal is the carbonaceous feed material, but it has not been extended seriously to biomass and other feedstocks. It is generally recognized that developing gasification methods to produce the synthesis gas poses one of the major technical and economic challenges to improving this technology. This paper reports a different slant on indirect liquefaction that could stimulate advancements in the efficiency and economics of the process for biomass.

BIOMASS GASIFICATION - A NEW APPROACH

The new approach to biomass gasification outlined here is predicated on the concept that it is better to gasify biomass to a CO₂-synthesis gas composed primarily of H₂ and CO₂, rather than a CO-synthesis gas composed primarily of H₂ and CO. The conversion to CO₂-syn gas, and its subsequent utilization, may be superior, both technically and economically, to the route through a CO-syn gas.

A comparison of the stoichiometry of the respective routes is shown in Reactions (1) and (3), respectively.



Both carbon-steam (C-H₂O) gasification reactions are endothermic. The enthalpy of the C-H₂O reaction to produce CO-syn gas is 31.4 kcal/g-mole, while only 21.6 kcal/g-mole are required for the CO₂-syn gas reaction. The difference between the two reactions is the exothermic (-9.8 kcal/g-mole) CO-shift reaction given in Reaction (2). Clearly, biomass is not carbon; nevertheless, the conclusions are the same except the steam gasification of biomass is even more facile than carbon (i.e., graphite), and the thermodynamics are more favorable.

Minimizing the energy requirements for the gasification portion of the overall sequence in the indirect conversion to fuels and chemicals eases the burden of the most costly and inefficient step in the overall process. Pinto and Rogerson (5) report the cost of the reformer/gasmaking portion of a steam-reforming methanol plant constitutes 45% of the total capital cost. Henery and Louks (6) have shown that the economics of producing synthetic natural gas (SNG), i.e., methane, from coal and lignite depend strongly on the

cost of adding heat to the steam-carbon reaction. The amount of heat supplied and the method by which it is supplied to the gasification reactions are highly critical to the economics. In the case of SNG, Henery and Louks (6) estimate the cost of the gasification heat is 1/3 the cost of product (SNG). Any process that takes advantage of exothermic gasification reactions (e.g., $\text{CO} + \text{H}_2\text{O} = \text{CO}_2 + \text{H}_2$ and $\text{C} + \text{H}_2 = \text{CH}_4$) in the gasifier can reduce external heat requirements and substantially improve process economics and efficiency. Calculations based on Reactions (1) and (3) indicate that CO_2 -syn gas requires 31% less energy to produce than CO-syn gas.

Another advantage of biomass in general is its reactivity allows sufficiently low temperatures (<750°C) to be employed so that reaction enthalpy can be supplied indirectly by a tube still reactant heat exchanger. Consequently, there is no need for pure oxygen or a plant to produce it, and a major expense and energy penalty to the gasification section of the operating plant is eliminated.

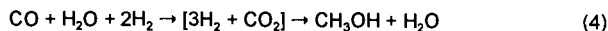
Because the reactivity of biomass varies among the different types (7,8), reaction conditions can be selected to favor the production of CO_2 -syn gas over CO-syn gas, including temperature, residence time, steam:biomass ratio, and the use of catalysts. The predicted gasification product composition is particularly sensitive to temperature and steam:biomass feed ratios. This sensitivity is shown in the equilibrium data in Table I, which indicate that the optimum conditions for producing CO_2 -syn gas are high steam:biomass ratio, low temperatures, and low pressures. At 1 atm, 600°C, and a steam:biomass (i.e., $\text{H}_2\text{O}:\text{C}$) mole ratio of 10:1, the product gas composition is 65.4% H_2 , 31.2% CO_2 , 3.0% CO, and 0.4% CH_4 . Since biomass has about 30 wt% oxygen, the amount of water required is predicted to be substantially less than 10:1.

While practically all gasification studies, irrespective of carbonaceous feedstock, have been conducted with the goal of producing CO-syn gas, there is sufficient experimental and theoretical evidence to suggest that, through reaction engineering principles, high conversions of feedstocks can be achieved, producing high yields of CO_2 -syn gas. Some of the predictions in Table I can be compared with experimental results under similar conditions shown in Table II.

CO- AND CO_2 - SYNTHESIS GAS CHEMISTRY

Work on the use of synthesis gas to produce a broad range of products began about 70 years ago in Germany with the production of fuels using cobalt catalysts (11-13). While this chemistry is loosely referred to as Fischer-Tropsch in recognition of the pioneering and extensive contribution of these individuals, there has been literally hundreds of significant contributors. The use of CO-syn gas has been the focus of this work, while CO_2 -syn gas has scarcely been considered.

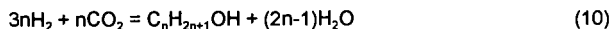
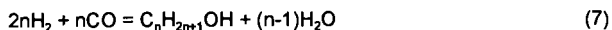
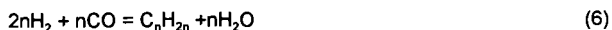
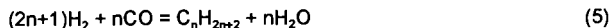
Table III illustrates the range of products that can be produced from CO-syn gas. Interestingly, optimum methanol synthesis over Cu/ZnO catalysts requires about 5% CO_2 in the inlet gas. If the CO_2 content is lower or higher, the methanol formation rate drops. Furthermore, the methanol formation apparently does not occur if the synthesis gas is free of CO_2 and H_2O . Russian investigators (18,19) have accounted for these observations by a mechanism where methanol formation is dominated by hydrogenation of CO_2 formed during reaction by the water gas shift reaction from CO:



Kuechen et al. (20) reported that a deactivated Cu/ZnO catalyst at 3-5 Mpa (30-50 atm) and 483-543K gave maximum rates of methanol synthesis with H_2 -CO-CO₂ syn gas ratio 70:0:30. The activation energy of methanol synthesis from CO_2 and H_2 was considerably lower than that from CO and H_2 . Cox et al. (4) reported the methanation of CO-free CO_2 -syn gas ($4\text{H}_2/\text{CO}_2$) in a packed bed reactor over supported nickel catalyst at 375°C, 100 psig, and space velocities of up to 7000 hr^{-1} .

REACTION COMPARISONS

Many of the synthesis schemes that have used CO-syn gas in the past appear to be possible using CO_2 -syn gas, as indicated here. The respective stoichiometries of aliphatic, olefin, and alcohol hydrocarbon formation from CO- and CO_2 -syn gases are shown in Reactions (5) through (10). The thermochemistry of some of the simpler homologs of these series of compounds is shown in Tables IVA and IVB. The data show that each are exothermic with favorable free energy changes at low temperatures and high pressures.



The advantage of using CO₂-syn gas in place of CO-syn gas may have significant overall process implications and, in some instances, reaction-specific benefits, as discussed below. For example, a comparison of the enthalpies of the CO- and CO₂-syn gases at 300°C shows the methanation to be about 18% less for the CO₂-syn gas (Reaction 8, n=1) than for CO-syn gas (Reaction 5, n=1), 35% less for the olefin formation (Reaction 9, n=2), 39% less for methanol formation (Reaction 10, n=1), and 29% less for ethanol formation (Reaction 10, n=2). Both CO- and CO₂-syn gas reactions are favored by pressure, but the CO-syn gas reactions are more favored than CO₂-syn gas. Comparative volume contractions for CO-syn gas versus CO₂-syn gas reactions are 50% versus 40% for methanation, 50% versus 37.5% for olefin formation, 66.5% versus 40% for methanol formation, and 66.7% versus 50% for ethanol formation. Hence, pressure can be used to considerable advantage to increase equilibrium conversions.

As expected from the enthalpies of reaction, the free energies are less for the respective CO₂-syn gas reactions. At 200°C, the respective free energy change (kcal/mole) for the CO- and CO₂-syn gas reactions are, respectively, -24.6 versus -19.5 for methanation, -13.46 versus -3.25 for olefin formation, 3.8 versus 8.9 for methanol formation, and -9.9 versus 0.3 for ethanol formation. For those reaction conditions with positive free energy changes, elevated pressures can be used to increase equilibrium yields, as is currently practiced in the commercial production of methanol from CO-syn gas. In the alcohol synthesis reactions, where free energy changes are not as favorable as for the other hydrocarbon synthesis reactions, higher pressures would be required to achieve equivalent equilibrium yields with the CO₂-syn gas.

Although some adjustments may be needed, these comparisons show the two synthetic gases to have comparable reactions for producing the desired products. Another salient feature of the new approach is that carbon deposition should not be the problem it is for CO-syn gas since the CO₂ counters the Boudouard reaction.



In addition, as can be seen from the thermodynamic data in Table IVB, synthesis reactions with CO₂-syn gas are less exothermic, reducing the difficulty of temperature control and expense of extra duty heat transfer equipment encountered when using CO-syn gas. Furthermore, lowering the concentration of CO alleviates a safety concern.

CONCLUSIONS

A new approach to indirect liquefaction of biomass is advocated based on the premise that it is easier to gasify the biomass to a CO₂-syn gas than to a CO-syn gas. Thermodynamic arguments are presented that show an energy savings of about 30%. Experimental data are presented that are consistent with the thermodynamic prediction that a CO₂-syn gas can be achieved through control of gasification conditions. Optimum gasification conditions are about 600°C, atmospheric pressure, and steam:biomass ratio equal to 10:1 in the presence of a gasification catalyst. The CO₂-syn gas under these conditions consists of 65.4% H₂, 31.2% CO₂, 3.0% CO, and 0.4% CH₄. Thermodynamic predictions have also been presented along with experimental results that indicate the range of products produced by catalytic conversion of CO₂-syn gas is comparable to products produced with CO-syn gas. Furthermore, carbon deposition and heat removal and temperature control are predicted to be more easily controlled with CO₂-syn gas chemistry. Even if catalytic conversion diversity with CO₂-syn gas is not as versatile as with CO-syn gas, the gasification to CO₂-syn gas represents an improvement in gasification efficiency, and the process can be used to produce fuel gas and hydrogen. While the discussion has focused on biomass, the concepts presented herein are appropriate for other carbonaceous materials such as coal and natural gas.

ACKNOWLEDGMENT

Pacific Northwest Laboratory is operated for the U.S. Department of Energy by Battelle Memorial Institute under Contract DE-AC06-76RLO 1830.

REFERENCES

- (1) Bridgwater, A.V. ed. *Advances in Thermochemical Biomass Conversion*. Blackie Academic & Professional/ Chapman Hall, Glasgow: 1994.
- (2) Overend, R.P.; Rivard, C.J. In *Proceedings First Biomass Conference of the Americas*, Vol. 1, pp. 471-497, 1993. NREL/CP-200-5768, National Renewable Energy Laboratory, Golden, Colorado.
- (3) Baker, E.G.; Mudge, L.K. *Catalysis in Biomass Gasification*. PNL-5030, Pacific Northwest Laboratory, Richland, Washington: 1984.
- (4) Cox, J.L. et al. *The Direct Production of Hydrocarbons from Coal-Steam Systems*. Research and Development Report No. 80, Office of Coal Research, U.S. Department of Interior: 1974.
- (5) Pinto, A.; Rogerson, P.L. *Chemical Engineering*, **1977**, 102-108.
- (6) Henery, J.P. Jr.; Louks, B.M. *Chem Tech.*, **1971**, 238-247.
- (7) Roberts, A.F. *Combustion and Flame*, **1970**, 14, 261-272.
- (8) Schiefelbein, G.F. "Biomass Gasification Research: Recent Results and Future Trends." PNL-SA-12841, Pacific Northwest Laboratory, Richland, Washington: 1985.
- (9) Lucchesi, A. et al. "Hydrogen by Pyrolysis-Gasification of Biomass." In *Proceedings of the Second International Symposium on Hydrogen Produced from Renewable Energy*, Cocoa Beach, Florida, October 22-24, 1985.
- (10) Mudge, L.K.; Baker, E.G.; Mitchell, D.H.; Robertus, R.J.; Brown, M.D. *Catalytic Gasification Studies in a Pressurized Fluid Bed Unit*. PNL-4594, Pacific Northwest Laboratory, Richland, Washington: 1983.
- (11) Storch, H.H.; Golumbic, N.; Anderson, R.B. In *The Fischer-Tropsch and Related Synthesis*. John Wiley & Sons: New York, 1951.
- (12) Pichler, H. In *Advances in Catalysis*. Frankenburg, W.G.; Komarewsky, V.I.; Rideal, E.K. eds., Academic Press: New York, 1952, Vol. 4.
- (13) Anderson, R.B. In *Catalysis*. Emmett, P.H. ed., Reinhold: New York, 1956, Vol. 4.
- (14) Mills, G.A.; Steffgen, F.W. *Catalysis Reviews*, **1973**, 8(2), 159-210.
- (15) Marschner, F.; Moeller, F.W. In *Applied Industrial Catalysis*. Leach, B.E. ed., Academic Press: New York, 1983, Vol. 2.
- (16) Hindermann, J. P.; Hutchings, G.J.; Kiennemann, A. *Catal. Rev.-Sci. Eng.*, **1993**, 35(1), 1-127.
- (17) Iglesia, E.; Reyes, S.C.; Madon, R.I.J.; Soled, S.L. *Adv. in Catalysis*, **1993**, 39, 221-302.
- (18) Rosovskii, A.Y. *Khim. Prom*, **1980**, 11, 652.
- (19) Kagan, Y.B. et al. *Kinet. Catal.*, **1976**, 17, 440.
- (20) Kuechen, C.; Hoffmann, U. *Chem. Eng. Sci.*, **1993**, 48(22), 3767-3776.

TABLE I. Predicted Equilibrium Gasification Product Compositions (1 atm)

Product, mol. %	500°C	600°C	700°C	800°C
<u>H₂O:C = 0.5</u>				
H ₂	38.1	49.3	50.9	49.8
CO ₂	36.8	25.1	11.1	2.9
CO	4.9	16.8	34.9	46.2
CH ₄	20.2	8.8	3.1	1.1
<u>H₂O:C = 1.0</u>				
H ₂	38.1	49.3	50.9	49.8
CO ₂	36.8	25.1	11.1	2.9
CO	4.9	16.8	34.9	46.2
CH ₄	20.2	8.8	3.1	1.1
<u>H₂O:C = 2.0</u>				
H ₂	38.1	50.7	57.1	57.1
CO ₂	36.8	25.3	17.2	14.4
CO	4.9	16.0	24.7	28.4
CH ₄	20.2	8.0	1.0	0.1
<u>H₂O:C = 3.0</u>				
H ₂	46.2	58.8	60.9	60.0
CO ₂	35.5	27.1	22.4	20.0
CO	3.9	10.9	16.4	20.0
CH ₄	14.4	3.2	0.3	0.0
<u>H₂O:C = 5.0</u>				
H ₂	56.9	63.8	63.2	62.6
CO ₂	33.8	29.3	26.9	25.0
CO	2.7	4.5	6.3	8.0
CH ₄	6.6	0.6	0.4	0.0
<u>H₂O:C = 10.0</u>				
H ₂	64.6	65.4	65.1	64.7
CO ₂	32.7	31.2	30.3	29.0
CO	1.5	3.0	4.6	6.3
CH ₄	1.2	0.4	0.0	0.0

TABLE II. Experimental Gasification Results

Feed Material	coal char	olive-husks	biomass
Catalysts	K ₂ CO ₃ /Ni-Al ₂ O ₃	none	Ni-Al ₂ O ₃
Steam/feed, lb/lb	3.8	-	5.7
Pressure, psia	30	15	15
Temperature, °C	560	747	735
SCF H ₂ /ton feed	90,000	35,000	not reported
Product(mol%, H ₂ O free)			
CO	1.9	6	5.8
CO ₂	36.6	25	29.9
H ₂	61.4	67	64.1
CO	1.9	6	5.8
CH ₄	0.0	2	0.2
Reference	4	9	10

TABLE III. Some Products Accessible Through CO-Synthesis Gas

Product	Reaction Conditions	Ref.
CH ₄	3H ₂ /CO, 350-400 °C, 50-100atm, 5,000-10,000 h ⁻¹ GSV, Ni/Al ₂ O ₃ Catalyst	14
CH ₃ OH	2H ₂ /CO, 230-300 °C, 50-100atm, Cu-ZnO Catalyst	15
C _n H _{2n+1} OH (n>1)	1.1H ₂ /CO, 260 °C, 130atm, 5,000-10,000 h ⁻¹ GSV, K-promoted MoS ₂ Catalyst	16
C _n H _{2n} (n=2-4)	1.4H ₂ /CO, 280 °C, 10atm, 340 h ⁻¹ GSV, Fe-Mn Catalyst	16
C ₅₊	2.1H ₂ /CO, 200 °C, 20atm, Co/SiO ₂ , 360 h ⁻¹	17

TABLE IVA. Comparative Thermochemistry of CO- and CO₂- Synthesis Gases (reactants and products in their normal states)

Reaction	Free Energy, kcal				
	25°C	200°C	250°C	300°C	350°C
5(n=1)	-36.04	-24.59	-21.78	-18.94	-16.06
6(n=2)	-31.48	-13.46	-9.34	-5.16	-0.95
7(n=1)	-6.97	3.76	6.64	9.56	12.50
7(n=2)	-32.89	-9.90	-4.17	1.60	7.40
8(n=1)	-31.26	-19.49	-17.15	-14.77	-12.34
9(n=2)	-21.92	-3.25	-0.07	3.18	6.49
10(n=1)	-2.19	8.86	11.27	13.73	16.22
10(n=2)	-23.34	0.31	5.09	9.94	14.85

TABLE IVB. Comparative Thermochemistry of CO- and CO₂- Synthesis Gases (reactants and products in their normal states)

Reaction	Enthalpy, kcal				
	25°C	200°C	250°C	300°C	350°C
5(n=1)	-59.78	-50.96	-51.38	-51.77	-52.13
6(n=2)	-71.26	-52.24	-52.76	-53.25	-53.70
7(n=1)	-30.63	-23.38	-23.72	-24.03	-24.31
7(n=2)	-81.83	-63.85	-64.34	-64.76	-65.13
8(n=1)	-60.47	-41.35	-41.88	-42.38	-42.85
9(n=2)	-72.64	-33.03	-33.76	-34.46	-35.13
10(n=1)	-31.32	-13.77	-14.22	-14.64	-15.02
10(n=2)	-83.21	-44.64	-45.33	-45.97	-46.56

METHANOL FROM BIOMASS VIA STEAM GASIFICATION

John A. Coffman
Wright-Malta Corp.
Plains Road
Ballston Spa, NY 12020

Keywords: steam gasification, biomass, methanol

ABSTRACT

R & D at Wright-Malta on gasification of biomass, and use of this gas in methanol synthesis, has now reached the stage where a demonstration plant is feasible. The gasifier has evolved into a long, slender, slightly declined, graded temperature series of stationary kiln sections, with box beam rotors and twin piston feed. The methanol reactor is envisioned as a smaller, more declined, graded temperature, water-filled stationary kiln, with a multi-pipe rotor. Input to the demo plant will be 100 tons/day of green (45% water) wood chips; output is projected at 11,000 gal/day of methanol and 7500 lbs/hr of steam. The over-all biomass to methanol system is tightly integrated in its mechanical design to take full advantage of the reactivity of biomass under a slow, steady, steamy pressurized cook, and the biomass pyrolysis and methanol synthesis exotherms. This is expected to yield good energy efficiency, environmental attractiveness, and economical operation.

INTRODUCTION

The oral presentation at the biomass symposium will consist primarily of pictures, drawings, graphs, and flow charts, illustrating the novelty in the mechanical equipment aspects of the W-M technology, as it has evolved over the past quarter-century. There is some novelty, too, in the steam gasification chemistry, the raw gas reformation into syngas, and the projected methanol synthesis. These aspects of the development will be emphasized in this written preprint.

STEAM GASIFICATION RESEARCH

Process parameters were determined in two bench-scale equipments: a "minikiln" and a "biogasser". One provided batch experimentation, giving a differential look at the process and an end point; the other permitted continuous operation and gave integrated data.

The minikiln was a rotating autoclave, about 1 ft in diameter and 3½ ft in length, electrically heated, with provision for steam injection under the bed and for product gas sampling and analysis. Test material, such as wood chips, corn stalks, or solid waste and sewage sludge, was placed in the barrel, the door bolted on, heating and rotation started, and the material tumbled in place, gradually heating, going on a simulated trip down a long kiln. At the end of the run, the minikiln was cooled, and the residue removed and weighed.

The biogasser was a long (10 ft), slender (2 in. ID), auger reactor, heated electrically, with provision for continuous feed of moist sawdust through lock valves into the cool end, and controlled release of product gas at the hot end. The solid residue dropped into a pressurized receptacle and was subsequently weighed. Water and condensable organics, if any, were stripped from the gas by passage through a condenser. The gas was analyzed by chromatography; its composition was representative of that expected from a commercial kiln.

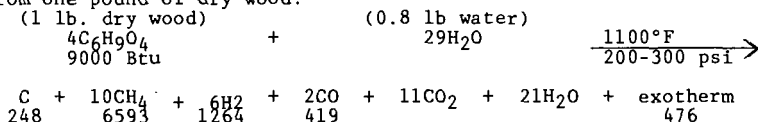
The bench-scale research showed that a slow, steady, pressurized cook, with alkaline catalyst and steam, under temperature gradually increasing to a top figure of 1100-1150°F is sufficient to gasify any type of biomass to 95-98% completion. No air or oxygen is required. It also showed that there is a broad optimum pressure at 200-400 psi. Lower pressure tends to slow the gasification process; higher pressure tends to throw the product mix toward higher molecular weight tar and coke, a la LeChatelier. It was determined that steam reformation of the intermediate pyrolysis liquids and steam gasification of the char go to completion under about the same conditions. Perhaps the vapors drift down the kiln, are absorbed into

char, and crack there. When conditions are right and char consumption is essentially complete, the gas also is clean, and burns with a pale blue, non-luminous flame.

The slow, steady temperature rise of the biomass charge, imposed by the inherently sluggish heat transfer of an indirectly heated kiln, is beneficial to the chemistry of steam gasification. Water itself is not sufficiently dissociated, even at 1100°F, to attack the decomposing biomass, although there will be some ionic hydrolysis in the region up to about 500°F. Rather, activation comes from the free radicals formed by breakage of chemical bonds in biomass polymers, starting at about 350°F, the weakest breaking first, then the next stronger, etc. Water participates in the radical chain reactions. With the slow temperature rise, radicals are generated in a slow, steady stream, on up through the brown and black charry stages. Char at, say, 900°F, is still not carbon; it is an amorphous high polymer with about one atom of hydrogen to two atoms of carbon, and still forms radicals (mostly atomic hydrogen) when heated to higher temperatures. And so the decomposing biomass reacts with water/steam all through its slow heat-up, and most of its substance, except inorganic matter, is gone by 1100°F.

(In contrast, a chip dropped into a fluid bed at 1100°F forms its radicals in a rush, wasting most of them. Steam reaction with the decomposing chip is thwarted, too, by the outpouring of gaseous products, and a substantial charry residue remains.)

The over-all gasification process is depicted in the balanced equation below. The proportions of the product gas are experimental data, being the nearest whole number composite of many runs in the biogasser at optimum conditions. (It is of interest to note that they are close to equilibrium even though equilibrium would not be expected at 1100°F in the absence of a metallic catalyst.) Wood is fresh white pine at 45% moisture. The numbers under the formulas represent the heat content in Btu's of each constituent, derived from one pound of dry wood.



Experimentation in the minikiln, using it in a differential thermal analysis mode, determined the magnitude and temperature occurrence range of the wood decomposition exotherm. Data obtained were in agreement with the calculated figure and with the literature. There was some degree of overlap between the water evaporation endotherm at higher pressures and the decomposition exotherm, but not enough to blunt it unduly. Calculation indicated that production equipment should be operable in regenerative mode without external heat supply, after initial warm-up and without a 2nd law pinch, provided that the moisture content of the feed material is not more than 50%. That is, the temperature differential between the backcoming gas in the heating pipes on the rotor vanes, and the on-going gasification process in the kiln, will be everywhere sufficiently large to sustain the process. This is particularly true in the methanol system, where the backcoming reformed gas will have unusually high enthalpy.

EQUIPMENT CHANGE AND SCALE-UP

The steam gasification process has been studied in five equipments in this order:

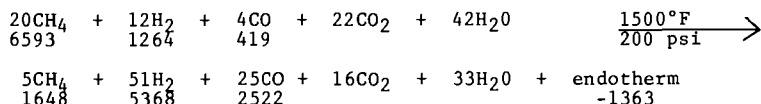
1. Bench-scale, batch type rotary kiln-15 lb charge.
2. Bench-scale continuous auger kiln-20 lbs/hr.
3. Process development unit, steam-heated auger kiln-500 lbs/hr.
4. Bench-scale, batch type rotor kiln-12 lb charge.
5. Mini-process development, rotor kiln-60 lbs/hr.

In all of the equipments, with comparable feed stocks, temperatures, pressures, heat cycles, and alkaline catalyst concentrations, the degree of gasification completeness and the composition of the product gas were, within experimental error, identical. There is no reason to expect this slow, steady process to change appreciably with further scale-up to

projected "standard" production units at, say, 12.5 green tons/hr.

REFORMING TO SYNGAS

If the gas is taken from the hot end of the kiln and raised in temperature from 1100 to 1500°F in the presence of an equilibrating catalyst, its composition will shift as shown in the equation below. This equation was derived from a W-M computer program which calculates the gas composition having the minimum Gibbs free energy as a function of temperature and pressure. Similar programs have been verified experimentally by other investigators in steam-reforming of natural gas.



Note that most of the methane has been steam-reformed to H₂ and CO, that some of the CO₂ has been reduced to CO, that most of the energy is now in the H₂ and CO, and that the ratio between these gases is now 2.04/1.00, just right for methanol synthesis. This gas composition shift is strongly endothermic, and the heat of reaction must be supplied by external heating.

(It is instructive to combine the gasification and shift equations, giving a situation which would prevail if the gasification were performed at a top temperature of 1500°F and 200 psi. The process is now 476-1363 = -887 endothermic. This does not mean that the wood decomposition exotherm has changed; it remains reasonably constant at about 700 Btu. It does mean that the over-all gasification process will range among varying degrees of endo- and exothermicity depending upon the final gas composition, which is in turn dependent upon temperature and pressure. Higher temperature and lower pressure throw it toward endothermicity and vice versa.)

Wright-Malta favors a lightly exothermic, self-sustaining gasification and a separate gas composition shift for reasons of equipment cost and process efficiency.)

METHANOL SYNTHESIS

As the syngas leaves the reformer, it gives a little of its sensible heat to the incoming gas, and then flows into the backcoming pipes on the gasifier vanes at about 1300°F. It exits the kiln at the feed end, is stripped of its water and all but a couple per cent of its CO₂, and is then compressed adiabatically from 200 to 1500 psi and 600°F.

Rather than use a scaled-down version of a commercial methanol process for the demonstration plant, W-M intends to use a new reactor design. It is, naturally, a stationary kiln (3 ft by 20 ft) declining about 15° from the horizontal, with about a 200 pipe rotor. In each pipe (1 in.) is a loosely fitting chain, and in each link is a copper catalyst pellet, kept bright and active by the mild chafing which occurs as the rotor slowly turns. Syngas drifts downward through the rotor pipes, condensing chemically into methanol vapor and physically into liquid, with the equilibrium shifting toward the right as the temperature falls. Water flows slowly, countercurrently up through the kiln, warmed by the methanol exotherm, its sensible heat, and heat of condensation, and boiling at the top end. Conversion of syngas to methanol is expected to be sufficiently accomplished (perhaps 60%) in a single, slow pass through the reactor so that recycling will be minimal.

The over-all biomass to methanol system is a tightly integrated package, taking full advantage of exotherms and sensible heat. The reformer will be heated by burning part of the purge gas (mostly methane); the remainder will be recycled through the twin piston feed into the gasifier. Steam raised in the methanol reactor, and in a heat recovery boiler atop the reformer, may be used, as in the demonstration plant, for space heating, or to generate electricity for powering the compressor and other auxiliaries. In the latter instance, net energy efficiency, raw biomass to fuel grade methanol, is calculated to be at least 70%.

Momentum is building to take seriously the need to move toward sustainable development through renewable energy. Biomass is, by far, the most versatile and widely distributed form of renewable energy, and environmentally attractive as well. In the present business climate, particularly here in the States, biomass to methanol would seem to be the best renewable energy venture.

A MILD, CHEMICAL CONVERSION OF CELLULOSE TO HEXENE AND OTHER LIQUID HYDROCARBON FUELS AND ADDITIVES.

J. Michael Robinson

Chemistry Department, The University of Texas of the Permian Basin
Odessa, TX 79762

Keywords: Biomass, Liquid fuels, Chemical reduction

INTRODUCTION

Biomass fermentations and high temperature and pressure pyrolysis processes that produce gas or liquid fuels are legion. They all have drawbacks. For example, the theoretical limit of ethanol production is 67% due to the loss of 1/3 of the available carbon as carbon dioxide gas during the fermentation. Pyrolytic reactions usually lose carbon as char and gases and may achieve about 80% carbon conversion.¹ Furthermore, pyrochemical processes usually require nearly dry feedstocks. Obviously, there remains a need for a variety of fuels from many sources, especially conventional liquid fuels. To resolve this fuel problem and to use a renewable resource, a strategy was selected to prepare valuable hydrocarbons from biomass by a chemical process.

Our initial goal was to develop an efficient multistep chemical process for the conversion of the principle components of biomass, cellulose and hemicellulose, into hydrocarbon fuels. Separation of these components and/or the use of selective reactions might allow for 100% carbon conversion by keeping the carbon chain intact. Furthermore, if initial reactions could be conducted in an aqueous medium, then the use of wet feedstocks would be possible. Overall, a six carbon sugar polymer, cellulose, would afford a single pure hydrocarbon product such as hexene. This is precisely what we have developed, a novel *chemical* process.

RESULTS AND DISCUSSION

Our use of the term *chemical* implies the typical mild conditions usually employed in glass vessels. This process consists of three to four separate reactions, the first two of which occur in water. **Scheme I** comprises a brief summary of the main reaction steps that achieve the strategic objectives of the organic portion of the process. For simplicity in this abstract, Scheme I is shown with cellulose rather than raw biomass, although the latter works as well.

Step 1 is a reductive depolymerization of carbohydrate biopolymers. Cellulose is simultaneously hydrolysed in dilute acid and catalytically hydrogenated to glucitol (commonly named sorbitol) in near quantitative yields.² Hemicellulose is similarly converted into xylitol and sorbitol. Lignin, if present, is simply removed by filtration after the reaction. While the acid is mild, the highly selective ruthenium catalyst is only active at the temperature shown. Thus, Step 1 uniquely provides the required polyols required for the next reaction and simultaneously provides a facile separation of lignin.

Step 2 of the process is also a key reaction: the chemical conversion of polyhydric alcohols to liquid hydrocarbons. The major part of all the reduction requirements occurs in this conversion. Reduction of five hydroxyl groups of sorbitol occurs while one hydroxyl group gives substitution. According to an early reference,³ sorbitol reacts with aqueous HI and red phosphorous to afford 2-iodohexane in 95% yield. By-product I₂ is consumed by phosphorous.

Our strategy to overcome the physical problems of I₂ phase separation as a solid or of using solid red phosphorous was to use homogeneous chemical agents that concomitantly reduce I₂ to regenerate HI.⁴ If the I₂ reacts quickly, it does not interfere with the polyol reduction reaction. Such use met with the unexpected results of simultaneous alkene formation and oligomerization. Considerable effort has been extended toward identifying the various products and the variables that control their formation.

Thus in Step 2, polyhydric alcohols such as sorbitol are reduced essentially quantitatively to a mixture of halocarbon and hydrocarbon compounds by reaction with hydriodic acid (HI) and a phosphorous type reducing agent, either phosphorous acid (H₃PO₃) or hypophosphorous acid (H₃PO₂). The reaction occurs in boiling aqueous solution at atmospheric pressure for about 1-2 hours. Reaction conditions were varied to give on one extreme about 99% 2-iodohexane and on the other extreme about 86% hydrocarbons with the remainder being halocarbons. The immiscible products are simply removed as a separate phase from the water solution. So Step 2 not only provides a highly reduced C₆ compound but also C₁₂, C₁₈, and C₂₄ hydrocarbons. These groups represent fuels in the range of gasoline, kerosene, diesel, and fuel oil, respectively. Material balances (yields) are 100%(±4%) and were determined by GC/MS analyses of isolated product.

Each hydrocarbon group is a mixture of alkene isomers. The higher homologues typically contain a ring. An example structure for the $C_{12}H_{22}$ isomers (1,2,4-trimethyl-3-propylcyclohexene, MW = 166) is shown in Scheme 1. Halocarbons detected were 2-iodohexane, isomers of $C_6H_{12}I_2$, and traces of $C_{12}H_{22}I_2$. Mannitol and xylitol gave similar results.

In contrast, we found that Step 2 products such as these do not form from glucose; it must first be reduced to sorbitol. Such products do not form on treatment of wood with HI.⁵ In fact, these authors found that H_3PO_2 greatly "suppresses the yield of oil products." Products obtained in this manner are complex mixtures of high molecular weight oils and tars containing oxygen and high percents of iodine, not specific molecular weight range small hydrocarbons as in our process.

Step 3 might be considered a cleanup reaction in that all of the remaining halocarbons in mixtures from Step 2 are subsequently converted to alkenes by an elimination reaction with potassium hydroxide (KOH) in boiling alcohol. Vast differences in boiling points of hexene (68 °C) from the other higher mass hydrocarbons, 200 °C and 300 °C, allow facile separation by distillation of the final mixture. The mixture of isomers in each group depresses the melting point and helps the fuel remain liquid.

The elimination of HI (Step 3) by KOH produces KI as insoluble by-product. KI can be recycled to KOH and HI by electrochemical means using Aqua-Tech's bipolar cells.⁶ Such regenerations are commercially economical. Hexene distilled after Step 3 is very low in iodine impurity, typically ranging from low teens to near 100 ppm. Further lowering of the iodine content is desired for two reasons: (1) potential corrosion due to the HI produced upon combustion, and (2) potentially expensive iodine replacement costs. However, 35 ppm iodine content only increases the cost of hexene by about \$0.002/gal.

There are several optional steps, one of which is shown as **Step 4** in Scheme I. Catalytic hydrogenation of hexene furnishes hexane, an important industrial solvent. Hydrolysis of 2-iodohexane to 2-hexanol is another optional reaction to a value added product.

Physical values, H/C ratio, and octane numbers are shown for these fuels and compared to conventional liquid fuels in Table 1. Hexene, for example, has a RON of 93, density of 0.68, and a H/C ratio of 2, all ideal for gasoline. The C_{12} hydrocarbons have several desirable properties (less volatile, highly branched, cyclic, partially unsaturated, and a H/C ratio of 1.8) that should contribute to a high RON. This group might be suitable as a narrow boiling point range gasoline. However, this C_{12} mixture should have a density of 0.8 and a bp of about 200 °C, similar to the values of kerosene. The C_{18} and C_{24} isomer mixtures likely fit into the diesel and fuel oil ranges. Oxygenates marketed today are also compared with 2-hexanol.

SUMMARY AND ECONOMIC PROJECTION

This multistep *chemical* process for reduction of biomass to liquid hydrocarbon fuels is the first of its kind. It stands in sharp contrast to other research areas that follow classical lines of bio-(fermentation) or thermal (pyrolysis) conversion. In fact, uncoupling the reduction process to a series of mild selective chemical reactions was the key to the problem. As a result, economic advantages abound. One particular advantage of this *chemical* process is that both Step 1 and Step 2 reactions take place in water as solvent, which allows the use of wet biomass. The water immiscible organic products of Step 2 simply coalesce as an upper layer facilitating their separation by mere decantation. Another benefit of the process is that the cyclic alkene dimers and trimers produced directly in Step 2 actually require less reduction, 10% and 13%, respectively, than hexene. These oligomeric hydrocarbons also do not require base treatment and subsequent reagent regeneration costs as do the haloalkanes. Step 2 is highly tunable, which allows a choice of products. Each simple reaction step can be driven to essentially quantitative yield resulting in the same high yield for the entire process.

While we may only use hydrogen in Step 1, and the optional Step 4, it is convenient at this time to estimate the total costs of reduction based on a typical price for hydrogen. Using a hydrogen cost of \$0.54/lb and a cost range of \$10 to \$40/ton for biomass (dry weight basis) containing 75% holocellulose, then total feedstock and reduction costs might be estimated as \$0.49 to \$0.64 per gallon for hexene. Similarly, the C_{12} and C_{18} isomers range from \$0.44 to \$0.60/gal. However, there are other chemical and mechanical costs associated with this multiple step process that will definitely contribute to overall process economics. Even if the real costs are twice as much, it might still be economical. Establishment of accurate economics will take some time. Total costs depend upon the exact steps, reagents, products, and precisely how the reagents are recycled. It is possible that the high quality, high value products available *via* this process may indeed be economically attractive in the near future, perhaps as fuel additives, even without a change in the margin of fossil fuels. Thanks to strong financial support from several sources, we are continuing to develop this process.

REFERENCES

1. Soltes, E.J. "Of Biomass, Pyrolysis, and Liquids Therefrom", Ch. 1 in ACS Symposium Series #376 "Pyrolysis Oils From Biomass; Producing, Analyzing, and Upgrading" Soltes, E.J. and Milne, T.A., Editors, American Chemical Society, Washington, D.C., 1988.
2. Sharkov, V.I. "Production of Polyhydric Alcohols from Wood Polysaccharides," *Angew. Chem. I.E.E.* 1963, 2, 405.
3. Vincent, C.; Delachanal "Work with Sorbitol" *Compt. Rend.*, 1890, 109, 677; *Beil.* 1918, First Work, Band I, System 59, 533.
4. Foster, L.S.; Nahas, H.G., Jr. "Hydriodic Acid: Regeneration of Oxidized Solutions," *Inorg. Synth.*, Vol. 2, 210, W.C. Fernelius, Ed., 1946.
5. Cooper, D.; Douglas, M.; Ali, O.; Afrashtehfar, S.; Ng, D.; Cooke, N. "A Low Pressure-Low Temperature Process for the Conversion of Wood to Liquid Fuels and Chemicals Using Hydrogen Iodide" *Canadian Bioenergy R&D Semin. [Proc.] 5th*, 1984, 455.
6. Mani, K.N. "Electrodialysis Water Splitting Technology," Aquatech Systems Report, Allied Signal, Inc., Warren, NJ, 1990.

ACKNOWLEDGMENT

This research has been supported by UTPB; the Robert A. Welch Foundation (Texas); the National Renewable Energy Laboratory (NREL); and the U.S. Department of Energy, Basic Energy Sciences, Advanced Research Projects. Special thanks are extended to Dr. Norman Hackerman, President Emeritus of Rice University and Chairman of the Welch Foundation, as well as to Dan Tyndall and Dr. Tom Milne at NREL who have been particular helpful. Many students have participated in the research and development of this process over the span of several years. Their assistance is greatly appreciated.

Scheme I

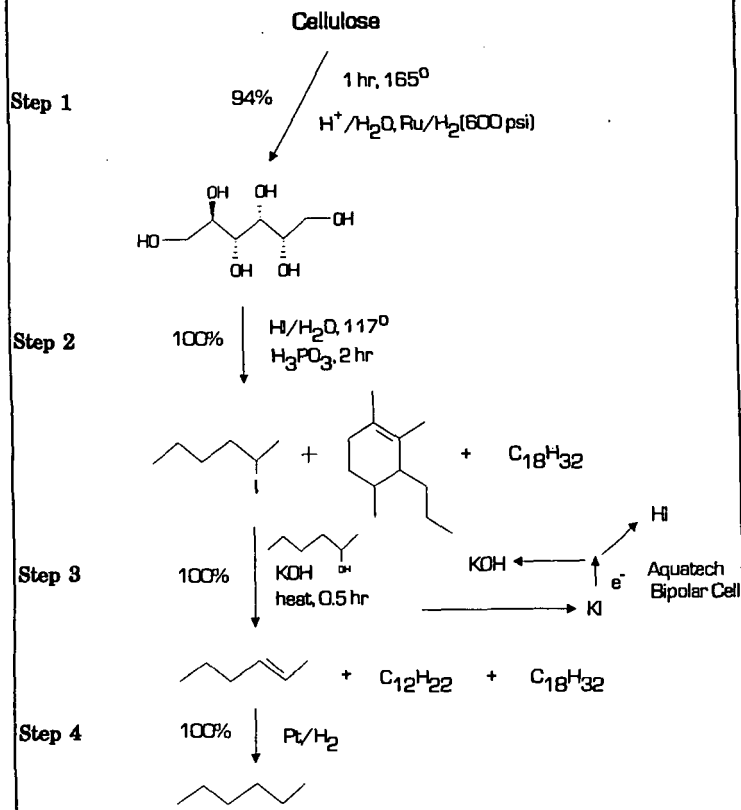


Table 1: Fuel Values

HYDROCARBONS

Compound	Formula	bp °C	RVP	d	H/C	Therm Val	Oct N
Hexane	C6H14	68	35	0.66	2.33	45 MJ/kg	25
Hexene	C6H12	69	0.67	2.0	(44.5)		93
gasoline	C4-C12	27-225	7-8	0.75	2.0	47.3	88
Dimers	C12H22	180-200		(0.76)	1.8		(high)
diesel	C14-C19	240-360	nil	0.84	2.1	43	
Trimers	C18H32	280-300		(0.8)	1.8		

OXYGENATES

Compound	Formula	bp °C	RVP	d	% O	Therm Val	Oct N
Methanol	CH4O	65		0.79	50	22.4 MJ/Kg	106
Ethanol	C2H6O	78	18	0.79	35	29.4	115
MTBE	C5H12O	56	8	0.74	18.2	38	110
ETBE	C6H14O	73	4	0.74	15.7		112
2-Hexanol	C6H14O	136		0.81	15.7	39	(high)

CATALYTIC THERMOCONVERSION OF CELLULOSE TO FUELS IN AQUEOUS MEDIUM

BABUL K. DATTA

Department of Chemical Engineering
Columbia University in the City of New York
NY 10027, USA

Keywords: Catalysts, Thermochemical, Aqueous.

ABSTRACT

Catalytic thermochemical liquefaction in aqueous medium was studied for conversion of cellulose to liquid fuels. There are 8 reactions were done by two different co-catalysts, (alkaline & acidic) with 5% Pt/Al₂O₃ in presence of 35 bar CO and H₂ as a reducing gas, at 300 °C. The duration of reaction time was 2 hours. During the reactions, catalysts and reaction time affected the process most dramatically. While the initial liquefaction (depolymerisation) of the cellulose is thermally controlled (pyrolysis), the subsequent conversion of the "Proto-oil" to liquid oils (deoxygenation) is mainly catalytically influenced. Some of the catalysts exhibited effective deoxygenation which resulted in the conversion of "Proto-oil" to a low oxygen content product. In run 7, conversion, oil production, H/C atomic ratio, calorific value is higher than others.

INTRODUCTION:

The conversion of cellulose to liquid fuels has been the subject of intensive studies during the last years¹⁻³.

The key problem in the liquefaction of biomass is the poor control of desired reactions. In pyrolytic liquefaction processes, the reactions are non selective, involving homolytic cleavage and free-radical reactions. In direct liquefaction, which uses CO, H₂, and water as reagent and catalysts, there is a complex sequence of reactions which probably starts out with the thermal breakdown of lignocellulosic materials and continues through the rearrangement, the reduction, the dehydration, the decarboxylation and other reactions to give a host of reactive compounds. These compounds can go further during the severe conditions of liquefaction process to lead to the polymerized, polymerisable and acidic compounds responsible of the poor yield and quality of the cellulose derived oil.

The crystalline regions in the cellulosic material make heterogeneous reactions occur slowly, as the close packing of the cellulose chains does not permit ease penetration by reagent molecules⁴. The use of homogeneous catalysts in these cases eliminates additional problems arising from the lack of effective contact between two solid phases, namely a heterogeneous catalyst and the biomass feedstock. Lindemuth⁵ believed that HCOO⁻ ion is the active species in a complex sequence of reactions that leads to oil formation.

The objective is to develop a consistent, quantified description of the liquefaction of cellulose, to examine the effect of co-catalysts with 5% Pt/Al₂O₃ in CO and H₂ atmosphere, quality of produced oils, and different types of water soluble components.

EXPERIMENTAL:

One liter capacity stainless steel autoclave (with rocker system) was used for each reaction with 1g different catalysts, 400g distilled water, 35 bar hydrogen gas and 300 °C temperature. All reactions were done for 2 hours. After cooling the autoclave, gasses were vented to the gas measurement system and collected samples for analysis in IR, GC. Then opened the autoclave for decant the aqueous layer and the rest of solid part was dissolved in acetone and refluxed for 3 hours, then filtered with vacuum pressure. After filtration, the solid part was char and catalyst; and the filtrate was rotaevaporated to separate acetone and oil. The remaining oil was separated by different solvents, such as Heptane and Toluene. The separated parts are called lights, waxes, asphaltenes and resins.

The aqueous phase contains a significant amount of reactive compounds, resulting from the breakdown of the cellulose. To understand of the nature of this complex, water soluble fraction, group separation was necessary before any identification was attempted. This was possible by solvent extraction. Prior to group separation, resinous substances from the water soluble were first precipitated with di-ethyl ether. The resulting ethereal soluble fraction was subsequently fractionated into four basic groups, namely; a) Carboxylic acids, (separated by 10% aqueous Na₂CO₃), b) Carbonyl compounds, (separated by 5% NaHSO₄), c) Phenolic compounds, (separated by 10% NaOH) and d) Solubilized/ Neutral hydrocarbons.

The four groups were identified by IR Spectroscopy.

IR - Perkin - Elmer IR Spectrophotometer (model 157) with range of 600 - 4000 cm⁻¹ was used.

Gas Chromatography - Pye Unicam G. C. (Series 204) fitted with dual detector system and coupled to a data processing computer (Hewlett - Packard - Data Dynamics 390) was used.

Catalysts - Johnson - Matthey Co. Cellulose - Powered pure cellulose (Solka-floc Brown Co., N. Y.).

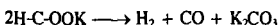
Suspension medium water - Distilled water. **Reducing gases** - Electrolytic hydrogen and Carbon-monoxide, BOC commercial grade-99.5%.

RESULTS AND DISCUSSIONS:

Table 1, lists the different reaction inputs, operating parameters and product distribution for runs 1-8. K₂CO₃ and SnCl₂ were used as a Co-catalysts with 5% Pt/Al₂O₃ for conversion of cellulose (Solka-floc) at 300°C and 35 bar of CO and H₂ as a reducing gas with 400 g water. In case of SnCl₂ in H₂ atmosphere, the amount of H₂O formation is larger than with K₂CO₃ and CO atmospheres due to the dehydration and catalytic deoxygenation of cellulose. Here Sn⁺² plays an important role which enters into the complex scheme of reaction to reduce cellulose fragments and liberate O₂, which reacts with H₂ from atmosphere or (from solvent H₂O) to form H₂O. This homogeneous hydrogenation of acidic catalyst contributes to dehydration of cellulose and leads to produce unsaturated substances that polymerise easily to form char. This effect, is directly proportional to the acidity of the medium. On the other hand, K₂CO₃ with CO atmosphere, CO reacts with H₂O (from solvent) to form CO₂ and H₂ (water gas shift reaction) instead of produce H₂O. Hence, SnCl₂ with H₂ produces large amounts of H₂O.

Moreover, SnCl_2 with H_2 atmosphere, maximum amount of water-soluble compounds were formed due to the strong hydrolytic action of the acidic catalyst. But in case of K_2CO_3 in presence of CO atmosphere, is reverse due to the neutralization of the organic acid compounds, higher conversion to gasification and decarboxylation (loss of CO_2) of water soluble fractions and cellulose fractions. CO probably has an additional role which inhibits the polymerisation of unsaturated compounds to form char.

The product gas recovery, shown that the gas formation is greater in presence of K_2CO_3 with CO reactions, which is probably due to CO took part in the water-gas shift reaction as well as $\text{K}_2\text{CO}_3 + \text{CO} + \text{H}_2\text{O}$ can form intermediate compound, possibly a potassium formate, which produces hydrogen, probably as hydried (H) ion. This ion reacts with the substrate (cellulose fragments), to remove oxygen as CO_2 and leads to the formation of oil also.



Net reaction: $\text{H}_2\text{O} + \text{CO} < \longrightarrow \text{H}_2 + \text{CO}_2$

Table 2 shows the elemental analysis of the feeds, char and oil of run (from 1-8).

The H/C atomic ratio is higher (1.26) with 5% $\text{Pt}/\text{Al}_2\text{O}_3 + \text{K}_2\text{CO}_3 + \text{CO}$ atmosphere in run 7, which may be due to elimination of higher amount of oxygen as a CO_2 by water-gas shift reaction. That means one carbon atom can eliminates two oxygen atoms as CO_2 from the reaction mixture. But in case of SnCl_2 with H_2 , reduction occurs by the elimination of only one oxygen atom (as H_2O) with two hydrogen atoms. The total elimination of oxygen (reduction) is double in case of $\text{K}_2\text{CO}_3 + \text{CO}$ than $\text{SnCl}_2 + \text{H}_2$. Moreover, the produced hydried (H) ion, from potassium formate is more active reducing agent than normal hydrogen atmosphere. So, it can easily more reduced the cellulose fragments for production of high amount and high quality of oils. Hence, the H/C atomic ratio and calorific value of the run 7 is greater than run 6 and others. is also high.

After solvent analysis, high amount of lights was formed than asphaltenes (in run 7) which was probably due to higher conversion of asphaltenes, resins and water-soluble fractions in presence of CO atmosphere into lights as well as gases (as CO_2 , CO and hydrocarbon gases) Which is shown in table 3.

From table 4, it is seen that when conversion increases, the production of water soluble fraction decreases and production of gases and oils increases. Moreover, ether soluble fractions from water soluble parts were also decreases on the same way which may due to the conversion of water soluble fractions into gases and oils. The ether soluble fractions were further separated by different solutions into different functional groups as carboxylic acid, carbonyl, phenolic and neutral hydrocarbons and identified by IR spectrum (shown in figure 1A to 2A).

From table 5, the G.C. analysis shown that K_2CO_3 in presence of CO atmosphere, CO_2 , CO gases are formed greater than the run with SnCl_2 in presence of H_2 which may probably due to water-gas shift reaction. The low concentration of hydrogen gases produced indicated that the hydrogen from the water-gas shift reaction is very reactive and reacts instantly with the cellulose fragments. The gases were identified by IR spectrum and GC chromatograms of run 5 to 8 and shown in figure 3A to 6A.

CONCLUSION:

- 1) In terms of conversion of cellulose, oil yield, quality of oil, calorific value of oil are higher in run 7, ($\text{K}_2\text{CO}_3 + 5\% \text{Pt}/\text{Al}_2\text{O}_3$ with CO atmosphere) in comparison with others.
- 2) The aqueous phase contains a significant amount of reactive compounds, resulting from the breakdown of the cellulose. The acidity of the aqueous phase is high ($\text{pH} \approx 3$) due to the presence of carboxylic acids. After reaction, when it was decanted from the autoclave, it looks as white after some while it becomes brown in color due to oxidation. After analysis of the water soluble fractions, it is seen that it contains carboxylic acids, carbonyl compounds, phenolic compounds and neutral hydrocarbon compounds, Table 5.
- 3) Using K_2CO_3 as a co-catalyst with 5% $\text{Pt}/\text{Al}_2\text{O}_3$ in presence of CO atmosphere, increased the yield of gaseous products at the expense of char and water soluble fraction. The improvement in the conversion has an reflection on the quantity and quality of the desired product.
- 4) The use of K_2CO_3 with 5% $\text{Pt}/\text{Al}_2\text{O}_3$ in presence of CO atmospheres had an enhanced effect on the catalytic conversion of cellulose.
- 5) Economically, 5% $\text{Pt}/\text{Al}_2\text{O}_3 + \text{SnCl}_2$ in presence of H_2 atmosphere is a viable catalyst for liquefaction of cellulose, because CO is more expensive than H_2 .

REFERENCES:

- 1) Adjaye, J.; R. K. Sharma and N.N. Bakhshi, "Characterization and Stability Analysis of Wood-derived Bio-oil", Fuel Process, Technol. 31, 241-256 (1992).
- 2) "Third liquefaction experts meeting", NRCC, Sherbrooke, Que., August 1983.
- 3) "Proceeding of the 14th Biomass Thermochemical" conversion contractor's Meeting, U.S. Department of Energy, Arlington, Virginia, June 1982.
- 4) J.P. Franzidis and A. Porteous, "Review of Recent Research of the Development of a Continuous Reactor for the Acid Hydrolysis of Cellulose" in "Fuels from Biomass and Wastes", D.L. Klass and G. H. Emert, ed.; Ann. Arbor Science publishers Inc. Ann Arbor, MI, (1981).
- 5) T. E. Lindemuth, "Carboxylyolysis of Biomass" in "Biomass Conversion Processes for Energy and Fuel" S. S. Sofer, O. R. Zaborsky, ed., 187-200, Plenum Press, NY, 1981.
- 6) A. R. Bowes, H. G. Shatwell, and A. W. Nash, "The Thermal Decomposition of Cellulose under Hydrogenation Conditions", J.Soc.Chem.Ind., 44, 507-511 T, 526T, 1925

Table 1. Reaction inputs, parameters and product distribution

Run	1	2	3	4	5	6	7	8
Feed type	Cellulose	Cellulose	Cellulose	Cellulose	Cellulose	Cellulose	Cellulose	Cellulose
Feed (g)	50.0	50.0	50.0	50.0	50.0	50.0	50.0	50.0
Catalyst	K ₂ CO ₃	Na ₂	K ₂ CO ₃	Na ₂	5% Pt/Al ₂ O ₃ + K ₂ CO ₃	5% Pt/Al ₂ O ₃ + Na ₂	5% Pt/Al ₂ O ₃ + K ₂ CO ₃	5% Pt/Al ₂ O ₃ + Na ₂
Catalyst (g)	1.0	1.0	1.0	1.0	5+5=1.0	0.5+0.5=1.0	0.5+0.5=1.0	0.5+0.5=1.0
Water, g	400.0	400.0	400.0	400.0	400.0	400.0	400.0	400.0
Reducing gas	H ₂	H ₂	CO	CO	H ₂	H ₂	CO	CO
Reducing gas (g)	1.6	1.6	22.12	22.12	1.6	1.6	22.12	22.12
TOTAL INPUT (g)	452.6	452.6	473.12	473.12	452.6	452.6	473.12	473.12
Temperature (°C)	300	300	300	300	300	300	300	300
Initial pressure (atm)	35	35	35	35	35	35	35	35
Heating up time (hr)	1.40	1.50	2.30	2.35	2.0	2.10	2.30	2.20
Reaction time (hr)	2.0	2.0	2.0	2.0	2.0	2.0	2.0	2.0
Max. Reaction press(atm) Final	280	280	290	285	295	292	310	300
Reaction press (atm)	37	36	40	38	40	44	38	36
TOTAL OUTPUT (g)	451.0	450.7	471.4	471.8	450.9	450.9	472.0	471.82
% Recovery from Autoclave	99.6	99.6	99.64	99.72	99.6	99.6	99.8	99.72
Product Distribution								
% Gas produced	16.0	11.56	18.76	28.8	12.8	15.96	31.76	26.40
% Water-soluble fraction	12.6	8.6	6.8	8.6	12.4	5.60	3.00	10.40
% Oil	17.6	40.0	38.6	21.2	24.4	40.0	50.00	20.60
% Char	19.0	8.0	6.4	14.6	12.0	7.0	3.00	11.00
% Water-produced	31.6	28.0	26.0	24.2	35.0	28.0	10.00	29.00
% TOTAL RECEIVED	96.8	96.76	96.56	97.4	96.6	96.56	97.76	97.4
% CONVERSION	75.64	89.59	92.28	78.9	78.68	93.73	96.94	81.44

Table 2. Elemental analysis

Run	1	2	3	4	5	6	7	8
Feedstock analysis								
% C	41.5	41.5	41.5	41.5	41.5	41.5	41.5	41.5
% H	6.1	6.1	6.1	6.1	6.1	6.1	6.1	6.1
% O*	52.4	52.4	52.4	52.4	52.4	52.4	52.4	52.4
% Ash	-	-	-	-	-	-	-	-
Char analysis								
% C	53.2	54.0	50.0	60.0	73.7	52.0	42.2	70.0
% H	4.9	4.5	3.9	5.5	4.6	4.2	4.0	4.2
% O*	28.0	15.0	12.0	23.7	21.7	8.9	6.8	10.8
% Ash	13.9	26.5	34.1	10.8		34.9	47.0	15.0
Oil analysis								
% C	75.6	77.8	78.0	68.9	78.0	74.5	75.3	73.9
% H	6.5	7.2	7.5	6.1	7.0	7.6	8.0	6.8
% O*	17.9	12.2	11.0	13.3	15.0	9.8	9.5	12.0
% Ash	-	1.0	3.5	11.7		8.1	7.2	7.3
H/C	1.02	1.10	1.14	1.05	1.07	1.21	1.26	1.09
O/C	0.177	0.117	0.10	0.146	0.144	0.098	0.094	0.146
Caloric value (Kcal/g)	7.5320	8.6512	8.6923	8.2513	8.3520	8.7215	8.7580	8.5571

Table 3. Product oil composition

Run	1	2	3	4	5	6	7	8
Product oil composition								
% Heptane soluble Lights.	35.8	50.2	55.0	38.3	41.6	61.2	63.5	46.7
% Heptane soluble (boil), Waxes.	8.90	13.4	14.8	12.3	12.0	13.8	15.0	12.3
% Toluene soluble Asphaltenes.	33.0	22.7	20.2	31.2	28.9	17.0	15.0	25.8
% Toluene insoluble, Resins.	22.3	13.7	10.0	18.2	17.5	8.0	6.5	15.2

Table 4. Extraction of different functional group(compounds) from ether soluble fraction of water soluble fraction.

Run	1	2	3	4	5	6	7	8
% Ether soluble fraction (from WSF*)	40.0	27.0	25.0	32.0	36.0	22.0	20.0	28.0
% A	14.2	9.0	8.5	9.6	10.2	7.0	6.4	9.0
% B	9.2	6.5	6.2	8.0	8.8	5.0	4.0	6.8
% C	4.5	2.2	2.5	2.0	4.0	2.0	3.0	1.6
% D	8.4	8.2	7.0	8.5	8.6	6.4	5.2	7.5
% E	2.2	0.6	0.5	1.5	2.8	1.0	0.6	1.1
% Total	38.5	26.5	24.7	29.6	34.4	21.4	19.2	26.0
% Recovery	96.25	98.0	98.8	92.5	96.0	97.0	96.0	93.0

A - Carboxylic acids (extracted by aqueous 10% Na₂CO₃ solution).

B - Heavy carboxylic acid

C - Carbonyl compounds (extracted by aqueous 5% NaHSO₄ solution).

D - Phenolic compounds (extracted by aqueous 10% NaOH solution).

E - Neutral hydrocarbons (etheral soluble compounds).

* WSF - Water soluble fraction

** All percentages are w/wt of ether soluble fraction

*** % of ether soluble fractions were obtained from Water soluble fraction by treating with di-ethyl ether.

Table 5. Product of gas distribution

Run	1	2	3	4	5	6	7	8
% CO	42.64	37.95	31.09	29.86	46.84	36.84	25.97	38.55
% CO ₂	24.21	24.68	52.25	50.09	25.06	40.26	61.04	50.90
% CH ₄	3.81	2.76	2.91	3.16	2.91	3.01	2.82	2.84
% C ₂ H ₆	0.59	0.57	0.59	1.02	0.60	0.59	0.63	0.65
% C ₂ H ₄	0.83	0.55	0.58	1.04	0.72	0.68	0.71	0.61
% C ₃ H ₈	1.14	0.71	0.66	1.09	0.85	0.55	0.81	0.67
% C ₃ H ₆	0.23	0.24	0.18	0.27	0.26	0.21	0.24	0.16
% n-Butane	-	-	-	-	-	-	-	-
% 1-Butene	-	-	-	-	-	-	-	-
% iso-butene	-	-	-	-	-	-	-	-
% Trans-2-butane	1.31	1.50	1.37	1.35	1.53	1.46	1.26	0.93
% Cis-2-butene	0.87	0.42	0.89	0.85	0.88	1.05	0.83	0.61
% Butadiene	1.72	2.09	1.75	1.70	1.72	1.86	1.72	0.85
% Total	77.35	71.47	92.27	90.43	81.37	86.51	87.04	96.77
% H ₂ + UP* [†]	22.655	28.53	7.73	9.57	18.63	13.49	12.96	3.23

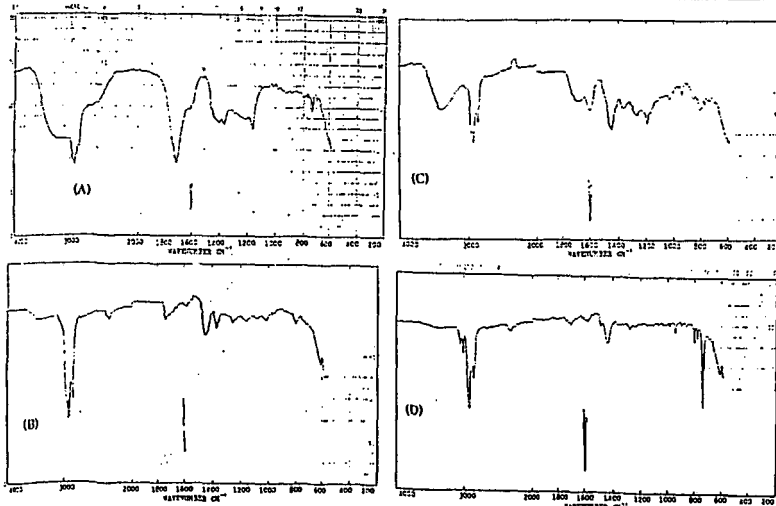


Figure 1A. IR spectra of aqueous extracts: (A) Na₂CO₃ extract (B) NaHSO₄. Figure 2A. IR spectra of aqueous extracts : (C) NaOH extract (D) Etheral-soluble .

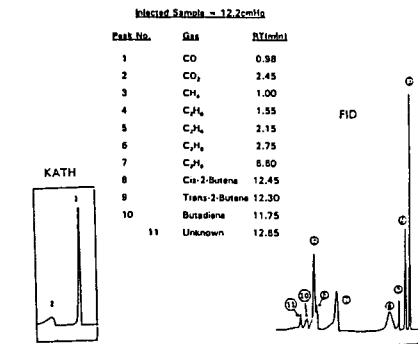
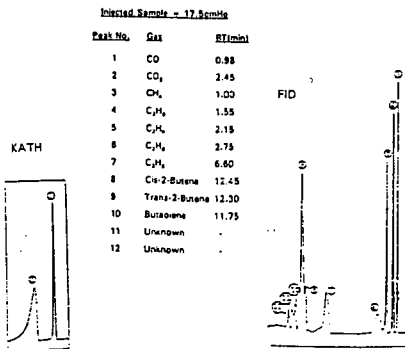
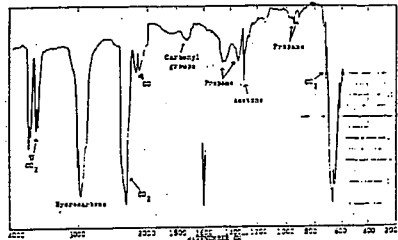
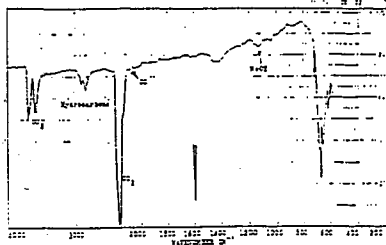


Figure 4A.

Figure 5A. The IR spectrum and GC chromatograms of the gaseous product from run 5

The IR spectrum and GC chromatograms of the gaseous product from run 6.

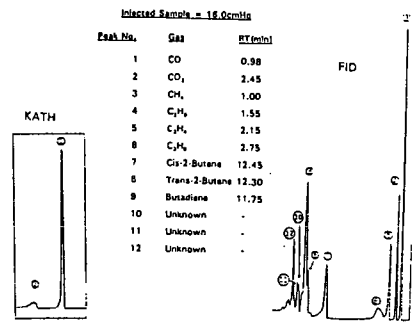
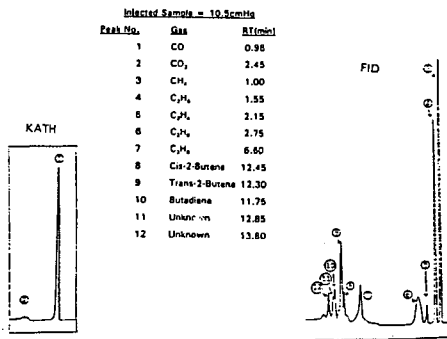
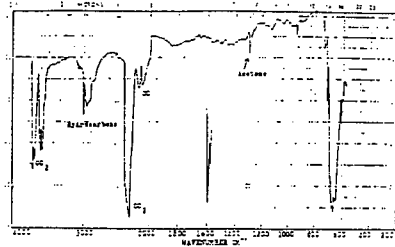
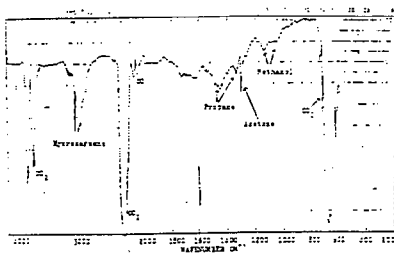


Figure 6A.

Figure 5A. The IR spectrum and GC chromatograms of the gaseous product from run 7.

The IR spectrum and GC chromatograms of the gaseous product from run 8

Deposition investigation in straw fired boilers

P.A.Jensen¹, M.Stenholm², P.Hald¹, K.A.Christensen³.

¹ Risø National Laboratory, Dept. of Combustion Research, P.O.Box 49, DK-4000 Roskilde, Denmark.

² dk-TEKNIK, Gladsaxe Møllevvej, DK-2860 Søborg, Denmark.

³ Technical University of Denmark, Dept. of Chemical Engineering, DK-2800 Lyngby, Denmark.

Key words: Deposition, straw, combustion.

Introduction

In Denmark straw has been applied as fuel at small combined power and district heating plants since the late 1980's. New equipment have been developed to handle and burn the straw. However, straw is by no means a trivial fuel, problems like fluctuations, deposition in the furnace, corrosion and a poor burn out have been observed at boiler plants. One of the problems has been, the large differences in the amount of deposition in the furnace chamber and on superheater tubes when applying different fuel parcels. Knowledge of how to characterize the straw for predicting the deposition properties in the boiler is needed. We will here present deposition experiments performed at two straw fired power plants with a fuel input of respectively 18 and 30 MW.

Some limited experiments have earlier been performed on smaller scale boilers^{1,2}, no clear correlation between laboratory analyses of the straw and deposition in the boilers was found. Combustion experiments on a combined wood and straw fired 18 MW stoker fired boiler have been performed³. Strong indications, of condensation of the mineral matter at different places in the boiler chamber, were seen.

Straw has typically a high content of potassium (0.5-1.3%), chloride (0.2-0.7%) and silicium (0.3-1.0%)⁴. KCl sublimates at typical combustion conditions and equilibrium calculations indicate that most of the potassium is in the gas phase at 900 °C⁵. The equilibrium calculations also indicate that a high Cl to K ratio gives a higher amount of K in the gas phase. The low melting point for some potassium species gives a high risk of the formation of hard deposits on furnace walls and convection tubes. A component as KCl melt at 771 °C, and KCl can contribute to melt formation at even lower temperatures when combined with other components as in deposits. Also the system K₂O - SiO₂ has a minimum melting point at 742 °C (68% SiO₂ and 32% K₂O).

Experiments

We have performed 12 one day experiments at full load at two straw fired power plants in the towns Haslev and Slagelse. At both places the straw was received in the form of Hesston bales. Other aspects than deposition were investigated during the experiments, however, this presentation contains only work concerning the deposition properties of the straw.

Haslev: A sketch of the boiler is shown in Figure 1. The bales are continuous fed in four rows into the four burners, where the combustion takes place on the surface of the front bales. The full load fuel input was around 5500 Kg/h corresponding to 18 MW.

Slagelse: (see Figure 2) The bales are reamed and the straw are fed by 9 screws into a moving grate boiler. The full load fuel input was around 7400 Kg/h corresponding to 30 MW.

Table 1 shows the 12 straw types that were applied for the experiments. Wheat, barley and rape were used with water contents of 11 to 16 %, chloride contents of 0.06 to 0.95 % (dry matter) and a potassium contents of 0.28 to 1.97 % (dry matter).

The experimental programme included air cooled deposition probes (around 1.8 meter long and with a diameter of 38 mm) inserted near the superheaters and in the boiler chamber. The deposition probes were kept as near as possible to 510°C as possible by the air cooling system. The fouling removal system, normally applied at the plants, in the form of the sootblowing and fonbal cleaning systems, was stopped during the experiments. After one experiment the deposition probes were withdrawn and the deposition was removed from the probes, the first fraction by a brush (loose deposit) and the second fraction by a steel brush and a knife (hard deposit). At the same position, as the deposition probes, temperature and the gaseous alkali content was measured. During all the experiments the operating conditions were monitored and the flue gas emissions were measured (HCl, CO, TOC, CO₂, O₂, NO_x and SO₂). Gaseous alkali measurements are in the developmental phase, and the results will be reported separately.

Aerosol samples were collected in the upstream of the fly ash filter. The aerosol size distribution was studied by a low-pressure cascade impactor and a scanning mobility particle seizer. It was possible to study particles from 0.01 to 2 micron.

In experiment 1 and 2 at Haslev and experiment 1,3,6,7 and 8 at Slagelse the amount of fed straw and the generated fly and bottom ash, was also measured. Detailed chemical analyses of straw, ash and deposits were performed.

Results

With respect to deposition wheat and barley were seen to behave reasonably similar, while rape was markedly different. The rape straw has a higher sulfur and calcium content but a much lower silicium content. In the following wheat and barley are discussed simultaneously while the experiment with rape is not included.

A very high amount of submicron aerosols was generated in the boilers. The mean diameter of the particles was around 0.3 micron. The particles consisted mainly of K, Cl and S. A large fraction of the alkaline in the fuel evaporate during the combustion and condensate as aerosols later in the furnace chamber. Figure 3 shows that a close correlation exists between the mass loading of submicron aerosols and the potassium contents of the straw. A detailed discussion of the aerosol formation mechanisms is given in reference 5.

In agreement with the aerosol measurements the fly ash is compared with the straw ash enriched with potassium, chloride and sulfur (see Table 2). The bottom ash has a slightly decrease in the same elements compared with the straw ash.

Table 3 shows chemical analyses of straw ash, bottom ash, fly ash and deposits from experiment 6 at Slagelse. A piece of loose deposits was analyzed with an environmental scanning electron microscope (ESEM) coupled with energy dispersive x-ray spectroscopy. The ESEM gave results as the proportion between the elements. In the table the elements are prescribed to give a total of 65%. The ESEM analysis gives information about the layer a few micron deep into the sample. Table 3 shows that compared with the fly ash the deposits are rich in silicium, this is probably caused by impaction of larger particles on the probe. This was not the case for all the experiments. The hard deposit of experiment 6 has a much higher chlorine to potassium ratio than the loose deposit. This was also observed in most of the other experiments. The ESEM analysis of the inner and the outer side of the deposit is reasonably similar and dominated strongly by potassium and chlorine. The surfaces are probably dominated by elements from the aerosols or from condensation of vapors.

During experiment number 6 two probes were inserted into the furnace chamber. Deposits at the extra probe were removed at different time intervals to study the dependency of residence time (see Table 4). It is seen that the total flux of deposition was reasonable independent of time while the fraction of hard deposit increased with the time.

The total deposition flux on the probes has been related to the potassium content in the straw. Figure 4 shows the results at the superheaters and Figure 5 the results in the furnace chamber. Similar to the aerosol generation a reasonable correlation with the water soluble potassium content in the straw is seen.

Figure 6 shows the flux of hard deposit in the furnace as a function of the chlorine content in the straw. A better correlation between the chlorine content of the straw and the hard deposits was seen than between the potassium content and the amount of hard deposits. With an increasing chloride content, the Cl to K ratio is also higher, this leads probably to condensation at a lower temperature (shown by equilibrium calculations in reference 6). With less potassium condensed prior to the probe, more potassium condensate directly on the probe surface. Also a high KCl content of the deposit gives a lowering of the deposit melting temperature.

Figure 7 shows the amount of hard deposits at the superheaters. Here, the picture is less clear. Because the temperature is lower the amount of hard deposits is lower and the measuring error much higher. Looking at Figure 6 and 7 it is seen that an increase in local temperature and in straw chlorine content gives an increase in the amount of hard deposit.

One experiment was performed with Rape straw. Large amounts of isolating deposits were generated in a short time and the temperature in the boiler increased fast. The experiment had to be stopped after 4 hours because of problems with the ash removal system.

Conclusion

It is the first time that such detailed measurements on straw fired boilers have been performed. Deposition formation on surfaces in the boiler can occur by different mechanisms: Condensation, impaction and termoforesis⁷. We think that if the deposition has been partly melted, or if it is generated to a high degree by condensation the deposition is harder and will be more troublesome for the boiler operators.

No correlation could be seen between the traditional laboratory generated ash softening and melting temperatures and the deposition in the boilers.

The results of the experiments with respect to deposition could be summarized in the following points:

- Large amounts of potassium evaporate and later condensate as aerosols.
- A high content of water soluble potassium gives a higher amount of total deposition.
- The local amount of hard deposits on convective surfaces is dependent on whether the alkaline condense as aerosols or directly on the boiler surfaces.
- Increasing local gas temperature gives a higher amount of hard deposits.
- A high chloride content of the straw gives a higher tendency for the formation of hard deposits.

References

1. Kjærboe, L. (1990). Slaggedannelse i fyringsanlæg. Case-stories. dk-TEKNIK (In Danish).
2. Thøllsen, H.Z. (1988). Halmens egenskaber til fyringsformål Slaggedannelse. Statens Jordbrugstekniske Forsøg. Beretning Nr. 40 (In Danish).
3. Baxter, L.L., T.R. Miles, T.R. Miles Jr., B.M. Jenkins, G.H. Richards and L.L. Oden (1993). Transformations and deposition of inorganic material in biomass boilers. Sandia National Laboratories, Livermore.
4. Undersøgelse af halms kemiske sammensætning - med relation til forbrænding og forgasning. Foretaget af bioteknologisk institut for Elsam/Elkraft. December 1994 (In Danish).
5. Christensen, K.A. (1995). The formation of submicron particles from the combustion of straw. Ph.D. thesis. Department of Chemical Engineering, Technical University of Denmark.
6. Hald, P. (1994). Alkali metals at combustion and gasification. Equilibrium calculations and gas phase measurements. Ph.D. thesis. Department of Chemical Engineering, Technical University of Denmark.
7. Baxter, L.L. (1993). Ash deposition during coal and biomass combustion: A mechanistic approach. *Biomass and Bioenergy* 4(2), 85-102.

Tables

Table 1. Straw applied for the 8 hour experiments.

Experiment	Straw type	Water content %	Chloride % of dry straw	Potassium (water soluble) % of dry straw
Has1	Wheat	15.1	0.29	0.57
Has2	Wheat	13.5	0.52	1.27
Has3	Barley	12.0	0.56	1.93
Has4	Wheat	14.6	0.44	1.01
Sla1	Wheat	15.0	0.06	0.28
Sla2	Wheat	13.3	0.20	0.74
Sla3	Barley	11.6	0.32	1.36
Sla4	Barley	13.6	0.95	1.97
Sla5	Wheat	13.9	0.51	1.07
Sla6	Wheat	13.2	0.86	1.50
Sla7	Wheat	16.1	0.14	0.48
Sla8	Rape	14.0	0.33	1.40

Table 2. Mean mineral composition (experiments 1 and 2 at Haslev and 1,3,6 and 7 at Slagelse) of Straw ash, bottom ash and fly ash.

Elements (dry sample)	Si	Al	Fe	Ca	Mg	Na	K	S	P	Cl	Sum
Mean in straw ash %	23.67	0.36	0.28	7.72	0.98	0.41	21.59	1.93	0.99	6.78	64.70
Mean in flyash %	7.12	0.17	0.45	2.74	0.42	0.43	37.36	3.21	0.75	22.44	75.09
Mean in bottom ash %	24.22	0.53	0.38	7.64	1.22	0.62	18.26	0.27	1.15	4.89	59.18

Straw ash were generated at 550C

Table 3. Mineral composition for experiment 6 at Slagelse of traw ash, bottom ash, fly ash, the furnace deposition probe and the inner and outer side of deposits (by ESEM).

Elements (dry sample)	Si	Al	Fe	Ca	Mg	Na	K	S	P	Cl	Sum
straw ash %	24.30	0.07	0.10	5.65	0.84	0.13	29.06	1.59	0.96	11.90	74.60
Fly ash %	2.15	0.11	0.28	1.22	0.16	0.57	50.64	3.12	0.65	33.00	91.90
Bottom ash %	28.03	0.30	0.26	7.86	1.33	0.26	17.43	0.14	1.18	0.73	57.53
Hard deposit %	10.28	0.11	2.52	4.07	0.60	0.15	32.38	1.96	1.09	19.00	72.16
lose deposit %	19.16	0.21	0.29	6.43	0.96	0.22	24.08	3.77	1.31	5.40	61.83
ESEM inner side, %	1.24	0.05	0.18	0.72	0.04	0.23	30.75	1.53	0.18	30.09	65.01
ESEM outer side, %	5.56	0.09	0.22	5.77	0.29	0.11	29.37	2.93	1.46	19.20	65.00

Table 4: Experiment 6 at Slagelse: Deposition in the furnace as a function of residence time.

Time the probe were inserted h	0.33	0.66	1.33	2.67	7.17
Total deposit flux g/m ² /h	96.1	64.2	69.2	59.6	67.4
Hard deposit flux g/m ² /h	1.99	0.76	1.12	10.1	41.96

Figures

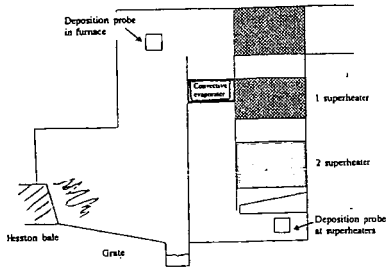


Fig. 1. Haslev straw fired boiler.

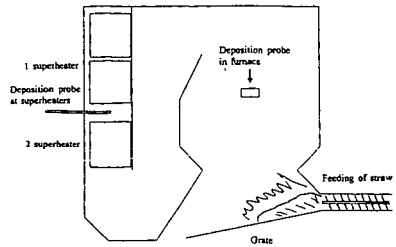


Fig. 2. Slagelse Straw fired boiler.

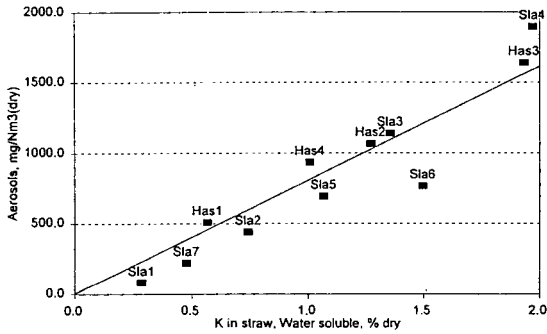


Fig. 3. Total aerosols (0.01 to 2 micron) in the flue gas as a function of water soluble K in the straw.

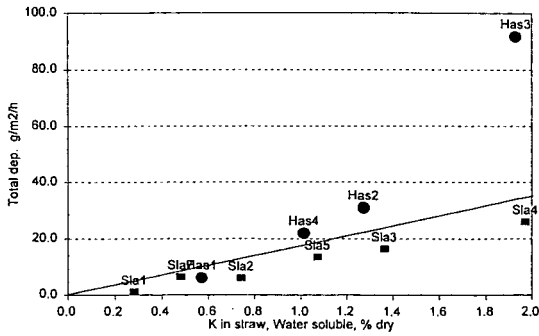


Fig. 4. Total deposition flux at the superheaters as a function of water soluble K in the straw.

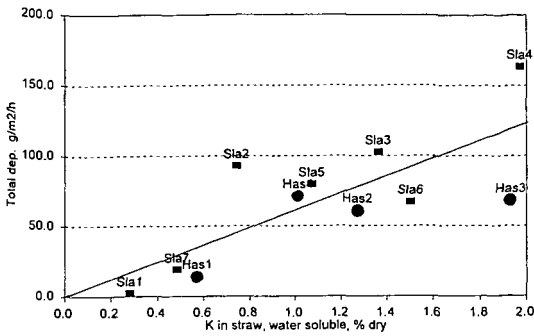


Fig. 5. Total deposition flux in the furnace as a function of water soluble K in the straw.

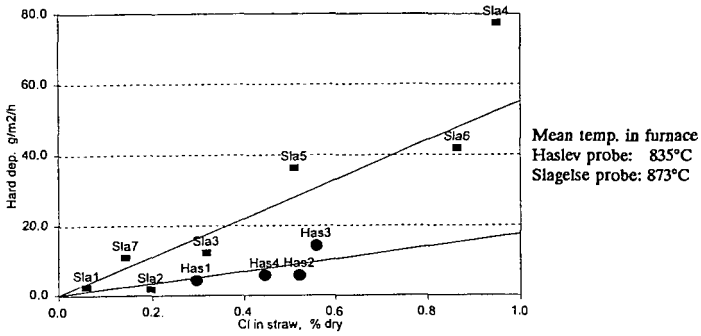


Fig. 6. Deposition flux of hard material in the furnace as a function of Cl in the straw.

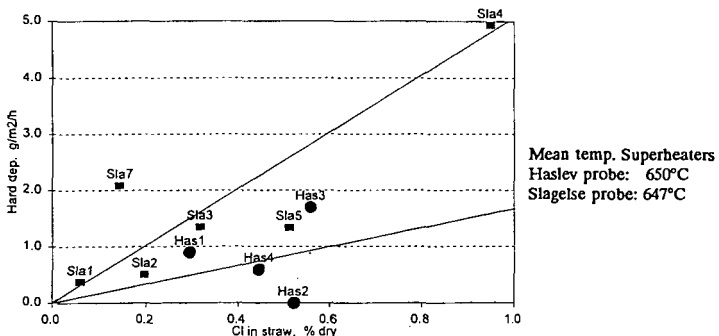


Fig. 7. Deposition flux of hard material at the superheaters as a function of Cl in the straw.

BED MATERIAL AGGLOMERATION IN PFB BIOMASS GASIFICATION

Nader Padban, Samuel Kiuru & Anders L. Hallgren
Dept. of Chem. Eng. II, P.O.B. 124 Chemical Center
University of Lund, S-221 00 Lund, Sweden

Keyword: Biomass, Bed material, Alkali induced agglomeration, Ash

1. Introduction

Small amounts of alkali compounds can drastically change the behavior of bed materials in fluidized bed gasification systems. Alkali-induced agglomeration and defluidization of the bed may cause severe operational problems and can be detrimental to the overall process. Enhanced tendency for agglomerations in the bed has been found in systems utilizing biomass or so called alternative solid fuels as feed-stock. The fuel alkali may add to the accumulation of alkali compounds in the bed. Adhesion tendencies between the particles seem to increase due to sticky layers of alkali condensations on the particle surfaces. In the present study an endeavor was made to establish a method for investigating suitable bed materials and the effect from biomass ash on the bed behavior in PFB biomass gasification. In this approach first results show that the composition of the particles in the bed, the temperature, and the mobility of the particles are of primary importance.

Agglomeration of bed material and problems caused by ash sintering in fluidized bed combustion/gasification processes has been reported frequently in the literature. According to Prabir et al [1] agglomeration of bed material can under certain conditions occur even at the temperatures below the ash fusion temperature and gas velocity higher than minimum fluidization velocity. Squire [2] and Sieggill [3] describe the defluidization phenomena as a direct consequence of stickiness of bed material. This could be caused by changed properties of bed material at a certain temperature or due to liquid deposition on the surface of the particles.

Ash agglomeration in a fluidized-bed coal gasifier may be influenced by the high surface tension of mineral matter. Capillary forces may draw mineral matter from the interior of a hot carbon particle in order to be accumulated as ash on the particle surface [2].

Gerald P. Huffman et al [4] investigated the high-temperature behavior of coal ash in reducing and oxidizing atmospheres. The results from that study suggest that significant partial melting of the ashes occurs at temperatures as low as 200-400 °C below the initial deformation temperature defined by ASTM ash cone fusion test. According to their experiments ash melting is accelerated by reducing conditions. In a reducing atmosphere the ash melting will mainly be controlled by the iron-rich corner of the FeO-Al₂O₃-SiO₂ phase diagram.

B.K.Dutta et al [5] propose that the softening temperature of a coal ash is lower in mild reducing atmosphere than in oxidizing or strongly reducing atmosphere. The decreased ash fusion temperature is caused by the fluxing effect of different iron oxides. Depending on the temperature, the state of these oxides will change and consequently even their fluxing effect. In an oxidizing atmosphere iron will be present as Fe₂O₃ and in mild reducing atmosphere as FeO, while in a strong reducing environment it tends to exist in metallic form. Ferrous oxide has the maximum fluxing effect on coal ash. Additionally, Dutta et al report that in the case of excess iron and in oxidizing atmosphere, the effect of alkali in decreasing the ash softening temperature may be very low or even insignificant.

R.G. Rizeq and F. Shadman [6] describe two different mechanisms for alkali-induced agglomeration of solid particles in coal combustors and gasifiers. In the case of low alkali concentration agglomeration is a result of formation of low-melting glassy phases on the

particle surfaces. In alkali rich conditions alkali salts will form a molten layer on the surface of particles which result in adhesion of particles. Their experiments even show that the minimum agglomeration temperature of some minerals can be decreased several hundred degrees depending on the alkali content.

In connection to the effect of alkaline compounds on ash sintering and deposit forming in peat gasification, Moilanen [7] show that there is a clear correlation between chemical composition and sintering strength of peat ashes at 800°C. According to those investigations the sintering strength of peat ashes rises by increased B/A (bas/acid) ratio in these ashes.

Up to now most research efforts considering ashes and bed materials have been concentrated to coal combustion and gasification processes. Since the bed material in these processes often differs from those used in biomass gasification there is a need for further investigations in this area. In gasification and combustion of biomass, where external bed material is used, not only the problems caused by ash melting and sintering but also problems created by reactions between bed material and ashes must be considered.

Previous work at the department of Chem. Eng. II [8] have shown that the agglomeration and cake forming phenomena in bed material in presence of alkaline compounds depend on both temperature and the kind of alkali present. The stable alkali compounds such as chlorides do not react with bed materials consisting of Al and Si at temperatures below 800°C, while unstable compounds such as alkali nitrates cause agglomeration of bed materials at the temperatures as low as 550°C. Therefore the knowledge about the composition of different alkali and other fluxing materials in ashes is necessary for predication of ash effects on bed material.

In the present work ash content and chemical composition of ashes for two different biomass has been investigated. The effect of temperature on the chemical composition of these ashes has been studied. Different mixtures of ash/bed material have been treated thermally to study the agglomeration or cake forming phenomena in the bed material.

2. Experimental

2.1 The Sample preparation

To study the temperature effect on ash chemical composition two different biomasses was preliminary ashed at 550°C. The ashing procedure has taken place in presence of air and at atmospheric pressure. The produced ashes were subsequently heated at 650°C and 900°C in 1 hour. The chemical composition of the ashes obtained from the temperature treatment was determined by **atomic absorption Spectrophotometry (AAs)** and **ion chromatography (IC)**.

Mixtures of ashes (obtained in 550°C) and bed material (consisting 99.5% of SiO₂) were used in investigating the agglomeration and cake forming phenomena caused by alkali in the bed material. The bed material/ash quotes for the samples were 0, 0.25, 1 and 4. In the preparation of mixtures the required bed material amount was placed as a layer on the weighted ash sample.

Samples were treated thermally in an oven to 900°C. The residence time at 900°C was one hour for all samples. **Scanning Electron Microscopy (SEM)** was then used for analyses.

2.2 Analysis procedures

Analysis for solid samples in the form of ashes, ceramics, glasses, minerals and etc. can be made in several different ways:

- i. X-ray fluorescence spectroscopy (XRF) is the most simple and accurate method without need for any cumbersome digestion procedure of the sample.
- ii. methods that require melting + digestion in order to transfer the solid sample into a solution before the real analysis can start. Such method may be ICP and AAS with flame and preferably with graphite furnace and IC.

For analyses, AAS with air-C₂H₂ and N₂O-C₂H₂ flame and IC were available. All elements Al, Si, Ca, Fe, Mg, Mn, K, Na, S and P can be analyzed by AAS with a graphite furnace. Since the last mentioned instrumentation was not available AAS with flame was used for all the mentioned elements except for S and P which were analyzed by isocratic IC. For phosphor a new analytical method for IC had to be developed and because sulfur cannot be analyzed on AAS, the next best way was to analyze both S and P by existing IC equipment. S and P separated in the IC column system as SO₄²⁻ and PO₄³⁻ ions. In the determining of S and P a small volume, typically 1 to 2 ml, filtered through 0.22 micron membrane filter, was introduced with a syringe or with a sample changer into a 50 µL loop. The anions of interest, SO₄²⁻ and PO₄³⁻, were separated and measured using a isocratic system comprised of a guard column, separator column, suppressor column and conductivity detector.

For the AAS analysis, 40-70 mg fine-grounded ash sample was mixed with 1:12 parts lithium methaborate dihydrate, LiBO₂·2H₂O in a graphite or platina crucible. The mixtures were then molted at 900°C in CO₂ atmosphere. The melt was dissolved in dilute nitric acid under stirring (10-15 hour). After appropriate dilutions the obtained solutions were analyzed by AAS for measuring the amount of Si, Al, Ca, K, Na, Fe, Mg and Mn in samples.

In the Scanning Electron Microscopy (SEM) studies the investigated areas were different for pure ashes and ash-bed material mixtures. In order to achieve a more general conception of the ash surfaces, in the case of pure ash the studied area was relatively large, however, for the characterization of different particles in mixtures point analyses (studied area~ 9µ²) were performed.

3. Results and discussions

Heating pure ashes results in a decrease in volume and the ash particles tend stick together. However the adhesion is not strong and can easily be destroyed by finger touch.

Agglomeration of bed material particles was observed in all ash-bed material mixtures, independently on ash/bed material quote. The size of the agglomerate for EB,biomass was much smaller than for those related to Salix. Generally the agglomerate size increases by increasing ash/bed material quote.

The AAS/IC (bulk) analysis of ashes from different-temperatures shows no significant temperature-related variations in chemical composition in ash of any sort. This could indicate that the ashes, already in the lowest ashing temperature, have reached a chemical equilibrium in solid /or condensed phase.

Comparison between the results from AA/IC and SEM shows considerable differences in chemical composition for both ashes. Generally Si, Al and K content determined by SEM analysis is much lower than those determined by AA/IC. Although

SEM analysis shows the chemical composition of the outer surfaces of particles (max. penetration = 3μ), the explanation can be that most of these elements are in the inner part of the ash particles. According to this assumption the outer shell will consist of oxides, sulfates, carbonates and phosphates of Ca, Mg, Mn and K.

The stronger agglomeration tendency for Salix mixtures may depend on the higher potassium content in these samples.

Table III shows some results of SEM point analysis studies for particles in the mixtures. The particles containing high silicon represent bed material grain from the agglomerates. These results indicate that the composition of the particle surface can vary drastically from one point to another in the same sample. Applied SEM analysis method has not shown to be satisfactory for larger surface examinations.

4. Conclusions

The ashes from biomasses are not homogeneous materials, and their chemical composition differ from one particle to another. Higher alkali content in ash surfaces contribute to a stronger agglomeration tendency in ash- bed material mixtures. The agglomerates consist of bed material particles surrounded by small particles rich in Ca and with varying concentration in K, P, S and another elements. Preliminary results indicate that agglomeration may be related to a wide range of low melting compounds consisting of this elements and Si. Studies of phase diagrams [9] show that since only the compounds containing alkali can have melting points lower than 900°C , we can not exclude the importance of alkali in agglomeration phenomena.

5. Acknowledgments

This work has financially been supported by the National Board for Industrial and Technical Development (Nutek)

References

1. Pabir Basu and A. Sarka; Agglomeration of coal ash in fluidized beds; Center of Energy Studies, Technical University of Nava, Halifax, Canada B3J 2X4.
2. A. M. Squiers et al; Behaviour of mineral matter in a fluidized bed gasifying cone; the ignifluid process; Trans. Brit. Ceram Soc. 1976, 75, 85-91.
3. J. H. Siegill; Defluidization phenomena in fluidized bed of sticky particles at high temperatures, PhD dissertation, The City University of New York, (1976).
4. G. P. Huffman et al; Investigation of the high temperature behaviour of coal ash in reducing and oxidizing atmospheres; US Steel Corporation, Research Laboratory, Monroeville, Pennsylvania 15146, USA.
5. B. K. Dutta et al. A study of the fusion characteristics of coal ashes: Softening temperature of coal ashes in a mild reducing atmosphere; Planning & Development Department, Fertilizer Corporation of India Ltd, Sindri.
6. R.G. Rizeq & F. Shadman; Alkali-induced agglomeration of solid particles in coal combustors and gasifiers; Chem. Eng. Comm. Vol. 81, pp. 83-96
7. A. Moilanen; Ash behaviour in gasification; Technical Research Centre of Finland; Laboratory of Fuel Processing Technology; Espoo, Finland.
8. N. Padban; Master thesis; Dept. of Chemical Engineering II, Lund University, Sweden.
9. Levin; Ribbins; McMurdie.; Phase diagrams for ceramists. American Ceramic Society, 1964- .

Table I. Composition of ashes in different temperatures ; analyzed by AAS/IC

Content, %		Si	Al	Ca	K	Na	Mg	Mn	Fe	S	P
EB,biomass	550°C	11.7	1.8	24.9	9.1	0.9	6.4	2.3	0.8	1.1	1.2
	650°C	12.6	1.9	25.1	9.9	1.3	7.0	2.6	0.9	1.1	1.6
	900°C	12.0	1.9	29.4	9.4	1.5	7.4	2.9	1.0	1.5	1.6
Salix	550°C	2.6	0.8	30.1	11.0	0.7	4.6	0.3	0.5	1.4	2.2
	650°C	1.6	0.9	29.5	12.1	1.0	4.3	0.3	0.7	1.6	2.5
	900°C	2.4	0.9	33.6	12.6	0.8	5.3	0.4	0.7	1.8	3.1

Table II. Ash composition for Salix and EB,biomass ; SEM studies

Content%	Si	Al	Ca	K	Mg	Mn	S	P
EB,biomass ash	3.02	0.78	37.33	3.58	4.56	9.97	2.23	4.27
	4.21	1.07	39.23	3.23	3.59	7.06	2.93	3.41
Salix ash	0.354	0.065	43.92	6.81	3.5	0.56	0.52	9.45
	0.68	0.089	43.82	6.01	2.78	0.73	2.66	7.69

Table III. Chemical composition of some particles in agglomerates ; SEM studies

Content%	Si	Ca	K	S	P
EB,biomass;ash/BM=0.25	24.64	18.48	2.04	1.08	2.48
EB,biomass;ash/BM=0.25	5.19	39.6	0.19	2.28	4.04
EB,biomass;ash/BM=1	2.87	52.53	2.58	2.58	1.48
EB,biomass;ash/BM=4	8.4	33.64	1.04	1.4	4.26
EB,biomass;ash/BM=4	34.38	10.75	0.41	0.68	1.83
Salix,ash/BM=0.25	34.36	6.25	13.51	0.17	0.0
Salix,ash/BM=0.25	5.33	38.19	1.64	4.18	7.17
Salix,ash/BM=0.25	1.17	40.30	0.24	3.94	10.97
Salix,ash/BM=1	41.92	3.09	0.27	0.27	1.72
Salix,ash/BM=1	2.78	42.23	1.4	0.54	11.89
Salix ,ash/BM=4	0.39	24.68	23.36	1.51	11.77
Salix ,ash/BM=4	0.42	57.2	0.89	0.57	5.7



SEM-photo of quartz sand particle embedded in alkali (50X).

LABORATORY ILLUSTRATIONS OF THE TRANSFORMATIONS AND DEPOSITION OF INORGANIC MATERIAL IN BIOMASS BOILERS

Larry L. Baxter¹, and Bryan M. Jenkins²

¹Combustion Research Facility
Sandia National Laboratories
Livermore, CA 94551-0969

²Dept. of Biological & Agricultural Eng.
University of California, Davis
Davis, CA 95616-5294

Keywords: combustion, biomass, inorganic material, ash

ABSTRACT

Boilers fired with certain woody biomass fuels have proven to be a viable, reliable means of generating electrical power. The behavior of the inorganic material in the fuels is one of the greatest challenges to burning the large variety of fuels available to biomass combustors. Unmanageable ash deposits and interactions between ash and bed material cause loss in boiler availability and significant increase in maintenance costs. The problems related to the behavior of inorganic material now exceed all other combustion-related challenges in biomass-fired boilers. This paper reviews the mechanisms of ash deposit formation, the relationship between fuel properties and ash deposit properties, and a series of laboratory tests in Sandia's Multifuel Combustor designed to illustrate how fuel type, boiler design, and boiler operating conditions impact ash deposit properties.

INTRODUCTION

Biomass-fired electric power generating stations are assuming increasingly prominent positions in energy and environmental issues in many regions of the world [Hustad and Sønu, 1992]. Such power stations typically are small (less than 50 MW_e net output), and rely on indigenous fuel supplies. Fuels for such facilities can be broadly classified into the categories of wood, agricultural residues, urban and municipal waste, and energy crops. Wood commonly represents the fuel of choice and the design fuel for biomass power stations. Wood's use is limited by availability, cost, and permitting agreements but in most cases not by fireside related problems (fouling, slagging, corrosion, etc.) in the boiler. The cost of wood fuel for such power stations in recent years was impacted by competition among the biomass power stations in some regions of the US, although such competition has waned in the last 18 months. At its peak, the cost of wood fuel in Northern California (USA) increased by over a factor of two from its baseline value prior to significant biomass combustion demand [Turnbull, 1993]. The availability of wood is beginning to decrease as a result of substantial reductions in logging associated with economic policy and wildlife protection. The probability of high fuel prices and unreliable availability motivate evaluation of new fuels for these combustors.

The motivation to develop new fuels for some power stations is driven by regulation and legal agreements more than by economics or availability. For example, under Title I of the U.S. federal Clean Air Act Amendments of 1990, states designate areas within their boundaries as attainment, non-attainment, or unclassifiable for each of six pollutants [1989]. Designations are based on either federal or state air quality standards. Operating permits for all biomass-fired power stations are based in part on their impacts on air quality. For power stations in or near non-attainment areas, permits often require a net *reduction* in the amount of pollutant (NO_x, particulate matter, etc.) generated in that area. This is accomplished by use of offset fuels, that is, fuels that would otherwise be burned in the field and produce higher levels of pollutants than what is produced if the same fuels are burned in a boiler. Agricultural byproducts generally and straw in particular represent common examples of offset fuels. Some power stations agree in their permits to consume sufficient offset fuel that they compensate for the pollutants produced from their overall operation, resulting in a net decrease in pollution as a result of operating the power plant.

Economic, long-term-planning, environmental, regulatory, and legal motivations can be strong for using offset or alternative fuels in biomass combustors. In addition, large and reasonably stable supplies of these fuels can be secured in many regions of the country. In practice, combustion of these fuels has proven difficult. Problems vary from fuels handling and storage to seasonal variations in both the amount and the quality of the supply. Arguably the most daunting issue, and the subject of this investigation, is the inorganic material in the fuel and its impact on the combustor. For example, essentially all biomass-fired power stations in

California that were designed and permitted based on using straw as an offset fuel opt to process straw by means other than combustion. These decisions are driven by the consistent experience of unmanageable bed agglomeration, slagging deposits, and convection pass fouling when burning straw. Several international studies have been completed in the general area of straw combustion [FEC Consultants Ltd., 1988; Livingston, 1991; Martindale, 1982; Martindale, 1984]. In many cases, addition of as little as 10 % straw to the boiler fuel supply for an electric power-generating facility causes an unscheduled shutdown within a few hours. Field experience with some other offset or alternative fuels (orchard prunings, nut shells or hulls, fruit pits, etc.) demonstrates borderline operation, with blend ratios limited to only 10-15 % when fired with wood [Miles, 1992; Miles and Miles, 1993; Miles, et al., 1993].

General mechanisms of ash deposition and laboratory/pilot-scale tests of bed agglomeration during straw combustion are discussed elsewhere [Baxter, 1993; Salour, et al., 1993]. The current investigation combines laboratory and field data in examining the causes of fireside problems during biomass combustion in a mechanistic way. Laboratory tests were conducted in a pilot-scale combustor and incorporated both *in situ* and *post mortem* analyses of ash deposit morphology, composition, and rate of accumulation. In separate reports, the details of an extensive series of laboratory and field tests of over a dozen biomass fuels and their ash-related combustion behaviors are discussed [Baxter, et al., 1995; Jenkins, et al., 1994; Miles, et al., 1994]. These sets of data are analyzed both separately and in comparison to demonstrate several of the most important aspects of ash behavior during straw combustion. This paper summarizes the laboratory findings during these investigations and illustrates many of the issues associated with the ash behavior of biomass fuels.

FACILITIES

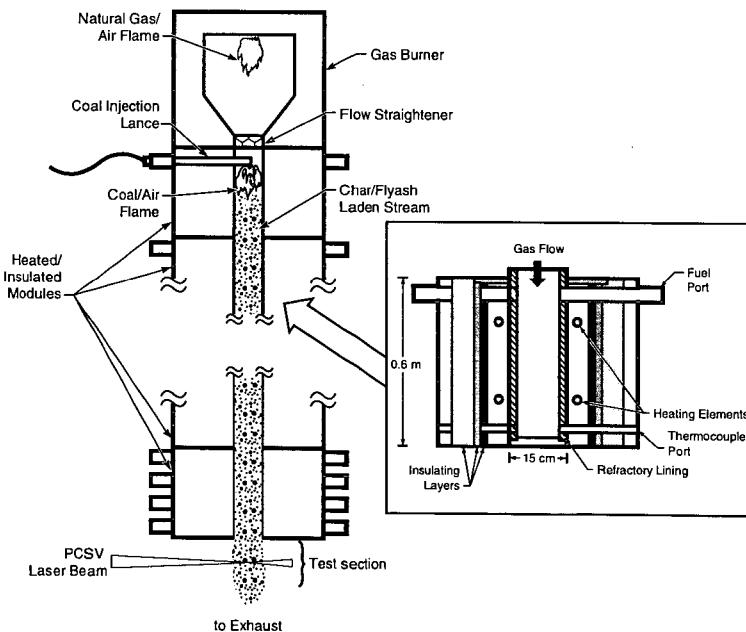


Figure 1 Schematic diagram of the Sandia Multifuel Combustor used in these combustion tests with modular guard heater inset.

The Multifuel Combustor (MFC) at Sandia was used to perform laboratory- and pilot-scale tests on ash deposition during combustion of the solid fuels indicated in Table I. The MFC is a pilot-scale (30 kW) down-fired, turbulent flow reactor that simulates the gas temperature and composition histories experienced by particles in combustion systems (Figure 1). A gas burner is used to provide a vitiated air to the remainder of the combustor. Gases from the burner flow through a series of modular sections that include guard heaters, fuel insertion ports, and thermocouple insertion ports. At the end of these modular heaters is the test section of the combustor. In this section, several air-cooled deposition surfaces that simulate waterwalls and convection pass tubes are injected in the particle-laden, vitiated flow. In the experiments described here, surface temperatures of these tubes are measured using thermocouples. Surface

temperature was held constant in each individual experiment but varied from 350 to 650°C among the several experiments performed. Further details about the MFC are available in the literature [Baxter, 1993].

Table 1 Biomass Fuels Tested in Sandia's Multifuel Combustor

Fuel	Moisture (% fuel)	Ash (% dry fuel)	Higher Heating Value (MJ/kg, daf)
		Herbaceous Fuels	
Rice Straw	11.22	19.17	18.74
Wheat Straw	8.39	8.08	19.31
Switch Grass	12.98	5.86	19.91
		Ligneous Fuels	
Almond Shells	7.52	2.87	19.83
Pistachio Shells	8.08	1.28	19.90
Olive Pits	6.97	1.83	21.97
Almond Hulls	8.02	5.75	20.00
Humus	12.51	34.64	12.89
		Commercial Fuels	
Urban Wood Fuel Blend	8.62	7.54	19.97
Nonrecyclable Paper	5.95	8.21	23.44
Wood/Straw Blend	9.25	7.33	20.56

The MFC was designed to simulate conditions in a coal combustor and has nominal fuel residence times of up to about four seconds. Typical fuel residence times in pulverized coal combustors are about two seconds. In the biomass tests, fuels were comminuted, typically to sizes less than 1 mm. This provided for nearly complete carbon conversion of the straws within the maximum residence time available in the combustor.

In all straw combustion tests, fuel was inserted into the MFC at a height of approximately 4.3 m (14 ft.) above the beginning of the test section. Ash deposits were collected from a simulated water wall and convection pass tube as well as from the internal ceramic liner of the MFC.

RESULTS AND DISCUSSION

Alkali metal behavior, in particular potassium, was identified at the beginning of the investigation as a concern. Traditional clean wood fuels contain little ash (< 1 %), and the ash contains relatively small amounts of potassium (5-20 %). The two commercial wood fuels indicated in Table 1 contain less clean sources of wood (urban wood waste, for example) and are blended with other, high ash fuels. The dominant ash components of clean wood include silicon and aluminum. Less traditional fuels, including essentially all of the nonprocessed herbaceous fuels and most of the nonprocessed agricultural residues, contain much more ash (Table 1) and higher potassium concentrations. Processed fuels, such as bagasse from sugar cane, often have very low alkali contents. The behavior of alkali is highlighted below (Figs. 2-4).

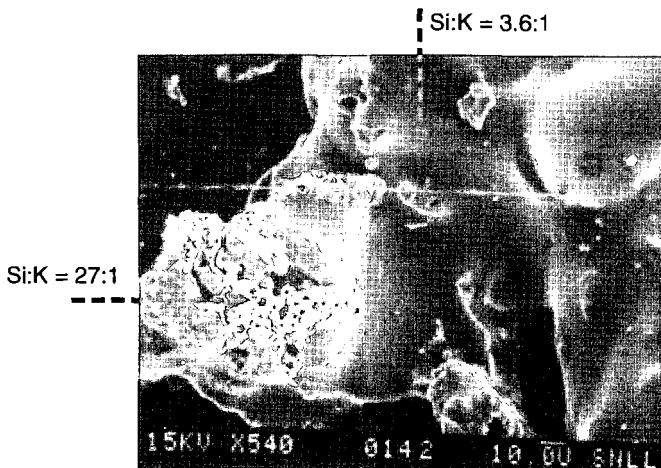


Figure 2. Elemental composition of different regions of a straw ash deposit.

Alkali materials in many forms are slightly volatile under combustion conditions. The resulting inorganic vapors react with other fuel or ash components to exacerbate ash deposition problems by two primary mechanisms. The first mechanism is the formation of molten deposits, an example of which is seen in Fig. 2. The silicon to potassium ratio of two regions of a straw deposit are indicated. The molten region has a silicon to potassium ratio of less than 4:1, whereas the same ratio in the granular region is over 25:1. Alkali metals generally decrease the melting point of silica by formation of alkali silicates. Potassium, the primary alkali metal in biomass, is more mobile during combustion than is common in, for example, coal. This leads to formation of soft or molten deposits for many nontraditional biomass fuels at lower temperatures than is common for coal or traditional woods.

The second mechanism of alkali metals contributing to ash deposition during biomass combustion is the formation of sulfated compounds. The low temperatures of steam tube surfaces promote the condensation of alkali vapors on surfaces. At surface temperatures, alkali sulfates are stable chemical species. The formation of an alkali sulfate layer of the deposit in intimate contact with the surface leads to the formation of a tenacious deposit. This is illustrated in Fig. 3, where the composition of an ash deposit was measured at the deposit crown, in the center of the deposit, and at the probe surface (positions A, B, and C, respectively). The concentration of sulfur monotonically increased as the measurement point approached the probe surface, with the ratio of sulfur at position C being over twice as high as at point A.

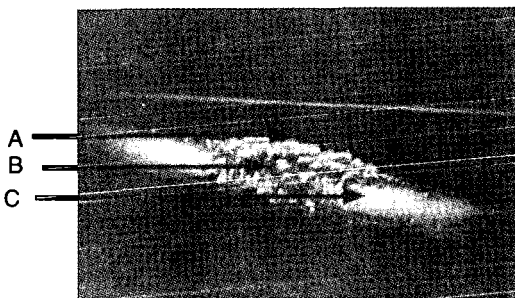


Fig. 3. Illustration of the formation of a sulfate bonding layer in a wheat straw ash deposit.

Similar behaviors are noted in the field experiments, as indicated in Fig. 4. The analysis compares the composition of the fuel ash and a deposit collected from a furnace surface that experiences little direct impact of particles. The amount of direct particle impaction on a surface depends primarily on boiler design. This deposit was collected from the wall opposite the furnace exit and convection pass entrance, where particles are directed away from the wall and into the convection pass. Very few impact on the boiler surface in this region. The vapors, on the other hand, are carried with the gases to the wall where they condense and react to form sulfates. As can be seen, the deposit composition is highly enriched in alkali metals and sulfur compared to the fuel ash composition. If boiler design or operating conditions change such that there is greater impact of particles in this region, the composition silica and other species associated with particles increases.

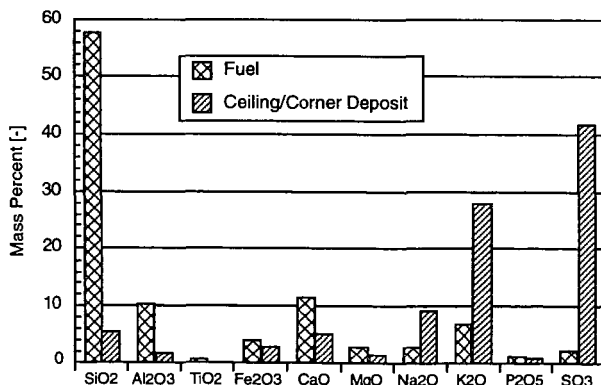


Fig. 4. Comparison between elemental composition of the fuel ash and a thin layer of reflective ash deposited on the ceiling and upper corner of the furnace. All compositions are expressed as oxides.

CONCLUSIONS

A series of laboratory and field tests illustrate the principal mechanisms of ash deposit formation during combustion of biomass fuels. Relationships among the amount and mode of occurrence of inorganic material in the fuel, boiler design, and boiler operating conditions that influence the type of ash deposit formed are discussed. Specific examples of ash deposit formation during combustion of straw are used to illustrate the mechanisms.

Important attributes of ash deposits are determined by the relative rates of particle impaction on surfaces, condensation, and chemical reactions. Deposit morphology, composition, tenacity, porosity, and reflectivity are influenced by the mechanism of deposition. For a specific fuel, the dominant deposition mechanisms vary with location in the boiler and with boiler operating conditions.

Distinguishing characteristics of biomass combustion include the large amount of silica and vaporizable alkali in the ash of nontraditional fuels and the tendency of the silica and alkali to combine chemically on heat transfer surfaces. Alkali vapors condense on cool surfaces to form thin, reflective, alkali-based deposits. The alkali chemically combines with sulfur to form sulfates. In regions where silicon-based fly ash particles accumulate on surfaces, alkali combines with the silica to form silicates. These alkali-silicates have melting temperatures near or below the prevailing gas temperatures. This leads to sintering and formation of molten phases in the deposit. The rate of sintering depends on both deposit temperature and the amount of alkali in the gas phase.

REFERENCES

- (1989). "Federal Register: Part III; Air Contaminants" (Final Rule No. 29 CFR Part 1910).
- Baxter, L. L. (1993). "Ash Deposition During Biomass and Coal Combustion: A Mechanistic Approach." *Biomass and Bioenergy*, 4 (2), 85-102.
- Baxter, L. L., Jenkins, B. M., Miles, T. R., Miles Jr., T. R., Oden, L., Bryers, R., Milne, T., and Dayton, D. (1995). "Ash Behavior in Biomass Boilers" No.
- FEC Consultants Ltd., O. (1988). "Straw Firing of Industrial Boilers" (Contractor Report No. ETSU B 1158). Energy Technology Support Unit: Department of Energy: United Kingdom.
- Hustad, J. E., and Sønju, O. K. (1992). "Biomass Combustion in IEA Countries." *Biomass and Bioenergy*, 2(1-6), 239-261.
- Jenkins, B. M., Baxter, L. L., Miles, T. R., Jr., T. R. M., Oden, L. L., Bryers, R. W., and Winther, E. (1994). "Composition of Ash Deposits in Biomass Fueled Boilers: Results of Full-scale and Laboratory Simulations". In *ASAE*, (pp. Paper No. 946007). St. Joseph, MI 49085-9659: ASAE.
- Livingston, W. R. (1991). "Straw Ash Characteristics" (Contractor Report No. ETSU B 1242). Energy Technology Support Unit: Department of Energy: United Kingdom.
- Martindale, L. P. (1982). "The Potential for Large Scale Projects Featuring Straw as a Fuel in the UK" No. ETSU.
- Martindale, L. P. (1984). "The Potential for Straw as a Fuel in the UK" No. ETSU.
- Miles, T. R. (1992). "Operating Experience with Ash Deposition in Biomass Combustion Systems". In *Biomass Combustion Conference*, Reno, NV:
- Miles, T. R., and Miles, T. R., Jr. (1993). "Alkali Deposits in Biomass Power Plant Boilers". In *Biomass Power Program*, Washington, DC:
- Miles, T. R., Miles, T. R., Jr., Baxter, L. L., Jenkins, B. M., and Oden, L. L. (1993). "Alkali Slagging Problems with Biomass Fuels". In *First Biomass Conference of the Americas: Energy, Environment, Agriculture, and Industry*, 1 (pp. 406-421). Burlington, VT: National Renewable Energy Laboratory.
- Miles, T. R., Thomas R. Miles, J., Baxter, L. L., Bryers, R. W., Jenkins, B. M., and Oden, L. L. (1994). "Boiler Deposits from Firing Biomass Fuels." *Biomass & Bioenergy*, (submitted).
- Salour, D., Jenkins, B. M., Vafaei, M., and Kayhanian, M. (1993). "Control of In-bed Agglomeration by Fuel Blending in a Pilot Scale Straw and Wood Fueled AFBC." *Biomass and Bioenergy*, 4(2), 117-133.
- Turnbull, J. H. (1993). "Use of Biomass in Electric Power Generation: The California Experience." *Biomass and Bioenergy*, 4(2), 75-84.

THE BEHAVIOUR OF ALKALI METALS IN BIOMASS CONVERSION SYSTEMS

Pia Hald
Department of Combustion Research
Risoe National Laboratory
Roskilde, Denmark

Keywords: alkali metals, gas phase measuring, equilibrium

INTRODUCTION

The development towards reduced environmental impact and improved energy efficiency has in recent years lead to development of new power technology and a renewed interest in the use of biomass in the power supply.

The advantage of substituting coal by biomass are that the emission of CO₂, which contributes to the greenhouse effect, is reduced. A disadvantage of biomass is that the problems concerning alkali metals often become more severe. That is due to the difference of how the alkali metals are bound in coal and biomass.

During combustion and gasification alkali metals may contribute to slagging, deposition, corrosion and fluidized bed agglomeration. Whether or where in the system the problems appear is related to the transformations of the alkali metals and these depend on fuel and process conditions.

The alkali metal remains in the ash fractions during the process or is released as gaseous alkali metal. The gaseous alkali metal reacts with the ash fractions or condense due to saturation. The alkali metals in the ash fractions, bottom ash and fly ash, may transform during the process dependent on which components are favoured.

Studies on the alkali metal transformations are carried out in order to predict and thereby reduce the mentioned problems. Tools to study the fate of alkali metals are measuring of gas phase alkali metal, equilibrium calculations and chemical analyses of solid materials as e.g. deposits.

The problems of alkali metals are known from coal conversion. With respect to coal the problems are mainly related to sodium and with respect to biomass the problems are mainly related to potassium. Hald (1994) contains a literature survey on alkali metals in coal conversion systems and compare coal and straw concerning alkali metals. A system for measuring of gas phase alkali metals was designed and the sampling efficiency was tested. A comprehensive equilibrium study was performed and the results organized in tables as an easy access to equilibrium results. How ash components contribute to melt formation is discussed. The use of the developed tools is demonstrated for a fluidized bed combustor and a gasifier. Theoretical and experimental discussions are mainly related to straw and coal, but the results may be used in the study of other fuels. Some results from Hald (1994) are presented below, arranged in the sections alkali metals in the fuel, alkali metals at equilibrium, gas phase measuring, alkali metals in a fluidized bed combustor and alkali metals in a straw gasifier.

ALKALI METALS IN THE FUEL

Using straw as fuel the alkali metal related problems become more pronounced than with coal, even though the content of the alkali metals may be quite similar. That is due to the difference of how the alkali metals are present in the fuels which is important for their fate during the conversion process.

The alkali metal alumina silicates are the alkali metal components in fuels which are the most stable and those with the highest melting points. Because of that alumina silicates are used as getter materials to reduce the amount of gas phase alkali metals and increase the melting points.

Alkali metals in a less stable form, easier released to gas phase during a conversion process, are those present as the more simple salts, e.g. KCl, NaCl and salts of carboxylic acids. Alkali metal not present as alumina silicates are in the following denoted the soluble alkali metals. Alkali metals as chlorides, carbonates and sulphates have relatively low melting points compared to the alkali metal alumina silicates.

Alkali metal related problems using coal are primarily due to sodium, although the potassium content often is higher than that of sodium. That is due to larger amounts of sodium in a soluble form.

In contrast to coal the content of Al_2O_3 in biomass is relatively small and the most alkali metals are present in a soluble form. Another important difference between coal and biomass is that getter materials may be present within the coal and react with the soluble alkali metal to form alkali metal alumina silicates.

The amount of melt formation depends on the combination of components and temperature. Equilibrium calculations will show which components are favoured.

ALKALI METALS AT EQUILIBRIUM

Equilibrium calculations may be used in the description of which components are favoured and what influence a change in process conditions will have. Exact amounts may be determined by gas phase measurements and chemical analyses of the solid materials.

An extensive equilibrium study was performed and some general tendencies for the alkali metals were revealed. The calculations involving more equilibrium equations were performed by use of an equilibrium model (Michelsen, 1989) assuming gas phase ideality and phases immiscible.

The ideal gas phase assumption was studied and shown to be acceptable for gasification/combustion gases, the relative deviation of the volume is maximum 4 % at pressures up to 80 atm in the temperature range 300 K to 2000 K. It was shown that with ideal liquid mixtures, containing alkali metals, present the gas phase content of alkali metals will be lower than if phases were immiscible.

General tendencies about which non-silicate alkali metal components to be favoured in ash materials or at condensation, at high and low temperature and at oxidizing or reducing conditions, could be arranged relatively to the ratios alkali metals to chloride (M/Cl) and alkali metals to sulphur (M_2/S), see Table 1. S, Cl and M describe the molar content of sulphur, chlorine and soluble alkali metals in the selected equilibrium system. The system can e.g. be the global system or a sub system as e.g. the gas phase. M_2 denotes M divided by two as alkali metals and sulphur form components in the mole ratios 2 : 1.

A general difference between coal and straw can be described by the mole ratios M_2/S and M/Cl, see Table 2. The sulphur content is lowest in straw and the chloride content in straw is in about the same range as in high chlorine coals.

Alkali metals, chlorine and sulphur from coal will be in the gas phase in the same ratios as given for the pure coal in Table 2. By use of Table 1 it is seen that alkali metals condensed from gas phase at coal combustion may be present only as M_2SO_4 . This agrees with what is described in the literature about sodium condensation in coal combustion systems.

With all soluble alkali metal, all sulphur and all chlorine from straw present in the gas phase, the mole ratios for the gas phase are as in Table 2. At combustion conditions Table 1 shows possibility for both alkali metal sulphates, carbonates and chlorides to condense when cooling the gas.

Results from measuring of potassium, chloride and sulphur in gas phase at straw combustion (those measurements mentioned in Jensen et al. (1995)) show that the chloride content typically exceeds the potassium content ($M/Cl < 1$). This leaves no possibility for alkali metal carbonate formation when the gaseous potassium condenses (see Table 2, $M/Cl < 1$ and $M_2/S > 1$). This is an example of how the equilibrium calculations and gas phase measurements may be used in the evaluation of deposition mechanisms.

Alkali metals are in the gas phase as $MCl(g)$ and $MOH(g)$. The distribution depends on the M/Cl ratio and the temperature. At temperatures above 800 °C no MCl will be found in solid or liquid form (see Table 1). This is true for a combustion or a gasification system using fuels with alkali metal contents similar or lower than straws. Both release of alkali metal from the fuel and the condensation of gaseous alkali metal are determined by kinetics. The equilibrium information about alkali metal chloride tells that with sufficient residence time of the fuel ash all alkali metal chlorides will be released to gas phase at temperatures above 800 °C and cooling a gas the alkali metal chlorides will not condense at temperatures above 800 °C.

Other examples of how the equilibrium calculations may be used to describe a change in the conversion system are 1) that more alkali metals will be present in gas phase with an increasing chloride to alkali metal ratio. 2) With coal as fuel, changing from reducing to oxidizing conditions, the amount of alkali metals present in gas phase may decrease due to condensation of alkali metal sulphates. With straw as fuel this change will not be as significant as straw contains much less sulphur than coal.

The tendency to melt formation will increase with increasing amounts of the alkali metal components with low melting points present. Those alkali metal components act as fluxing agents for the other ash components. Calculating freezing point depression by equation (1) it may be evaluated to which extent the ash component denoted i contributes to melt formation.

$$\Delta T = T^* - T = - \frac{R}{\Delta H_m} \cdot T^* \cdot T \ln(x_i) \quad (1)$$

ΔT is the freezing point depression, T^* the melting point of the pure solid i (equals freezing point), R the gas constant, ΔH_m the molar melting enthalpy for component i and x_i the mole fraction of the component i in the mixture. At temperatures above T no solid phase of component i will be present. The freezing point curve for a component i can be described by the set of T, x_i . Freezing points of a number of components at $x_i = 0.8$ were calculated, the results are given in Table 3. A material as Al_2O_3 has a high melting point and a high melting enthalpy leading to a very small freezing point depression. A component as SiO_2 has a low melting enthalpy which give a large freezing point depression.

One important differences between coal and straw is that SiO_2 in straw is present as pure SiO_2 instead of as alumina silicates. The melting point of SiO_2 is significantly reduced by the presence of components with low melting points and may therefore contribute to melt formation also at the lower temperatures.

GAS PHASE MEASURING

A sampling system for gas phase measuring was designed in order to measure the amount of alkali metals in the gas phase. The sampling system comprises a probe and bubblers. The probe carries an alumina condenser, which is moderately inert to alkali metals.

A verification of gaseous alkali metal sampling systems has been needed as alkali metals may condense as small aerosol particles possibly evading the sampling system. Therefore a laboratory system to study the sampling efficiency was developed. The sampling efficiency was studied with $KCl(g)$ in the range of 250 - 500 ppm(v) and with $NaCl(g)$ in the range of 0.5 - 250 ppm(v). The results show that 94 ± 6 % of alkali metals are captured with a gas flow of 5 NI/min.

Soluble alkali metal in particles sampled coincident with the gas phase alkali metal may contribute to the measured gas phase result and in every sampling it may be evaluated to which extent.

Sampling with filter should be investigated, this could be done with the laboratory system used for studying sampling efficiency. Different things may be taken into account, typical filter materials react with or adsorb the gaseous alkali metal and a filter cake may react with or release gaseous alkali metal until equilibrium is obtained. In the alkali metal measurings mentioned in Jensen et al. (1995) the use of a quartz filter was tested, the results will be reported later.

ALKALI METALS IN A FLUIDIZED BED COMBUSTOR

The alkali metal behaviour is described for a 80 MW Circulating Fluidized Bed Combustor (CFBC), Grenaa Denmark. The CFBC is fed with a fuel mixture of coal and straw (heating value of about 50 % of straw and coal, respectively). Limestone is added for in bed removal of sulphur. The use of coal in combination with straw decreases the tendencies of bed material agglomeration, deposition and corrosion.

Potassium and chloride contents were measured in the CFBC, after the cyclone in front of two heat exchangers. The content of potassium was in average 100 ppm(v) and of chloride in average 110 ppm(v). This is about 25 % of total soluble potassium introduced and about 60 % of the total chloride introduced.

The gas temperature at the measuring point was about 800 °C, the maximum gas temperature in the system, about 920 °C, was in the top of the cyclone. Nordin (1993) reports for a fluidized bed system that the temperature at the surface of a burning particle may be about 150 °C higher than the gas temperature. This means that the particle temperature could have been above 1000 °C.

Deposits on the two heat exchangers were analyzed and the results are given as oxides. The first heat exchanger met by the gas contained about 5 % potassium as K_2O and the second about 30 %. The analyses of the deposits and equilibrium calculations indicated condensed alkali metal sulphates not to form to the extent of equilibrium at the location of measuring. The rate of condensation is such that the potassium is found in the deposit on the second heat exchanger.

A scanning electron microscopy analysis of the first micron layer (tube side) of the deposit on the second heat exchanger showed a first layer of potassium sulphate.

The introduced fuel combination has the ratios $M_2/S < 1$ and $M/Cl > 1$. When adding limestone for the capture of sulphur it can be explained as the ratio M_2/S increases, but gas phase measurements indicated a M_2/S ratio < 1 . By use of Table 1 it is seen that gaseous potassium will deposit only as potassium sulphate. This agrees with the chemical analyses of the deposit.

The kind of bed material may influence on the extent of melt formation, bed materials were evaluated and the influence of addition of limestone discussed. The bed material should have a relatively high melting point together with a relatively high melting enthalpy (see equation (1)) as e.g. CaO and Al_2O_3 (see Table 3). It may be considered which components may be formed as e.g. CaO will react with sulphur to form $CaSO_4$. A material which captures the alkali metals forming compounds with higher melting points may be preferred. Addition of limestone gives a possibility for reduction of the extent of melt formation as 1) the ratio $CaSO_4$ to K_2SO_4 increases (eutecticum at 875 °C), 2) the concentration of ash in the bed material decreases and 3) CaO itself contributes only to melt formation to a minor extent (see Table 3).

ALKALI METALS IN A STRAW GASIFIER

Potassium measurements were performed in a 50 kW moving bed straw gasifier, Laboratory of Energetics, The Technical University of Denmark. The gasifier was operating 12 hours during which the ash materials were accumulated in the system. The maximum temperature was about 950 °C in the top of the reactor where the fuel was introduced. The temperature was reduced downwards in the reactor, and the produced gas left in the bottom where the gas temperature was about 750 °C.

The potassium content was measured to 450 ppm(v) in the outlet gas at a temperature of 750 °C, that is 35 % of the total potassium content in the straw. The result is in reasonable agreement with equilibrium calculations at a temperature of 750 °C. It can not be known whether the measured potassium content has been released on the way downwards in the reactor or if it is an equilibrium established due to the accumulation of ash material.

Equilibrium calculations for the total system show that potassium in condensed form will be present as chlorides and carbonates if potassium silicates are not included in the calculations. This could also be found by the use of Table 1 and Table 2. If potassium silicates are included in the calculations the carbonates will not form. This is one of the general results, the alkali metal silicates are favoured to the carbonates.

The amount of potassium in the gas phase at 750 °C is the same whether potassium silicates are included in the calculations or not. The possible potassium silicates are $K_2O \cdot (SiO)_x$, where $x=2$ below 950 °C and $x=4$ above 950 °C.

CONCLUSION

Results of equilibrium calculations combined with gas phase measurements of the alkali metals, chlorine and sulphur were demonstrated as useful tools in the investigation of the alkali metal behaviour at gasification and combustion.

REFERENCES

- Barin I.: Thermochemical Data of Pure Substances, VCH (1989)
- Hald P.: Alkali metals at Combustion and Gasification, Equilibrium Calculations and Gas Phase Measurements, Department of Chemical Engineering, The Technical University of Denmark, Ph.D.-thesis (1994)
- Jensen P.A., Stenholm M., Hald P., Christensen K.A.: Deposition investigation in straw fired boilers, Risoe National Laboratory, Denmark (1995)
- Michelsen M.L.: Calculation of multiphase ideal solution chemical equilibrium, Fluid Phase Equilibria 53, 53-80 (1989)
- Nordin A.: On the chemistry of combustion and gasification of biomass fuels, peat and waste; environmental aspects, Ph.D.-thesis, University of Umeå (1993)
- Weast R.C.: CRC Handbook of Chemistry and Physics, 63rd edition, CRC Press (1983)

Table 1 Mole ratios M_2/S and M/Cl describing which condensed non-silicate alkali metal components are favoured at low or high temperatures (T) and at reducing (Red.) or oxidizing (Ox.) conditions.

		$M_2/S \leq 1$ $M/Cl \leq 1$	$M_2/S \leq 1$ $M/Cl > 1$	$M_2/S > 1$ $M/Cl \leq 1$	$M_2/S > 1$ $M/Cl > 1$
Ox.	$T < 800 \text{ }^\circ\text{C}$	M_2SO_4	M_2SO_4	M_2SO_4 MCl	M_2SO_4 M_2CO_3 MCl
Ox.	$T > 800 \text{ }^\circ\text{C}$	M_2SO_4	M_2SO_4	M_2SO_4	M_2SO_4 M_2CO_3
Red.	$T < 800 \text{ }^\circ\text{C}$	MCl	M_2CO_3 MCl	MCl	M_2CO_3 MCl
Red.	$T > 800 \text{ }^\circ\text{C}$	-	M_2CO_3	-	M_2CO_3

Table 2 Mole ratios M_2/S and M/Cl in coal and straw.

	Coal	Straw
M_2/S	< 1	normally > 1
M/Cl	< 1	> 1

Table 3 Freezing points at $x_i = 0.8$ and ΔT at $x_i = 0.8$. Melting enthalpies and melting points for the pure components (T^*).

Component	ΔH_m (kJ/mol)	T^* ($^\circ\text{C}$)	$T_{x_i=0.8}$ ($^\circ\text{C}$)	$\Delta T_{x_i=0.8}$ ($^\circ\text{C}$)
$K_2O \cdot (SiQ)_4$	49.0	770	730	40
KCl	26.3	771	699	72
$CaCl_2$	28.5	772	705	67
NaCl	28.2	801	730	71
Na_2CO_3	29.6	850	776	74
$Na_2O \cdot (SiQ)_2$	35.6	874	809	61
Na_2SO_4	23.8	884	788	96
K_2CO_3	27.6	901	815	86
$NaBO_2$	33.5	967	887	80
$K_2O \cdot (SiQ)_2$	41.0	1045	971	74
K_2SO_4	34.4	1069	978	91
$MgSO_4$	14.6	1127	916	211
$CaSO_4$	27.6	1457	1277	180
SiO_2	9.6	1723	1167	556
Al_2O_3	111.1	2054	1967	87
CaO	79.5	2614	2432	182
MgO	77.8	2852	2635	217

ΔH_m -values are from Barin (1989) and T^* from Weast (1983).

Mechanisms of Alkali Metal Release During Biomass Combustion

David C. Dayton and Thomas A. Milne
National Renewable Energy Laboratory
Industrial Technologies Division
1617 Cole Boulevard
Golden, CO 80401-3393

Keywords: alkali release, biomass combustion, molecular beam mass spectrometry

Introduction

The conversion of biomass materials into electricity via combustion poses several technical and economic challenges. One of the more pressing technical challenges associated with biomass combustion is fouling and slagging in combustors. Accelerated fouling and slagging in current biomass combustion facilities has been linked to the alkali metal content of the fuel. Alkali metal release during biomass combustion causes significant problems in terms of severe fouling and slagging of heat transfer surfaces in boilers thus reducing efficiency, and in the worst case leads to unscheduled plant downtime¹. Future biomass to electricity facilities that will incorporate integrated combined cycle systems that use biomass combustion gases directly to drive an aeroderivative turbine² will have even lower tolerances for alkali metal vapor release because accelerated erosion and corrosion of turbine blades results in shorter turbine lifetimes.

Hot gas cleanup methods are sought that reduce the amount of alkali vapor in biomass combustion gases to acceptable levels, thus minimizing fouling and slagging. This would be facilitated by a detailed understanding of the mechanisms of alkali release during biomass combustion as well as identifying these alkali vapor species and how these vapors lead to fouling and slagging. Our experimental approach to these issues is to identify the form of alkali metal vapors from directly sampled hot gases liberated from the combustion of small biomass samples in a variable temperature quartz tube reactor employing a molecular beam mass spectrometer (MBMS) system to monitor the combustion event. The baseline condition chosen for studying alkali metal release during biomass combustion was 1100°C in 20% O₂ in helium (simulated air). This temperature is approaching the maximum turbine inlet temperatures used for the next generation of direct biomass-fired turbines for power production. Under these conditions, the large excess of oxygen assured complete combustion and the furnace temperature was high enough to insure the partial volatilization of alkali metal containing species. By screening a large variety of biomass samples for alkali metal release, it may be possible to determine combustion conditions that minimize alkali metal release. These results may also be used to identify methods for reducing the alkali metal vapor content of the hot combustion gases.

Experimental

The release of alkali metal vapor species during biomass combustion was monitored and studied using a direct sampling, molecular beam mass spectrometer (MBMS) system. The MBMS system is ideally suited for studying the high temperature, ambient pressure environments encountered during the present alkali metal screening studies. The integrity of the sampled, high temperature combustion gases is preserved by the free-jet expansion because chemical reactions are effectively quenched and condensation is inhibited. The nature of the free jet expansion and the subsequent formation of a molecular beam allows reactive and condensable species, such as alkali metal containing vapors, to remain in the gas phase at temperatures far below their condensation point for long periods of time in comparison to reaction rates. The details of the apparatus and its application to studying alkali metal release during switchgrass combustion are described in the literature³⁻⁵.

Small (20-60 mg) samples were combusted in a tubular quartz reactor that was placed in a standard two-zone, electric clam-shell furnace³ set at either 1100°C or 800°C. Biomass samples were loaded into hemi-capsular quartz boats of such a size that approximately 40 mg of ground, loosely packed, material filled the boat, depending on the feedstock. The actual boat temperature and flame temperature were not measured, however, the hot gas temperature in the vicinity of the sample boat could be monitored with a type-K (chromel-alumel) thermocouple. A mixture of oxygen (20%, 10%, or 5%) in helium flowed through the reactor from back to front at a total gas flow rate of 4.4 standard liters per minute. Combustion gases had a residence time of about 0.1 seconds in the reactor before reaching the sampling orifice. When appropriate, steam was added to the reactor atmosphere by injecting water into the rear of the furnace through a needle fed by a syringe pump. Stainless steel shot was packed around the tip of the needle to increase the surface area for water evaporation. This provided a steady flow of 20% steam by volume.

The end of the reactor was fitted around the tip of the sampling orifice positioned at the downstream end of the quartz tube reactor to sample the high temperature, ambient pressure biomass combustion gases. The orifice protruded into the furnace to keep it at an elevated temperature and thus prevent condensation on the sampling cone. The actual temperature of the orifice was not routinely measured, however, when the furnace temperature was set at 1100°C the tip of the orifice was observed to glow orange. Sampled gases underwent a free jet expansion into the first stage of the differentially pumped vacuum system. The expanded gases were skimmed by a second conical skimmer (1 mm orifice diameter) at the entrance to the second stage forming a molecular beam that was directed into the ionization region of the mass spectrometer in the third stage of the vacuum system. Ions were formed by electron impact ionization of the sampled gases with a nominal electron energy of 25 eV. The ions were filtered by a triple quadrupole mass analyzer and detected with an off axis electron multiplier. The mass spectrometer was scanned continuously at a rate of approximately 100 amu/sec. In this configuration, a complete mass spectrum was recorded once every 1.0 to 1.5 seconds. Background subtraction from the total ion signal yielded corresponding mass spectra at a given time during the combustion event or averaged over a given phase of the combustion event.

A total of 23 different biomass feedstocks have been screened for alkali metal vapor release under four different combustion conditions. Only the results from one combustion condition, 1100°C and 20% oxygen in helium, will be discussed below. The list of feedstocks is as follows: planer shavings of lodgepole pine (*Pinus contorta*); eucalyptus (*Eucalyptus saligna Sm.*); poplar (*Populus deltoides x nigra var. Caudina*); corn stover (*Zea mays L.*); switchgrass (*Panicum virgatum L.*); wheat straw (*Triticum aestivum.*); rice straw; (Sandia) switchgrass (*Panicum virgatum L.*); pistachio shells (*Pistacia vera*); almond shells (*Prunus amygdalus*); almond hulls (*Prunus amygdalus*); wood waste #1; wood waste #2; waste paper, Danish wheat straws (*Triticum aestivum*) from Slagelse and Haslev (Danish power plants) (SLAG001, SLAG002, and HAS001); alfalfa stems (*medicago sativa L.*) (IGT001 and IGT002); summer switchgrass (*Panicum virgatum L.*); Dakota switchgrass (*Panicum virgatum L.*); and two willows (*Salix viminalis*, *Salix alba*, tops only). This set of feedstocks can be divided into various classes of biomass identified as woody feedstocks, herbaceous feedstocks, grasses, agricultural residues, and waste feedstocks. It will become apparent that the varying nature of the feedstocks results in unique differences in terms of alkali metal release during combustion.

Results and Discussion

The combustion of the solid biomass samples occurs in three distinct phases: the combustion phase, the char combustion phase, and the ash cooking phase^{4,5}. The details of the combustion event are available in the literature⁵. Based on these studies, it became obvious that the most important information concerning the species and amount of alkali metal released during biomass combustion was contained in the mass spectra averaged over the char combustion phase. Mass spectra averaged during the char combustion phases of all 23 feedstocks screened for alkali metal release qualitatively reflected the feedstock composition as determined from the ultimate and ash analyses. Although the ultimate analysis can be used to determine the total amount of alkali metal in a given feedstock, it does not reflect how much alkali metal is released into the gas phase nor the form of the alkali metal released.

The mass spectra averaged during the char combustion phase of the woody feedstocks (pine, eucalyptus, poplar, and willow) revealed that little alkali metal was released. As an example, the char phase mass spectrum averaged during the combustion of willow is presented in Figure 1. The mass spectral results are consistent with the ultimate and ash analyses for this willow sample that indicate low alkali metal levels. The only indication of alkali metal release is the detection of K⁺, however, the parent alkali metal species which yield this fragment could not be identified. Based on previous results⁴, the primary mechanism for alkali metal release during the combustion of low alkali containing woody feedstocks involves the vaporization or decomposition of potassium sulfate.

In general, the straws and grasses (switchgrass, wheat straw, alfalfa stems, and rice straw) contain high levels of potassium and chlorine. The mass spectrum averaged during the char phase of rice straw combustion is shown in Figure 2. Based on the composition of rice straw (shown in the inset) determined from the ultimate and ash analysis of the sample, this feedstock has high levels of both potassium and chlorine. As a result, strong mass spectral signals are observed at $m/z=74$ and 76 , corresponding to the KCl parent ions. In fact, the fragment ions of the KCl dimer (K₂Cl⁺ at $m/z = 113$ and $m/z = 115$) were also observed. Significant intensity was also observed at $m/z=39$, the K⁺ fragment. The intensity of these signals is a function of the amounts of potassium and chlorine available in the feedstock. For high chlorine containing feedstocks, like rice straw, it is also possible to identify HCl released during combustion. The dominant mechanism for alkali metal release during

the combustion of feedstocks with high potassium and chlorine contents is through the vaporization of potassium chloride.

The agricultural residues, pistachio shells, almond shells, and almond hulls, tend to have high potassium content but low chlorine content. In fact, the almond hulls have the highest level of potassium of all 23 feedstocks studied. The mass spectrum averaged over the char phase of almond hulls combustion is shown in Figure 3. The dominant alkali metal species observed in the char phase mass spectra averaged during almond hulls combustion were potassium hydroxide ($m/z = 56$) and potassium cyanate, KOCN ($m/z = 81$). The high nitrogen content in addition to the high potassium content of the almond hulls and the oxidizing combustion conditions contribute to the formation of KOCN. At this time it is not clear whether KOCN is directly released or KCN is released and then reacts with oxygen to form the cyanate. The relatively low chlorine level of the almond hulls forces the alkali metal release to other thermodynamically stable forms.

The waste feedstocks (wood waste #1, wood waste #2, and waste paper) are not as bad as their name implies in terms of alkali metal release. These feedstocks tend to have relatively low alkali levels, and as a result, it was difficult to identify any alkali species in the mass spectra averaged over the char combustion phases of these feedstocks. The waste feedstocks do have moderately high chlorine levels (0.13 w%). However, HCl was the only chlorine species identified in the char phase mass spectra.

Multiple alkali release mechanisms can occur simultaneously during biomass combustion depending on the feedstock composition. This is most apparent from the mass spectral results recorded during the char phase of alfalfa stems combustion shown in Figure 4. Alfalfa stems have a high potassium, chlorine, and nitrogen content. As a result, there is substantial alkali metal released in the form of KCl, KOH, and KOCN.

Once the major biomass combustion products were identified, including the major alkali metal containing species released, correlations were sought between the mass spectral data and the ultimate analysis data for the 23 feedstocks screened. The chlorine content determined in the ultimate analyses correlated well with the mass spectral intensities of identifiable chlorine containing species, HCl and KCl, monitored at $m/z=36$ and 74 (HCl^+ and KCl^+ , respectively). Most of the available chlorine is released into the gas phase and can be accounted for during biomass combustion⁶.

The potassium content of a given feedstock does not correlate as well with the parent and fragment ions (KOH^+ , KOCN^+ , KCl^+ , and K^+) identified in the char phase mass spectra that result from the dominant gas phase potassium species. The overall potassium content of a given feedstock does not necessarily correspond to a high level of alkali metal vapor released during biomass combustion⁶. Almond hulls have the highest potassium content of the 23 feedstocks, yet combustion of almond hulls does not release the most potassium vapor (KCl, KOH, and/or KOCN). Rice straw has a high potassium content, however, it also has the highest chlorine content of any of the 23 feedstocks. As a result, significant alkali metal vapor is released as KCl during rice straw combustion. Alfalfa stems and switchgrass also have a high potassium and chlorine content that accounts for the above average alkali metal vapor released during combustion. It appears that those feedstocks with high potassium and the higher chlorine levels tend to release more alkali metal vapors (based on an average of the 23 feedstocks studied) than those feedstocks with high potassium and low chlorine contents.

Conclusions

The MBMS technique has proven to be a valuable and versatile tool for studying alkali vapor release during biomass combustion. The most significant parameter which affects alkali vapor release is the feedstock being combusted. While each individual feedstock appears to have its own unique combustion properties, these feedstocks can often be grouped together into classes of feedstocks. Woody feedstocks have comparatively little alkali content and low levels of chlorine. Consequently, combustion of woody feedstocks leads to very little alkali vapor release, usually via a mechanism involving the vaporization of potassium sulfate.

Herbaceous feedstocks, grasses and straws contain very high levels of alkali and chlorine compared to the woody feedstocks. Large amounts of alkali metal, in the form of potassium chloride, are released into the gas phase during combustion of herbaceous feedstocks which results in a high fouling and slagging potential for these feedstocks. The results of these alkali screening studies implicate the chlorine content of a given feedstock as a facilitator of alkali release⁶.

While chlorine content has been linked to substantial alkali vapor release, it is not essential. The agricultural residues still release significant amounts of alkali vapor during combustion, however, the

alkali is in the form of the hydroxide and potassium cyanate instead of the chloride. These studies identify a new mechanism for alkali metal release that involves the formation of potassium cyanate. This mechanism of alkali transport seems to be dominant during the combustion of feedstocks that have high potassium and nitrogen contents.

Having identified these dominant gas phase species it should be possible to identify how these alkali metal containing species contribute to fouling and slagging in industrial combustion systems. Methods can now be sought to sequester or reduce the level of these species in the gas phase if they prove to be major precursors to deposit formation. Additives to the bed material in fluid bed combustors can be sought to capture these species after they are released. Alkali getter beds or separate hot gas cleanup units can be designed knowing that the major alkali species in the gas phase have been identified based on the feedstocks screened in this study.

Acknowledgements

The authors are grateful for the support of the Solar Thermal and Biomass Power Division of the Department of Energy Office of Energy Efficiency and Renewable Energy. Special thanks go to Richard L. Bain and Ralph P. Overend for both programmatic and technical support and guidance. Mr. Gerald Cunningham of Hazen Research, Inc. is acknowledged for providing feedstocks and their analyses. We would also like to acknowledge the efforts of Thomas R. Miles, Sr. and Thomas R. Miles, Jr. of Thomas R. Miles Consulting Engineers and Dr. Larry Baxter of Sandia National Laboratories Combustion Research Facility.

References

1. Turnbull, J.H., *Biomass and Bioenergy*, 1993, 4, pp. 75-84.
2. Bain, R.L. and Overend, R.P., *Advances in Solar Energy: An Annual Review of Research and Development, Volume 7*. Ed. Karl W. Boer, American Solar Energy Society. Chapter 11, 1992.
3. Evans, R.J. and Milne, T.A., *Energy and Fuels*, 1987 1, pp. 123-127.
4. French, R.J., Dayton, D.C., and Milne, T.A., "The Direct Observation of Alkali Vapor Species in Biomass Combustion and Gasification," NREL Technical Report (NREL/TP-430-5597). January 1994.
5. Dayton, D.C., French, R.J., and Milne, T.A., submitted for publication in *Energy and Fuels*.
6. Dayton, D.C., R.J. French, and T.A. Milne, "Identification of Gas Phase Alkali Species Released During Biomass Combustion," Proceedings of the Bioenergy '94 Conference, October 2-6, 1994, Reno, NV. p. 607.

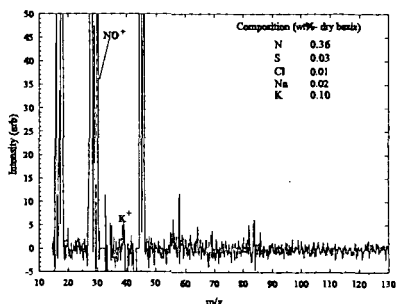


Figure 1: Mass spectrum averaged over the char phase of willow combustion at 1100°C in 20% oxygen in helium. The signals have been normalized to the $^{34}\text{O}_2^+$ signal measured before sample insertion. The composition in the inset is from the ultimate and ash analyses of the feedstock on a moisture free basis.

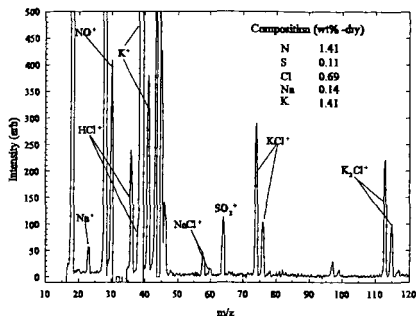


Figure 3: Mass spectrum averaged over the char phase of rice straw combustion at 1100°C in 20% oxygen in helium. The signals have been normalized to the $^{34}\text{O}_2^+$ signal measured before sample insertion. The composition in the inset is from the ultimate and ash analyses of the feedstock on a moisture free basis.

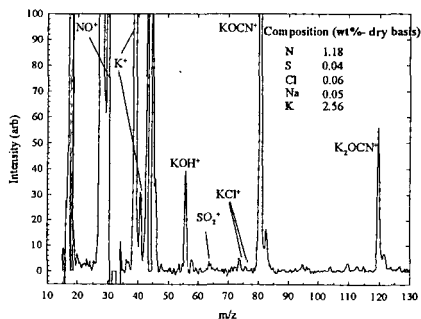


Figure 4: Mass spectrum averaged over the char phase of almond hulls combustion at 1100°C in 20% oxygen in helium. The signals have been normalized to the $^{34}\text{O}_2^+$ signal measured before sample insertion. The composition in the inset is from the ultimate and ash analyses of the feedstock on a moisture free basis.

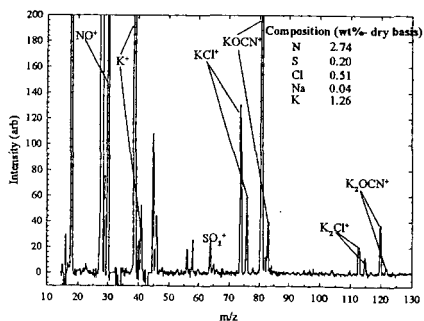


Figure 2: Mass spectrum averaged over the char phase of alfalfa stems combustion at 1100°C in 20% oxygen in helium. The signals have been normalized to the $^{34}\text{O}_2^+$ signal measured before sample insertion. The composition in the inset is from the ultimate and ash analyses of the feedstock on a moisture free basis.